Norwegian University
of Life Sciences

Master's Thesis 2023 30 ECTS

Faculty of Chemistry, Biotechnology and Food Science
Dr. Daniel Straume

Incorporation of branched stem-peptides in the cell walls of penicillin-resistant *Streptococcus pneumoniae*: which PBP is responsible?

Johanne Moldstad
Master of Science in biotechnology and chemistry

Acknowledgments

This master´s thesis was completed as part of the Master of science in biotechnology and chemistry at the Norwegian University of Life Sciences (NMBU), in the Molecular Microbiology (MolMik) research group at the Faculty of Chemistry, Biotechnology and Food Science (KBM), January to May 2023. The thesis makes up 30 ECTS of the master's degree.

I would like to begin by thanking my supervisor, Dr. Daniel Straume, for all guidance in the practical lab work and the writing process. I have learned a lot from you.

I would also like to thank Ragnhild Sødal Gjennestad for everything I have learned from these past months working with you. I am very grateful for the immense patience you have shown me and for answering all my questions.

The MolMik group all deserves thanks for making my time in the lab into the great experience it was. Thank you all for being available to answer questions and encourage me when I was working on some stubborn transformations and isolating cell walls for weeks. Especially big thanks to Zhian Salehian for all the help you have provided for me in all aspects of the lab work. I have highly appreciated the excellent mood you bring to the lab. My fellow master´s student also deserves thanks for making our time together in the lab enjoyable.

Thank you to my friends, especially Sigrid Fu and Julie. Sigrid Fu for encouraging me to do things other than just master´s thesis work, and Julie for being a great fellow student these past two years. I really appreciate our friendship.

Lastly, I would like to thank my family. My parents have been so supportive throughout my entire course of study, especially these past two years of my master's degree. I highly value the advice and encouragement you give me when the workload feels overwhelming at times. Thank you for putting up with all my complaints while writing my thesis. I would especially like to thank my mother for proofreading every report I have ever handed in, including this one. Thanks to her, all my reports have been grammatically correct and had a great sentence structure. Thank you both for always being "in my corner."

Table of contents

Abstract

Streptococcus pneumoniae is an opportunistic pathogen that colonizes the upper respiratory tract of 10% of the human population. Infections from this bacterium include otitis media, sinusitis, and pneumonia, but it also causes severe systemic infections, including bacteremia and meningitis. Annually this pathogen is responsible for around 1 million deaths worldwide. The common treatment for infections caused by *S. pneumoniae* is β-lactam antibiotics (e.g., penicillins), which target so-called penicillin-binding proteins (PBPs) responsible for cell wall synthesis. PBPs are enzymes that, through transglycosylation and transpeptidation reactions, synthesize the peptidoglycan layer, which surrounds the cytoplasmic membrane of most bacteria. The cell wall precursor molecule is called a muropeptide and consists of a di-saccharide with a pentapeptide attached to it. The peptide part can be either linear or branched, meaning that it has two extra amino acids added to it. The pneumococcal cell wall consists of both branched and linear muropeptides. β-lactam resistant isolates often have an increase in branched muropeptides in their cell wall. A protein called MurM is required to create branched muropeptide precursors. When knocking out *murM* in resistant strains, they are resensitized to penicillin, strongly suggesting that incorporating branched muropeptides in their peptidoglycan is critical for penicillin resistance.

The hypothesis for this study is that a low-affinity version of PBP2b either prefers branched structured muropeptides or is less active, leading to compensating cell wall synthesis by one of the other PBPs. A low-affinity PBP means that it will have a lower affinity towards penicillin and bind penicillin less than the wild-type strain does (Chambers, 1999). To study this, knockout strains of *pbp2b* and single knockouts of the class A PBPs (*pbp1a*, *pbp1b,* and *pbp2a*) were created and phenotypically tested for changes in their cell wall composition. The strains RSG77 and Pen6 were chosen to be the foundational genetic backgrounds for this study because they are both highly resistant strains with a high level of branching in the cell wall. RSG77 is a strain created at the MolMik group. The mutant strains were imaged by microscopy to see what changes the knockouts had on the morphology of them. The knockout mutants of *pbp2b* as well as the class A PBPs all showed an expected change in morphology, based in findings form the literature. The Δ*pbp2b* strains had a morphology where the cells were shorter and grew in chains, whilst the class A PBP mutants deviated little from the genetic background. The composition of the high-affinity PBPs present in each strain, were visualized by fluorescently labelling them with bocillin FL and SDS-

PAGE. The bands where no penicillin would bind, was either where the PBP had been knocked out or where it was a low-affinity PBP instead. An HPLC analysis of all strains was performed to investigate changes in the amount of branching present in the cell wall. The HPLC results showed no major differences in the cell wall when *pbp2b* or either of the class A PBPs (*pbp1a*, *pbp1b*, and *pbp2a*) was knocked out.

Sammendrag

Streptococcus pneumoniae er et opportunistisk patogen som koloniseres i den øvre delen av respirasjonssystemet hos om lag 10% av verdens befolkning. Infeksjoner forårsaket av denne bakterien inkluderer mellomørebetennelse, bihulebetennelse og lungebetennelse, men den kan også forårsake mer alvorlige systemiske infeksjoner som bakteriemi og hjernehinnebetennelse. Dette patogenet er ansvarlig for omtrent 1 million dødsfall årlig på verdensbasis. Den vanligste måten å behandle *S. pneumoniae* infeksjoner på, er med β-lactam antibiotika (for eksempel penicillin). Den angriper såkalte penicillin-bindende proteiner (PBPer) som er ansvarlige for celleveggsyntesen. PBPer er enzymer som, gjennom transglykosylerings- og transpeptideringsreaksjoner, syntetiserer peptidoglykanlaget som omgir den cytoplasmiske membranen hos de fleste bakterier. Forløperen til celleveggen er et molekyl som kalles muropeptid. Den består av et disakkarid med et pentapeptid festet til seg. Peptiddelen kan enten være lineær eller forgreinet, hvilket betyr at den har to ekstra aminosyrer festet til seg. Celleveggen til pneumokokker består av både lineære og forgreinede muropeptider. β-laktamresistente isolater har ofte en forøkning i antall forgreinede muropeptider i celleveggen. Et protein som heter MurM er nødvendig for at det skal dannes forgreinede forløpere. Ved å slå ut *murM* i resistente stammer, blir de resensibilisert til penicillin, hvilket sterk indikerer at inkorporeringen av forgreinede muropeptider i peptidoglykanen er kritisk for penicillinresistens.

Hypotesen for denne studien er at en lavaffinitetsversjon av PBP2b enten foretrekker en forgreinet struktur på muropeptidene, eller så er den mindre aktiv, noe som fører til kompenserende celleveggsyntese av en av de andre tilgjengelige PBPene. Det at en PBP er lavaffinitet betyr at den har en lavere affinitet mot penicillin, og vil derfor binde mindre penicillin enn de som ikke er det (Chambers, 1999). For å studere dette ble det laget mutantstammer hvor *pbp2b* og klasse A PBPene (*pbp1a*, *pbp1b* og *pbp2a*) var slått ut hver for seg. Disse ble fenotypisk testet for å se om det var noen endringer i deres sammensetting av celleveggen. Stammene RSG77 og Pen6 ble valgt til å være den genetiske bakgrunnen i denne studien, fordi de er begge høyresistente stammer og de har et høyt antall forgreinede muropeptider i celleveggen. RSG77 er en stamme som er laget av MolMik gruppen. Mutantstammene ble avbildet ved mikroskopi for å se hvilke morfologiske endringer som skjedde når de ulike PBPene var slått ut. Basert på informasjonen som finnes om disse utslåingene fra før av, så hadde både Δ*pbp2b* og klasse A PBP mutantene en forventet

morfologisk endring. Δ*pbp2b* stammene hadde en morfologi hvor cellene var kortere og vokste i kjeder, mens mutantene uten klasse A PBPene hadde lite endring fra den genetiske bakgrunnen. Sammensettingen av høyaffinitets-PBPene som var til stede i hver stamme ble visualisert med fluorescerende merking med bocillin på SDS-PAGE. Der hvor båndene ikke vises er enten PBPen slått ut eller så er det en lavaffinitets PBP istedenfor. En HPLC analyse av alle stammene ble gjennomført for å undersøke endringer i mengden forgreininger som var til stede i celleveggen. Resultatene fra HPLC viste ingen store endringer i celleveggen til klasse A PBPene. I de stammene hvor *pbp2b* var slått ut i RSG77, var det et lite skifte og mengden forgreininger var større når PBP2b var til stede. Disse endringene ble ikke observert for de samme mutantene i Pen6.

1 Introduction

1.1 *Streptococcus pneumoniae* – an important human pathogen

Streptococcus pneumoniae (pneumococcus) is a Gram-positive opportunistic pathogen that will colonize in the upper respiratory tract of approximately 10% of the human population (NCIRD, Division of bacterial diseases, 2022; van der Poll & Opal, 2009). This bacterium causes infections like otitis media, sinusitis, and pneumonia but can also cause severe systemic diseases, including bacteremia and meningitis (van der Poll & Opal, 2009). Annually the pathogen is responsible for around 1 million deaths worldwide (Troeger et al., 2018). Bacterial respiratory tract infections are typically treated with β-lactam antibiotics (e.g., penicillin). However, since the first incident of penicillin resistance seen in pneumococci in 1969, the number of resistant isolates has increased (Cornick et al., 2012). In 2017, the World Health Organization (WHO) published the global priority pathogen list to help guide and prioritize research and development in the global fight against antibiotic resistance. Of these, penicillin-non-susceptible *S. pneumoniae* is categorized as a priority three pathogen, which indicates a medium threat, below high and critical categories (*WHO*, 2017).

S. pneumoniae is found in the genus *Streptococcus*, making it a low GC Gram-positive bacterium belonging to the phylum Firmicutes (Figure 1). *Streptococcus* can be divided into six main categories based on phylogeny. These groups are the pyogenic, anginosus, mitis, salivarius, bovis, and mutans groups, and *S. pneumoniae* is found in the mitis group. This was seen from 16S rRNA analyses (Kawamura et al., 1995).

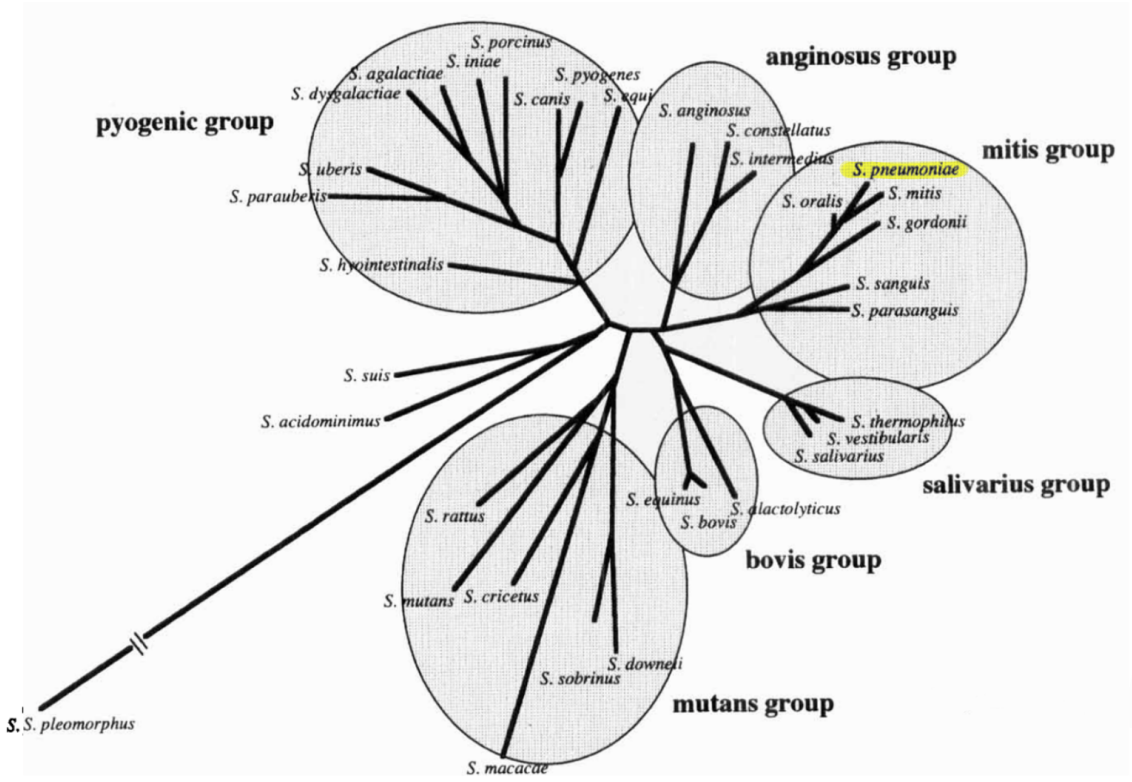

Figure 1 The phylogenetic relationship between all species of *Streptococcus*. The phylogenetic groups are the pyogenic, anginosus, mitis, salivarius, bovis, and mutans. Figure modified from Kawamura et al., 1995.

The natural habitat of streptococci is in humans' and animals' mucus membranes (Hardie & Whiley, 1997). Pneumococci will colonize in one of two ways: it can either be a persistent and non-invasive colonizer, or it can be invasive. Low-level and long-lasting transmission is possible by the constant carriage of pneumococci. By doing this, the pneumococci can establish a reservoir of bacteria in the human population. About 10% of adults and 60% of children always have detectable amounts of pneumococcal colonization in their mucus membranes in the upper respiratory tracts (van der Poll & Opal, 2009).

Bacterial pneumonia caused by *S. pneumoniae* is recognized as one of the leading causes of disease and death among infants and children younger than five years old, causing as many as 826 000 deaths in the year 2000. This was roughly half of the deaths related to pneumococci that year (O'Brien et al., 2009). A study by Wahl et al. in 2018 indicates that the number of *S. pneumoniae*-related deaths decreased between 2000 and 2015 in children under five years. This, however, might

be an underestimation due to uncertainties in how many deaths involving pneumonia are related to pneumococci (Wahl et al., 2018).

S. pneumoniae is mainly transferred between hosts in liquid secreted from the respiratory tract, often within a household or between children. Pneumococci are not considered a highly contagious pathogen due to their ineffective route of infection compared to other bacteria, so isolation of infected patients is rarely seen or needed (van der Poll et al., 2009).

S. pneumoniae produces several colonization and virulence factors. Some of these are the polysaccharide capsule, surface proteins, and pneumolysin, a pore-forming toxin. The role of the capsule for *S. pneumoniae* is mainly to aid in escaping the host´s immune system, which can cause harm to the cell. The capsule also has a role in colonization, where it securely attaches the cell to the host. The capsule will also protect the cell from some antibiotics (Nelson et al., 2007). Among the virulence factors, the polysaccharide capsule is, therefore, the most predominant one (Mitchell, 2004). An unencapsulated version of the laboratory strain R6 was found to be avirulent compared to its predecessor (Cornick et al., 2012). The capsule's composition can vary, giving rise to different serotypes. To this date, more than 100 different serotypes have been discovered of *S. pneumoniae* (Ganaie et al., 2020). Generally, people infected with *S. pneumoniae* only carry one serotype at a time, although it is possible to have multiple serotypes at once (Hare et al., 2008). The duration of colonization of pneumococci varies significantly between the different serotypes (T. Smith et al., 1993).

The number of invasive pneumococcal disease cases decreased immensely in children once the vaccine was introduced. After this introduction, however, an increase in the prevalence of serotypes not susceptible to vaccines followed (Weil-Olivier et al., 2012). This shows that solutions are still needed to fight the threat pneumococci pose to our society. What gives *S. pneumoniae* the ability to become resistant to new drugs and escape vaccines quickly is its ability to undergo natural transformation (Rice, 2002; Straume et al., 2014).

The choice of treatment against community-acquired pneumonia has, since the late 1940s, been β-lactam antibiotics. This caused a decrease in disease and death, but it also caused overconsumption and misdiagnoses due to a lack of information and training about proper dosage (Cornick et al., 2012). This led to the first discovery of a penicillin-resistant *S. pneumoniae* strain in 1967 (Hansman & Bullen, 1967). Using β-lactam antibiotics caused selection pressure on strains of *S.*

pneumoniae to evolve for survival. This evolution is done by either natural transformation or spontaneous gene mutations causing resistance. Natural transformation is much faster than evolutionary changes in the genome (Chewapreecha et al., 2014; Straume et al., 2014).

These antibiotic-resistant pneumococci are still concerning for the general public's health. Therefore, investigating antibiotic resistance mechanisms is crucial for stopping the spread and stagnation of new multiresistant strains (Cornick et al., 2012).

β-lactam antibiotics are, as previously mentioned, the most common way to treat bacterial infections. These antibiotics will inhibit the synthesis of new peptidoglycan because they bind covalently to the PBPs in the cell wall, which leads to no new peptidoglycan being synthesized, and the cell will not divide or repair itself properly (N. H. Georgopapadakou & Liu, 1980; Tipper & Strominger, 1965). When penicillin inhibits one or more of the PBPs, depending on how essential the PBP is, the result is often cell death (Spratt, 1977).

1.2 Peptidoglycan synthesis in *S. pneumoniae* – an overview

The cell wall has many vital functions for the bacterium. Some of those are maintaining the cell shape, preventing it from bursting due to the internal turgor, harboring teichoic acids and proteins anchoring to the cell wall, and their interactions (Bui et al., 2012). Pneumococci are oval-shaped cocci (Zapun, Vernet, et al., 2008b). This shape is obtained by a combination of peripheral and septal cell wall synthesis, performed by different types of machinery called the elongasome and the divisome, respectively (see section 1.4) (Higgins & Shockman, 1976; Zapun, Vernet, et al., 2008b). The main component of the cell wall is peptidoglycan, which is built up of glycan strands that are crosslinked by shorter peptides called stem peptides (Rogers et al., 1980) (Figure 2). The glycan strands consist of alternating N-acetylmuramic acid, called MurNAc, and of N-acetylglucosamine, called GlcNAc (Vollmer et al., 2008). In *S. pneumoniae*, the peptide has the sequence L-Ala-D-iGln-L-Lys-D-Ala-D-Ala (Garcia-Bustos et al., 1987). Cross-linking of the strands is mainly done between the carboxyl of the fourth D-Ala residue of one peptide and the epsilon amino group of the third L-Lys of the other peptide. This linkage can eighter be direct or contain a short bridge of peptides (Vollmer et al., 2008).

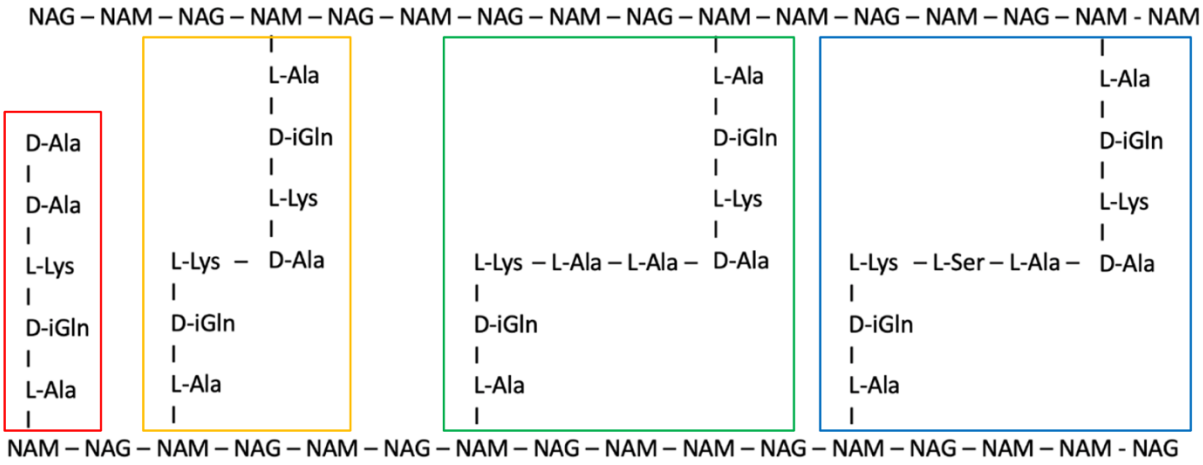

Figure 2 The structure of peptidoglycan in *S. pneumoniae*. Peptidoglycan comprises long chains of glycan, which exchange between units of N-acetylglucosamine (GlcNAc) and of N-acetylmuramic acid (MurNAc). The glycan strands are connected via cross-links, which are short peptides. These can be eighter linear or branched. A single peptide is shown in the red square, followed by a linear cross-linked muropeptide in the yellow square. The two branched versions of muropeptides are shown in the green and blue squares and are the ones to occur in pneumococci. Figure modified from Zapun et al., 2008a.

Peptidoglycan is synthesized from a precursor molecule called lipid II (Figure 3). Synthesis of lipid II includes the formation of GlcNAc and MurNAc with a Uridin diphosphate (UDP) attached to them and having the stem peptide bound to MurNAc. The UDP works as a carrier of the precursors (Barreteau et al., 2008). First, the stem peptide is assembled by four enzymes essential to the cell. These enzymes are the Mur ligases, consisting of MurC, MurD, MurE, and MurF. These ligases make MurNAc into a pentapeptide complex (Duncan et al., 1990; Liger et al., 1995; Michaud et al., 1990; Pratviel-Sosa et al., 1991). Then MurNAc is assembled and attached to the membrane by being anchored to a membrane carrier lipid. This is done by MraY, which forms lipid I (Ikeda et al., 1991). A molecule of UDP-GlcNAc will then be relocated onto the MurNAc end of the lipid I by MurG. This new peptide is lipid II (Bupp et al., 1993).

In pneumococci, it is common to amidate the second stem peptide residue on the alpha-carboxylic group in lipid II. The reaction will be catalyzed by the protein complex consisting of MurT and GatD. This complex is essential in *S. pneumoniae* because the lipid II precursor needs to be modified by amidation for an efficient cross-linking (S. R. Filipe et al., 2000). Therefore, the following modification is adding a branch to lipid II. The branch consists of 2 L-amino acids, which will be added to the third position in the stem peptide. This reaction is catalyzed by the

ligases MurM and MurN (S. R. Filipe et al., 2001). These enzymes are not essential for pneumococci to grow but are vital for some strains' ability to resist β-lactam antibiotics (Vollmer et al., 2019).

At this point, the precursor lipid II will be transferred from the cytoplasm to the periplasm. This is done by the flippase MurJ (Sham et al., 2014). When lipid II has been flipped into the periplasm, it will be used by peptidoglycan polymerases called penicillin-binding proteins (PBPs) as a substrate for synthesizing the cell wall (Ghachi et al., 2005). For lipid II to form polymers, two reactions must occur. First, transglycosylation will form glycan strands, and then transpeptidation will cross-link the glycan strands into the existing peptidoglycan layer via stem peptide cross bridges (Goffin & Ghuysen, 1998). The cross-linking can be eighter direct or indirect (Figure 2) (Garcia-Bustos et al., 1987). The indirect links are often referred to as branching in the cell wall. PBPs can either do both reactions or only the transpeptidation. Class A PBPs (PBP1a, PBP1b, and PBP2a in *S. pneumoniae*) have both transglycosylation and transpeptidation activity, while the class B PBPs (PBP2x and PBP2b in *S. pneumonaie*) only have the transpeptidation abilities (Berg et al., 2013; Kell et al., 1993). The class C PBP (PBP3) is the only D-Ala, D-Ala (D, D)-carboxypeptidase in pneumococci (Morlot et al., 2005).

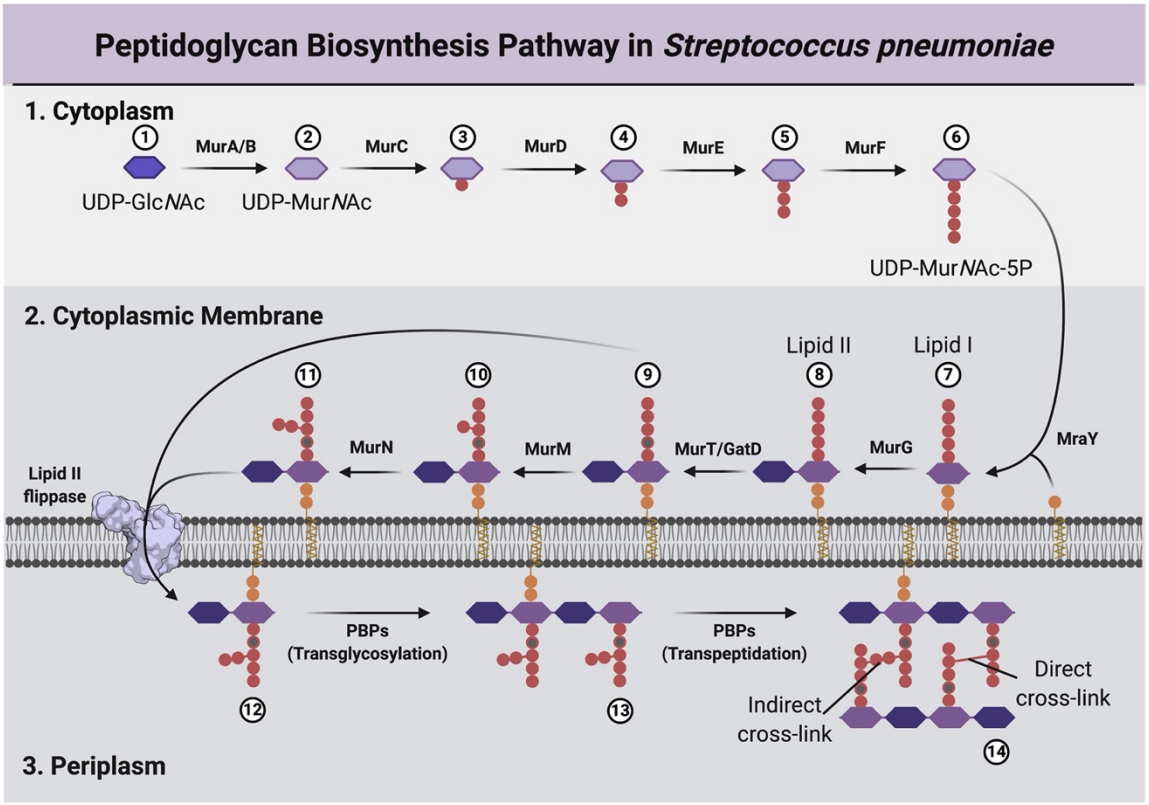

Figure 3 Peptidoglycan biosynthesis pathway in *S. pneumoniae*. An overview of all reactions occurring during synthesizing of new peptidoglycan in pneumococci. See the main text for more information about the process. Figure from York et al., 2021.

The class B PBPs that perform only the transpeptidation reaction were long believed to depend on class A PBPs for transglycosylation of the glycan chains. However, it has been found that enzymes that perform these reactions cooperate with the class B PBPs. These enzymes are known as SEDS (shape, elongation, division, and sporulation) transglycosylase (Henriques et al., 1998) and perform transglycosylation. The class B PBPs can perform the transpeptidation (Berg et al., 2013; Kell et al., 1993). PBP2x belongs to class B and is a part of a complex together with the SEDS transglycosylase FtsW, which is involved in the septal cross-wall formation (Noirclerc-Savoye et al., 2013). Another member of the class B family, PBP2b, forms a complex with the SEDS transglycosylase RodA, which is responsible for peripheral peptidoglycan synthesis (cell elongation) (Meeske et al., 2016).

In *S. pneumoniae*, the transpeptidation of the chains can give a direct crosslink, or an indirect crosslink, also called a branched crosslink. The branched crosslink found the most abundantly in strains resistant against β-lactam antibiotics is L-Ser-L-Ala or L-Ala-L-Ala (Bui et al., 2012; Severin & Tomasz, 1996). The amount of branching found will vary between pneumococcal strains (Fiser et al., 2003).

Evidence from biochemical, genetic, and cellular analyses indicate that the synthesis of new peptidoglycan and the murein hydrolase activity in the cell is regulated and coordinated by two large protein complexes: the elongasome and the divisome (Egan & Vollmer, 2013; Trouve et al., 2021; Typas et al., 2011). The divisome is responsible for septal peptidoglycan synthesis, and the elongasome oversees the elongation of the cell by performing peripheral peptidoglycan synthesis (Den Blaauwen et al., 2008; Goehring & Beckwith, 2005). The septal synthesis separates the dividing pneumococcal cell in the middle. This forms two new cells called daughter cells from the original one (Du & Lutkenhaus, 2017). The peripheral synthesis also starts at the middle of the cell's division ring and builds new peptidoglycan strands to elongate the dividing cell (Lamanna et al., 2022). The proteins in both the divisome and the elongasome are organized into multiple rings, often one ring for the divisome flanked by two more elongasomal rings. They form around the center of the cell wall before it divides by FtsZ, FtsA, and EzrA (Fleurie et al., 2014; Perez et al., 2019). FtsZ will polymerize and form the Z-ring, a ring consisting of tubulin-like proteins (Massidda et al., 2013). The Z-ring is recruited to the midcell closely associated with the cytoplasmic membrane and is stabilized by FtsA and ZipA (de Boer, 2010).

After the Z-ring has been made, the rest of the proteins in the divisome are arranged around the Z-ring (Pinho et al., 2013). When the cell starts dividing, the septal peptidoglycan synthesizing machinery moves to one side of the closing septum along with FtsZ in circular movements. The machinery for peripheral peptidoglycan synthesis remains at the outer perimeter of the septal disk (Land & Winkler, 2011). The cross wall made by the divisome will be divided into two daughter cells by murein hydrolases (Zapun et al., 2008b). See sections 1.4.1 and 1.4.2 for more details on the divisome and elongasome.

1.3 Penicillin-binding proteins

As previously described, penicillin-binding proteins (PBPs) are enzymes that have essential roles in the late stages of peptidoglycan synthesis. The enzymes perform transglycosylation and peptide cross-linking of the peptidoglycan layer in the cell wall. PBPs have penicillin-binding domains, either carboxypeptidases or transpeptidases (Zapun, et al., 2008a). The periplasmic domain of the PBPs is anchored to the cytoplasmic membrane, and the catalytic domain is on the outside of the membrane (Suvorov et al., 2007). The domains have three conserved motifs, which are SXXK, (S/Y)XN, and (K/H)(S/T)G. These are the characteristic active sites for the family of active-site serine penicillin-recognizing enzymes (ASPRE). β-lactam antibiotics will bind to the motifs and inhibit the enzyme's activity (see below). The central part of the catalytic mechanism of the SXXK motif is the serine (S) (Zapun, et al., 2008a).

S. pneumoniae has two classes of high-molecular-mass PBPs and one of low-molecular-weight. The two classes of high-molecular-mass are *pbp1a*, *pbp1b*, and *pbp2a* in class A and *pbp2x* and *pbp2b* in class B (Berg et al., 2013; Sauvage et al., 2008; Zapun, Vernet, et al., 2008b). The PBPs in class A have been biochemically recognized as bifunctional glycosyltransferase transpeptidases (Goffin & Ghuysen, 1998).

The class A PBPs can be knocked out individually, and a double knockout of *pbp1a* and *pbp1b* and of *pbp1b* and *pbp2a* are possible. However, making the double knockout Δ*pbp1a*Δ*pbp2a* has been found to be lethal for the cell, indicating that the two enzymes might have an essential overlapping function that can be compensated by the presence of the other PBP (Berg et al., 2014; Paik et al., 1999). PBP2x and PBP2b have been proven essential enzymes (Kell et al., 1993). Compared to the class A PBPs, they are not bifunctional and only possess a transpeptidase activity. PBP2b and PBP2x have the same enzymatic activities but have different roles biologically (Di Guilmi et al., 1998; Ghuysen, 1994). The only low-molecular-mass PBP in *S. pneumoniae* is PBP3, found in class C (Hakenbeck & Kohiyama, 1982). It is a D-Ala, D-Ala (D, D)-carboxypeptidase in pneumococci. It trims off the last residue of the pentapeptides to reduce the readiness of donors interested in the reaction causing transpeptidation. By doing this, the D,D-carboxypeptidase limits the interlacing of the peptidoglycan (Morlot et al., 2004). (Morlot et al., 2005). PBP3 is present in the entire bacterial surface at the beginning of cell division, except in the future division site. This

indicates that the placement of the high-molecular-mass PBPs mid-cell depends on how much peptidoglycan substrate is available to them (Morlot et al., 2005).

The high-molecular-mass PBPs are multimodular and control the polymerization and insertion of peptidoglycan into existing cell walls. Topologically, they comprise a cytoplasmic tail, an anchor attached to the membrane, and two domains (Sauvage et al., 2008). As previously mentioned, the domain of the PBPs in the periplasm is anchored to the cytoplasmic membrane. A transmembrane segment does this. This leaves the small N-terminal domains to stick out into the cytoplasm. (Typas et al., 2011). The domains are joined together by a linker, where the peptidoglycan synthesis transpires at the cytoplasmic membrane (Goffin & Ghuysen, 1998). The C-terminal of both classes has transpeptidase activity. The transglycosylation in class A comes from the N-terminal domain. The function of the N-terminal in class B PBPs has not been entirely determined, but is thought to interact with proteins involved in cell division and therefore have a role in morphogenesis. PBP2x has an additional domain that consists of two repeated units (Sauvage et al., 2008).These units are together called a PASTA (Penicillin-binding proteins and Serine/Threonine kinase associated) domain (Yeats et al., 2002). This PASTA domain in PBP2x has the believed function of a sensor to know the location of peptidoglycan which has not been cross-linked yet (Maurer et al., 2012), but it is also confirmed to be a β-lactam-binding domain (Yeats et al., 2002).

Transpeptidation is the cross-linking of two peptide strands from adjoining glycan strands. This occurs by cleavage of the D-Ala-D-Ala bond in one peptide, forming an intermediate of enzyme and substrate. This reaction releases the terminal D-Ala and creates the energy needed during the transpeptidation reaction. In total, the whole reaction will form one new peptide bond. This bond is between the fourth D-Ala of the donor and one of the amino acids in the bridge of the acceptor (Scheffers & Pinho, 2005).

As previously mentioned, PBPs transpeptidase activity is inhibited by β-lactam antibiotics. This will interrupt the cell wall by binding covalently to the active site of PBPs. Since these proteins are involved in peptidoglycan synthesis, the formation of a new cell wall will be disrupted when the penicillin binds covalently. This leads to disruption of the cell wall and eventually lysis of the cell (Georgopapadakou et al., 1980). The penicillin will attach to the transpeptidase domain of PBPs (Bycroft et al., 1985). β-lactams can do that because they mimic the D-Ala-D-Ala peptide both structurally and chemically, which the transpeptidase domain in PBPs will bind to. The

hydrolyzation of the complex made up of β-lactam antibiotics and the transpeptidase domain of PBPs, will be hydrolyzed slowly. Hence, this prevents any further reactions from taking place in the bound PBP. The structure of the dipeptide N-Acyl-D-Alanyl-D-Alanine and the β-lactam share the same negative electrostatic potential regions, which is indicated in Figure 4 by arcs (Zapun et al., 2008a).

The complex formed by β-lactam antibiotics and the transpeptidase domain of PBPs resembles the mechanism of the first step in transpeptidation (N. Georgopapadakou et al., 1977; Tipper & Strominger, 1965). When the β-lactam ring is open, the transpeptidase serine can perform a nucleophilic attack on the β-lactam ring (Ehmann et al., 2012).

These drugs got their name because of the 4-membered β-lactam ring in the middle of the molecule (Figure 4). The ring is attached to eighter a five- or six-membered heterocyclic ring. That ring is eighter saturated or not. How chemically reactive the β-lactam ring is will be based primarily on what kind of ring it is attached to (Dalhoff et al., 2006). β-lactam antibiotics are categorized into subclasses. The subclasses are divided based on the variety of the second ring attached (Bycroft & Shute, 1985). Cephalosporins are related to penicillin structurally and consist of a β-lactam ring with a six-membered ring attached to (Hsieh & Ho, 1975).

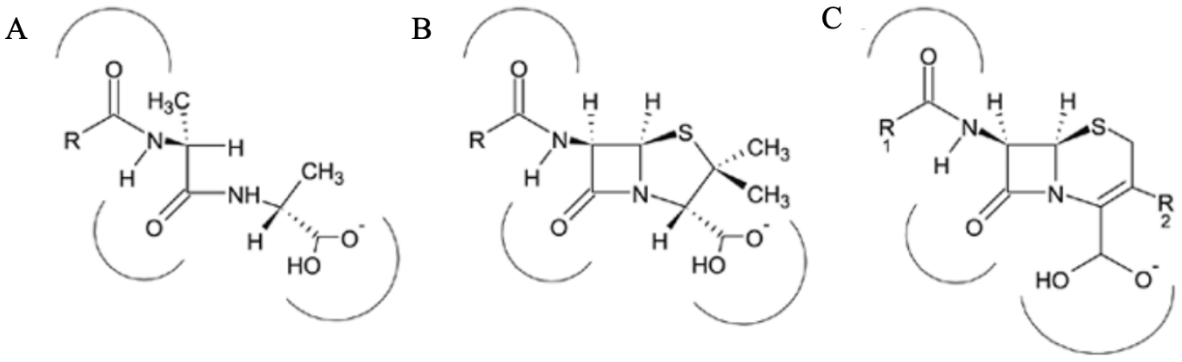

Figure 4 Comparison of the shape of A) the stem peptide D-Ala-D-Ala in peptidoglycan and the structure of B) penicillin and C) cephalosporins. The β-lactam ring is in the middle of the molecules in B) and C). Figure from Zapun et al., 2008a.

1.4 The difference between septal and peripheral cell wall synthesis in *S. pneumoniae*

S. pneumoniae is an oval-shaped cocci resulting from the combined activity of the divisome (septation) and the elongasome (cell elongation) (Higgins & Shockman, 1976; Zapun, Vernet, et al., 2008b). The activity of these peptidoglycan synthesizing multi-protein complexes is strictly regulated and coordinated during cell division, involving numerous proteins (Figures 5B and 6) (Briggs et al., 2021). The following two sections outline the basic principles of how the divisome and elongasome work.

1.4.1 The divisome synthesizes the septal cell wall

An essential protein in the divisome is the tubulin homolog FtsZ (Löwe, 1998). The role of FtsZ is to polymerize into fibers that act as a scaffold for the peptidoglycan synthesis machinery. The FtsZ monomers polymerize at one end of the FtsZ fiber and dissociate at the other ends, known as FtsZ treadmilling. The FtsZ treadmilling drives the processive movement of the divisome in circumferential movements perpendicular to the cell's long-axis (McCausland et al., 2021).

As the division begins, parts of FtsZ and other proteins will move toward the equatorial regions of the cell, where the two daughter cells will form. The proteins are being recruited there by MapZ. MapZ does this recruitment by creating a ring structure around the middle of the cell and separating when the cell is elongated. This is called the MapZ-ring (figure 5 A). MapZ will, after this, position the FtsZ-ring by directly interacting with FtsZ (Fleurie et al., 2014). MapZ is a bitopic protein. This membrane protein binds its C-terminal domain to the extracellular peptidoglycan layer and its N-terminus to FtsZ in the cytoplasm. When division starts, MapZ creates the MapZ-ring in the middle of the cell and splits it into two rings so one can enter each daughter cell (Fleurie et al., 2014). How MapZ recognizes the center of the cell is yet to be determined. Still, it is thought to involve recognition of a particular cell wall structure found at mid-cell, most probably derived from the previous division event (Briggs et al., 2021).

When the last components of the divisome are assembled (Figure 5 B), the cell needs to begin the production of more peptidoglycan. In the divisome, this is performed by the FtsW/PBP2x complex, which synthesizes the septal cross-wall that separates the two daughter cells (Morlot 2003, Noirclerk, in vitro…, berg 2014). This is done by FtsW creating the glycan strands and PBP2x creating the cross-linking between the peptides (Berg et al., 2014).

The septal cross-wall must be cleaved down the middle to separate the daughter cells. This is performed by the PcsB/FtsE/FtsX complex. PcsB is an extracellular cell wall hydrolase that interacts with the membrane protein FtsX. FtsE is a cytoplasmic ATPase. FtsE will hydrolyze ATP upon an unknown signal to induce a conformational change in FtsX. This will, in turn, lead to the release of the catalytic domain of PcsB. PcsB is placed in the middle of the cross-wall, which then is cleaved (Bartual et al., 2014).

LytB is a peptidoglycan hydrolase responsible for physically separating the two daughter cells after the separation done by the PscB/FtsE/FtsX complex is complete. The daughter cells will only be attached via a thin cell wall filament, which will be cut by LytB (García et al., 1999). In addition, it also cleaves the β -1,4 - glycosidic bond between GlcNAc and MurNAc (De Las Rivas et al., 2002).

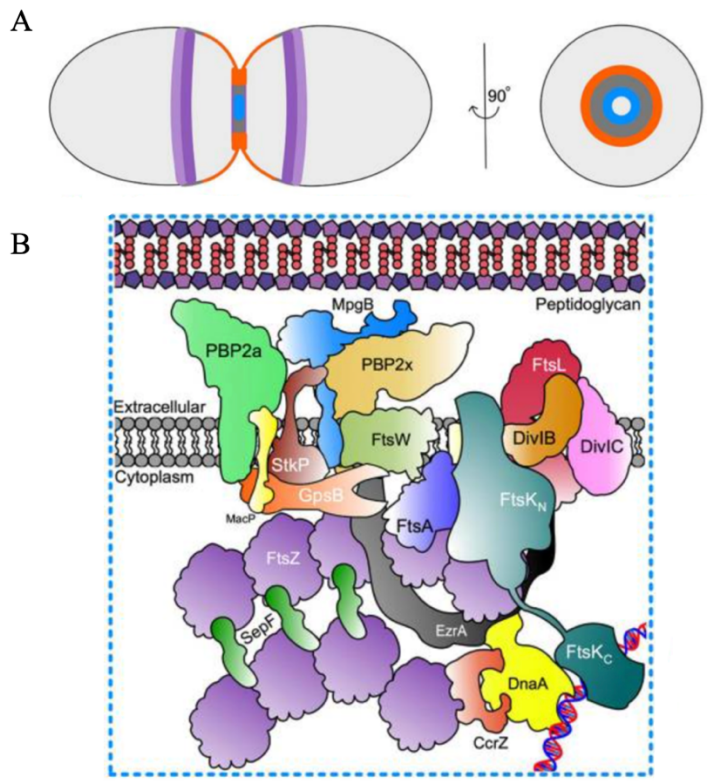

Figure 5 The FtsZ-ring and the MapZ-ring are active in the septal peptidoglycan synthesis in *S. pneumonia*. Their position in the cell during cell division are shown in A). The FtsZ-ring is shown in dark purple, and the MapZ-ring is shown in light purple. The septal cell wall is shown in blue, and the peripheral cell wall is indicated in orange. Some of the proteins in the divisome involved in the septal peptidoglycan synthesis are shown in B). For functions of some of the proteins and information about peptidoglycan synthesis, see the text, as well as 1.2 and 1.3. Figure modified from Briggs et al., 2021.

1.4.2 The elongasome synthesizes the peripheral cell wall

The elongasome is also guided by FtsZ in a circular motion on either side of the divisome. After the elongasome has been positioned correctly in the cell wall, the RodA/PBP2b complex is responsible for the peptidoglycan synthesis. This is important for the cell's ability to elongate (Henriques et al., 1998).

Two of the proteins in the elongasome are MreC and MreD. The function of both MreC and MreD has yet to be entirely determined (Figure 6) (Wachi et al., 1989). MreC has three domains where the first is an amino-terminal tail located in the cytoplasm, the second one is a membrane domain, and the third domain is a coiled-coil domain which is used to create MreC dimers. This domain is found extracellularly (Van Den Ent et al., 2006). MreD has five hydrophobic transmembrane domains spanning the membrane (Leaver & Errington, 2005). MreCD has been found to direct the peripheral synthesis of peptidoglycan and control where PBP1a is in the cell and how active it is (Land & Winkler, 2011). In addition, PBP1a has the role of producing new glycan strands for the peptidoglycan synthesis (Tsui et al., 2016).

When cell division starts, PBP2b is found in the outer ring of the peripheral peptidoglycan synthesis complex (Tsui et al., 2014). PBP2b is a transpeptidase and needs a transglycosylase to synthesize peptidoglycan. PBP2b creates a complex with the transglycosylase RodA to perform the peripheral synthesis of peptidoglycan (Henriques et al., 1998). RodA will polymerize lipid II into glycan strands, and PBP2b will cross-link the new glycan strands to existing strands in the peptidoglycan layer of the cell wall (Sjodt et al., 2020). RodA is a glycosyltransferase in the SEDS family. This protein works with PBP2b to synthesize new peptidoglycan during cell division (Gérard et al., 2002). In *S. pneumoniae*, the complex RodA/PBP2b is a part of the “Rod” complex in the elongasome. This complex also consists of proteins like MreC, MreD, and RodZ. RodA is an essential protein for pneumococci (Land & Winkler, 2011). It has the same function as FtsW, but RodA is in the elongasome, while FtsW is in the divisome (Gérard et al., 2002).

StkP is a Serin/Threonine protein kinase that regulates peptidoglycan synthesis (Beilharz et al., 2012; Fleurie et al., 2012). StkP interacts with several proteins involved in cell division and peptidoglycan synthesis, which leads them to become phosphorylated (Fenton et al., 2018; Nováková et al., 2005; Sasková et al., 2007). Studies have shown that StkP is vital in regulating cell wall synthesis. It also controls that the septum is closed correctly. StkP signals information

about the status of the cell to proteins involved in the division of the cell. It works as a regulator regarding timing in the cell division process. Because of its many roles during cell division, StkP is active during both the septal and the peripheral cell division (Beilharz et al., 2012; Fleurie et al., 2012).

EloR is one of the proteins phosphorylated and activated by StkP. This phosphorylation is essential for the cell (Stamsås et al., 2017). EloR is made up of three domains. The first is on the N-terminal and is a Jag domain, the second is a KH-II domain, and the last is at the C-terminal and is an R3H domain (Grishin, 1998; Valverde et al., 2008; A. Winther et al., 2019). This protein does not have a membrane-bound segment. EloR is in a complex with KhpA. If this complex no longer works in a cell, it loses shape and becomes shorter. This is consistent with what the loss of the elongasome function indicates. The cell will no longer depend on the PBP2b/RodA complex (see below). It is known that EloR is located in the midcell, but it is not yet known what causes EloR to migrate there (Stamsås et al., 2017). Point mutations in *eloR* leading to inactivation of the domain binding the RNA suggest that the phosphorylation done by StkP leads to an unbound RNA being released. It is unknown how this leads to the elongation of the cell (A. R. Winther et al., 2021).

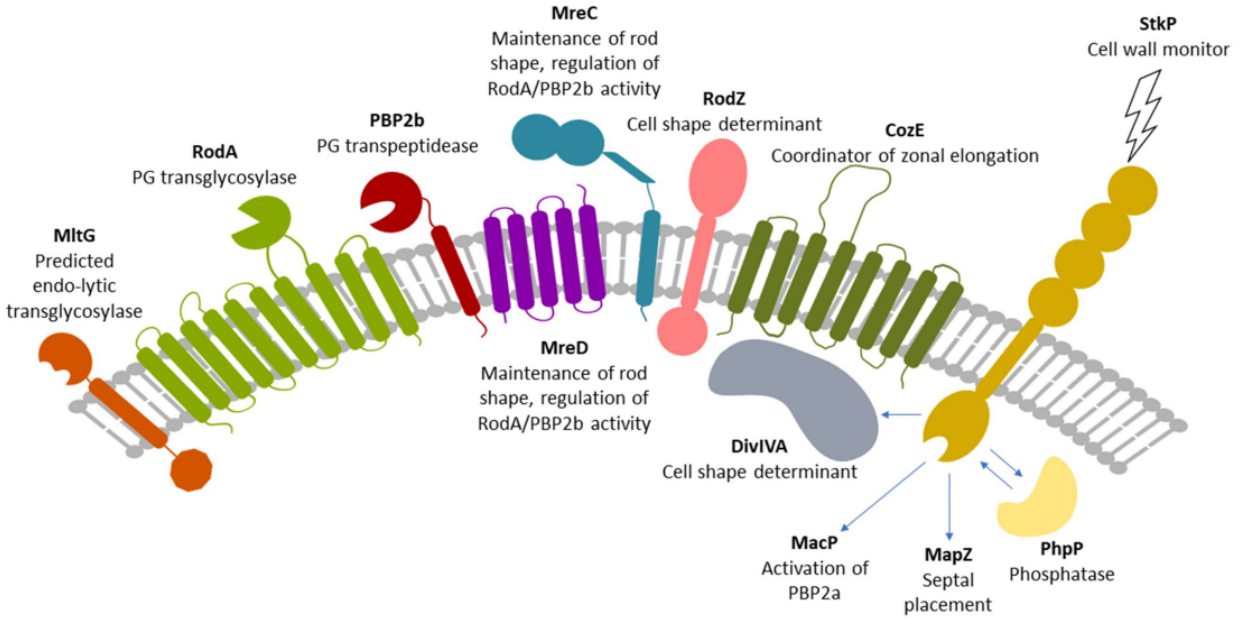

Figure 6 The division complex elongasome in *S. pneumoniae* and the relationships between some of the involved proteins. The elongasome is responsible for the peripheral peptidoglycan synthesis. For functions of the proteins and information about peptidoglycan synthesis, see the text, as well as 1.2 and 1.3. Figure from Winther, 2020.

1.5 Natural competence – the pneumococcal way to acquire new genetic traits

S. pneumoniae was the first bacteria to be confirmed to have the ability to undergo natural transformation (Griffith, 1928). Pneumococci are incredibly adaptable because of their ability to experience natural transformation (Figure 7). This ability in pneumococci is what gives rise to β-lactam resistance (Johnsborg et al., 2007). To do natural transformation, *S. pneumoniae* induces a set of genes that brings the cell into a physiological state known as the competent state. During competence, pneumococci can take up extracellular DNA (Tomasz, 1966). If the DNA is homologous to its genomic DNA, the transformed DNA can be incorporated into the recipient cells' genome via homologous recombination. Incorporating DNA into the recipients genome enables the cell to acquire new traits to handle its environment better, which leads to greater diversity among the bacteria (Feil & Spratt, 2001; Soucy et al., 2015).

Competence in *S. pneumoniae* is regulated by a quorum-sensing-based system encoded by the *comCDE* genes (Håvarstein et al., 1996). The *comC* gene encodes for a pre-peptide secreted by the ComAB transporter. During export, the N-terminal signal sequence of ComC is cleaved off to

produce a mature peptide of 17 amino acids, called the competence stimulating peptide (CSP) (Håvarstein et al., 1995). ComD is a histidine kinase membrane receptor and ComE is the cognate response regulator. ComD works as the receptor for CSP. When CSP binds to ComD, it autophosphorylates the receptor. The phosphate group is transferred from ComD to ComE (Håvarstein et al., 1996; Straume et al., 2014). When ComE gets phosphorylated, it induces the transcription of early competence genes, including the *comCDE* genes (Boudes et al., 2014; S. N. Peterson et al., 2004) (Straume et al., 2014). This results in a positive feedback loop (Ween et al., 1999). This loop is what induces the competent state. It will also cause the extracellular concentration of CSP to increase. The produced CSP can induce competence in nearby cells spreading the signal rapidly through the population. (Håvarstein et al., 1995)

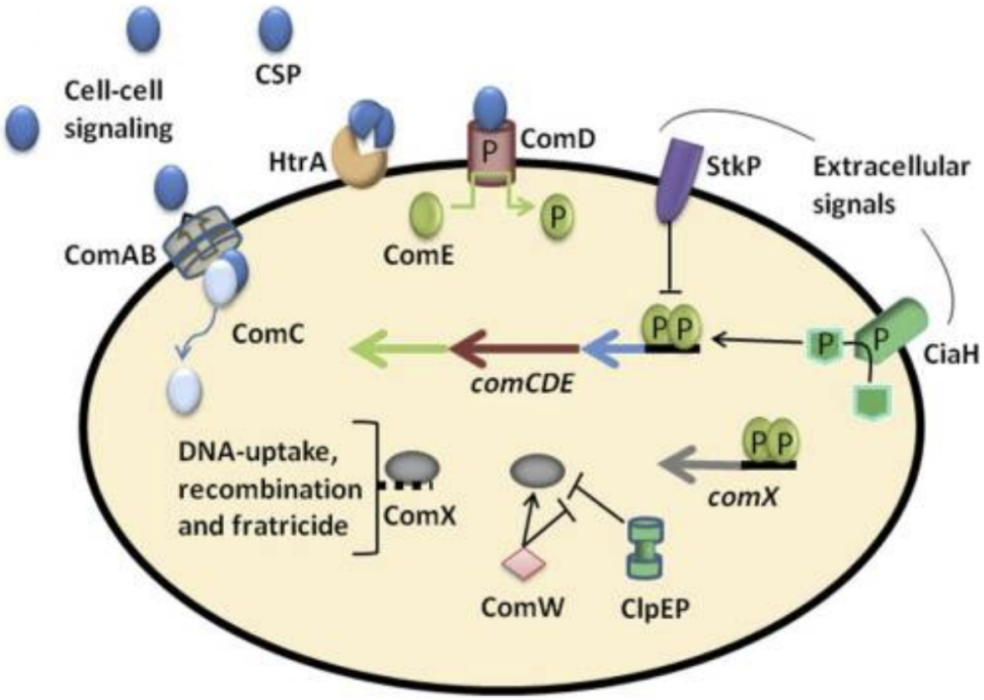

Figure 7 An illustration of natural transformation and competence regulation in *S. penumoniae*. Extracellular signals in the form of competence-stimulating peptides (CSP) lead to the activation of a competent state in *S. pneumoniae*. *S. pneumoniae* uses the regulatory system ComCDE and the ABC transporter ComAB to regulate its competent state. When this is activated, the cell is competent and can take up naked extracellular DNA and incorporate the DNA into its genome by homolog recombination. When the concentration of CSP reaches a threshold concentration, the cells induce fratricide, which is when competent cells excrete enzymes that will lyse non-competent cells nearby. This enables the competent cells to take up genes from the lysed cells in their environment. See the text for more information. Figure modified from Berg et al., 2012.

Along with the *comABCDE* genes, the genes encoding ComX are also a part of the early genes (Peterson et al., 2000). ComX will function as a sigma factor which will begin the transcription of genes used later in competence induction (Campbell et al., 1998; Lee & Morrison, 1999). These genes are called late genes and consist of about 80 genes. The late genes are involved in the uptake of DNA and homologous recombination of DNA into the cell's genome (Peterson et al., 2000; Straume et al., 2014). When the cells decrease the competent state, this is primarily facilitated by DprA, one of the 80 late competence genes induced by ComX (Lee & Morrison, 1999; Mortier-Barrière et al., 2007). This decrease in competence state is caused by an interaction between DprA and ComE, blocking the transcription from ComE. This will result in the cell slowly exiting the competent state (Quevillon-Cheruel et al., 2012).

Natural transformation is the primary driver of spreading antibiotic resistance genes among pneumococci. Since pneumococci can undergo a natural transformation, they are susceptible to the uptake of resistance genes, which can give rise to a resistance towards β-lactams (Johnsborg et al., 2007). The surfacing of pneumococci resistant to a new generation of penicillin will most likely be powered by transformations (Lattar et al., 2018).

1.6 Penicillin resistance in pneumococci

The first choice in the treatment of community-acquired pneumonia has, since the late 1940s, been β-lactam antibiotics (Cornick & Bentley, 2012). However, increasing numbers of penicillin-resistant isolates are registered in the healthcare systems. Pneumococci do not express β-lactamases, enzymes that catalyze the hydrolysis of the ring in the β-lactams. This leaves the antibiotic inactive (Bycroft & Shute, 1985). Instead, the strains resistant against β-lactams have altered their PBPs to make them challenging to acylate by β-lactams (Hakenbeck et al., 1980; Zighelboim & Tomasz, 1980). The resistance towards penicillin has been shown to involve different alterations in PBP2x, PBP2b, and PBP1a. The PBPs become altered by recombining genes between closely related pneumococci so that the cells acquire new traits. This is easily done by *S. pneumoniae*, a naturally competent bacterium (Grebe & Hakenbeck, 1996; Nagai et al., 2002). The reason some pneumococci have low-affinity PBPs can be both the result of point mutations and the uptake of low-affinity genes through transformation and homolog recombination (McGee et al., 2001).

As described in previous sections, the pneumococcal cell wall consists of both branched and linear muropeptides. Analyses of strains resistant towards β-lactams have shown that these often have an increase in branched muropeptides. Ongoing studies have shown that incorporating branched muropeptides into the peptidoglycan layer is essential to keep the resistance level of the cell. Conversely, if the branching decreases, so does the resistance towards penicillin (see 1.7 for more information).

1.7 Background and Aim of Study

So far, researchers have yet to look much into which of the PBP(s) are essential for the increased incorporation of branched muropeptides in penicillin-resistant pneumococci. However, previous work conducted by former master's student Maria Victoria Heggenhougen in 2019 in the Molecular Microbiology (MolMik) group at NMBU, indicated the addition of low-affinity PBP2b increased the relative amount of branched muropeptides in the cell wall. Additionally, a separate study by Berg et al. in 2013 found that depletion of PBP2b in *S. pneumoniae* led to a higher ratio of branched muropeptides in the cell wall. Considering this, recent results from Ph.D. student Ragnhild Sødal Gjennestad at the MolMik group indicate that PBP2b depends on branched structured muropeptides to function correctly.

Ragnhild Sødal Gjennestad made a *S. penumoniae* strain, which is resistant to penicillin and depends on branched muropeptides to maintain its resistance (Figure 8, RSG77). Previous results indicate that when the bacteria start expressing a low-affinity PBP2b, it becomes dependent on branching. If this is because this version of PBP2b prefers to cross-link in a branched manner or because it has a lower affinity, it can cause other PBPs to take over, for example, the class A PBPs, and these can prefer branching. To test this, *pbp2b* and all class A PBPs were knocked out separately, and the cell wall composition was analyzed.

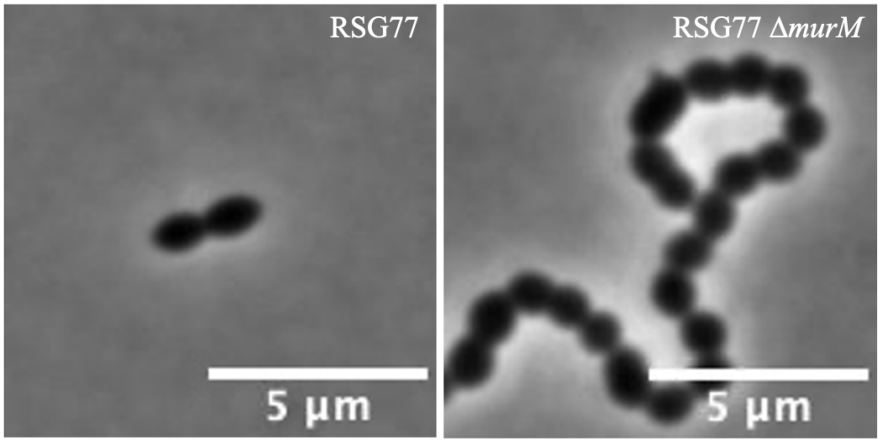

Figure 8 *murM* deletion caused a short and chained morphology in the strain RSG77. Cells were grown in C-medium until OD~0,4 and observed utilizing phase contrast microscopy (1000x magnification). The strain RSG77 is derived from a penicillin-sensitive *S. pneumoniae* R6 and serial transformed and selected based on increasing penicillin G concentration. Whole genome sequencing and experimental data revealed that mutations in a specific part of *pbp2b* are necessary for resistance to drop in a *murM* deletion mutant. Unexpectedly, the *ΔmurM* mutant (right image) also displayed a morphology like when *pbp2b* is depleted.

Considering the research conducted at the MolMik group mentioned above, it is highly interesting to investigate the contributions of the different PBPs to a branched cell wall. Since a branched structured cell wall is one of the main characteristics to penicillin-resistant pneumococcal isolates, the significance of finding its main contributor is of high importance. The results from the MolMik group strongly indicate that branched muropeptides are essential for the elongasome. Further, the results conducted by Heggenhougen in 2019 show that low-affinity PBP2b could be a key for increased branching. Therefore, this study aims to investigate the effect of low-affinity PBP2bs in incorporating branched muropeptides and attempt to uncover any of its possible collaborators in the matter.

2 Materials and methods

2.1 Strains

Table 1 *S. pneumoniae* strains used in this study, including a description of the genotype and characteristics of each strain.

Strain	Genotype and characteristics	Reference
DS507	RH425 *ΔmreC::*janus, Kan^R	Dr. Daniel Straume
SPH465	RH425 C547T substitution in *mreC*	Stamsås et al., 2017
SPH156	Δ*pbp2b*::janus, PcomX:*pbp2b*, Kan^R	Berg et al., 2013
KHB104	RH20 *Δpbp1a::*janus Kan^R	Dr. Kari Helene Berg
KHB105	RH20 *Δpbp2a::*janus Kan^R	Dr. Kari Helene Berg
KHB106	RH20 *Δpbp1b::*janus Kan^R	Dr. Kari Helene Berg
AW73	RH425 Δ*mreC*, Kan^R	Dr. Anja Ruud Winther
RH425	R704, but streptomycin resistant, Ery^R, Sm^R	Johnsborg & Håvarstein, 2009
RSG77	RSG46 transformed with gDNA from Uo5	Ragnhild Sødal Gjennestad
RSG171	RSG77, but *eloR::DEL*, Sm^R	Ragnhild Sødal Gjennestad
RSG173	Pen6 med *rpsL*(RH425) --> Sm^R	Ragnhild Sødal Gjennestad
RSG189	Pen6 but *eloR::DEL*	Ragnhild Sødal Gjennestad

Table 2 *S. pneumoniae* strains made in this study, including a description of the genotype and characteristics of each strain.

Strain	Genotype and characteristics	Reference
JM1	RSG77 Δ*mreC*::janus, Kan^R	This work
JM2	RSG77 Δ*pbp1b*::janus, Kan^R	This work
JM3	RSG77 Δ*pbp1a*::janus, Kan^R	This work
JM4	RSG77 Δ*pbp2a*::janus, Kan^R	This work
JM5	RSG173(Pen6) Δ*pbp1b*::janus, Kan^R	This work
JM6	RSG173(Pen6) Δ*pbp2a*::janus, Kan^R	This work
JM7	RSG77 Δjanus::*mreC**, Sm^R	This work
JM8	RSG77 Δ*eloR*:DEL Δ*pbp2b*::janus, Kan^R	This work
JM9	RSG173(Pen6) Δ*pbp1a*::janus, Kan^R	This work
JM10	RSG77 Δjanus::*mreC** Δ*pbp2b*::janus, Kan^R	This work
JM11	RSG173(Pen6) Δ*mreC*::janus, Kan^R	This work
JM12	RSG173(Pen6) Δ*eloR*::DEL Δ*pbp2b*::janus, Kan^R	This work
JM13	RSG173(Pen6) Δjanus::*mreC**, Sm^R	This work
JM14	RSG173(Pen6) Δjanus::*mreC** Δ*pbp2b*::janus, Kan^R	This work

2.2 Primers

Table 3 List of all primers used in this study. Included is a short description of the primers as well as the nucleotide sequence.

Name of primer	Description	Sequence 5´ à 3´	Reference
GS223	853 bp upstream *mreC*	ATGGATAGTATGATTTTGGGG	Straume et al., 2017
GS224	998 bm downstream *mreC*	CTACGAGCTTGTTTTTCCAAC	Straume et al., 2017
Janus F	Janus, F	GTTTGATTTTTAATGGATAAT GTG	
KHB129	*pbp2b*-upstream fragment (ca 1000 bp upstream)	CGATAAAGAAGAGCATAGGA AG	Berg et al., 2013
KHB132	*pbp2b*-downstream fragment (ca 1000 bp downstream)	TCCCAATCAATGGTTTCATTG G	Berg et al., 2013
KHB135	Sequencing primer, ca 200 upstream for *pbp2b*	ATGAGTCATACTGGAAGACTA G	Dr. Kari Helene Berg
MTS1F	1000 bp upstream *pbp2a*	GCACAACTTGTTCGTACTCTT G	Marita Terese Sæther
MTS4R	900 bp downstream *pbp2a*	AGGTTTACTTCTGCAACTGTG	Marita Terese Sæther
MTS5F	1000 bp upstream *pbp1a*	CCTTGTGTTCATAGCGAGG	Marita Terese Sæther
MTS8R	1000 bp downstream *pbp1a*	AAAACGGCTTTGGTAGCAGAT G	Marita Terese Sæther
MTS9F	1100 bp upstream *pbp1b*	GCCTGTACTTGGTAGTTTGG	Marita Terese Sæther
MTS12R	1000 bp downstream *pbp1b*	GACTATTCCAGTATAGCAC	Marita Terese Sæther
RSG48	1600bp downstream *pbp2b*	GACGCATGACAGCCACCAC	Ragnhild Sødal Gjennestad
RSG49	1500bp downstream *pbp1a*.	GCAGGTAAGACCTACCGTG	Ragnhild Sødal Gjennestad
RSG50	1500bp upstream *pbp1a*.	GCCGCTTCAAGGGGTTCTG	Ragnhild Sødal Gjennestad
RSG51	1500bp upstream *mreC*.	GTGCCAAGTCAAGGGAGTG	Ragnhild Sødal Gjennestad
RSG52	1400bp downstream *mreC*.	CACGGACAGGTGCTGCTG	Ragnhild Sødal Gjennestad

2.3 Peptide

Table 4 The peptide used in this study. Included is the sequence of amino acids and the concentration of the stock solution.

Peptide	**Sequence of amino acids**	**Concentration of stock solution**	**Supplier**
CSP-1	N-EMRLSKFFRDFILQRKK-C	100 µg/mL	Research genetics Inc.

2.4 Enzymes, different nucleotides, and molecular weight marker

Table 5 List of the enzymes, nucleotides, and molecular weight markers used in this study.

Name	Concentration of stock solution	Product number	Supplier
1 kb DNA ladder	500 µg/mL		Merck
dNTPs (dATP, dGTP, dCTP, dTTP)	10 mM	4026/4027/4028/4029	TaKaRa
Phusion®, High-Fidelity DNA polymerase	2 U/µL	01341935	Thermo Scientific
REDtaq® 2x Master Mix		5200300-1250	VWR Life Science
DNase	10 mg/mL	120M7016V	Sigma
RNase	10 mg/mL	061M15701V	Sigma
Trypsin	1.6 U/µg	93615	Fluka
5x Phusion® High-Fidelity buffer		F-518	Thermo-Fisher Scientific
LytA	1.7 mg/mL		Isolated by Dr. Daniel Straume

2.5 Antibiotics

Table 6 List of the antibiotics used in this study.

Antibiotic	Concentration of stock solution	Product number	Supplier
Kanamycin	100 mg/mL	SLBW6738	Sigma Aldrich
Streptomycin	100 mg/mL	SLBP6412V	Sigma Aldrich
Bocillin-FL	25 µM	B13233	Life technologies

2.6 Kit

Table 7 The kit used in this study.

Name	**Purpose**	**Product number**	**Supplier**
NucleoSpin® Gel and PCR Clean-up	Extraction of DNA from agarose gel	740609.250	Macherey-Nagel

2.7 Chemicals

Table 8 List of all chemicals used in this study. Included in the list is chemical formula and product number.

Chemical	Formula	Product number	Supplier
Acetic acid	CH_3COOH	1.00063.1011	Merck
Acetone	CH_3COCH_3	1.00014.2500	Merck KGaA
Acetonitrile	HC_3CN	34998	Sigma-Aldrich
Acrylamide	C_3H_5NO	79-06-1	Sigma-Aldrich
Adenosine	$C_{10}H_{13}N_5O_4$	01890	Sigma-Aldrich
Agarose		20767.298	VWR Chemicals
Ammonium persulfate	$(NH_4)_2S_2O_8$	7727-54-0	BioRad
Bacto TM Todd Hewitt		249240	Becton, Dickinson and Company
BactoTM Casitone		225930	Becton, Dickinson, and Company
B-merkaptoetanol	C_2H_6OS	M6250	Sigma-Aldrich
Biotine	$C_{10}H_{16}N_2O_3S$	19606	Sigma-Aldrich, Fluka
Bisakrylamide	$C_8H_{12}N_2O_4$	868-63-3	Merck
Bovine Serum Albumin		A7906	Sigma-Aldrich
Bromophenol blue	$C_{19}H_9Br_4O_5SNa$	B-8026	Sigma-Aldrich
Calcium chloride anhydride	$CaCl_2$	21075	Sigma-Aldrich, Fluka
Calcium pantothenate	$C_{18}H_{32}CaN_2O_{10}$	C8731	Sigma-Aldrich
Choline chloride	$C_6H_{14}NO \cdot Cl$	C1879	Sigma-Aldrich
Copper sulphate pentahydrate	$CuSO_4 \cdot 5H_2O$	61240	Sigma-Aldrich, Fluka
Di-sodium hydrogen phosphate	Na_2HPO_4	1.06580.1000	Merck
Dipotassium phosphate	K_2HPO_4	1.05104.1000	Merck KGaA
EDTA	$C_{10}H_{14}N_2Na_2O_8 \cdot 2H_2O$	1.08418	Merck
Glass beads		G4649	Sigma-Aldrich
Glucose 20%	$C_6H_{12}O_6$	G7021	Sigma-Aldrich
Glutamin	$H_2NCOCH_2CH_2CH(NH_2)CO_2H$	49419	Sigma-Aldrich, Fluka
Glycerol 50%	$C_3H_8O_3$	49781	Sigma-Aldrich
Glycine	$C_2H_5NO_2$	G7126	Sigma-Aldrich
Hydrochloric acid, 37%	HCl	7647-01-0	Acros Organics BVBA
Iron(II)sulphate heptahydrate	FeSO4 · 7H2O	44970	Sigma-Aldrich, Fluka
L-Asparagine monohydrate	$C_4H_8N_2O_3 \cdot H_2O$	A8381	Sigma-Aldrich
L-cysteine hydrochloride monohydrate	$C_3H_7NO_2S \cdot HCl \cdot H_2O$	30130	Sigma-Aldrich, Fluka
L-tryptophan	$C_{11}H_{12}N_2O_2$	93660	Sigma-Aldrich, Fluka
Lithium chloride	LiCl	62476	Sigma-Aldrich
Magnesium chloride hexahydrate	$ClMg \cdot 6H_2O$	M2393	Sigma-Aldrich
Manganese (II) chloride	$MnCl_2$	416479	Sigma-Aldrich

Manganese(II)chloride tetrahydrate	$MnCl_2 \cdot 4H_2O$	31422	Riedel-de Haën
Monosodium phosphate	NaH_2PO_4		
N,N,N,N-tetramethyl ethylene diamine (TEMED)	$C_6H_{16}N_2$	T9281	Sigma-Aldrich
Nicotinic acid	$C_6H_5NO_2$	72309	Sigma-Aldrich, Fluka
peqGREEN		PEQL37-501	Saveen Werner
potassium chloride	KCl	1.04936.1000	Merck KGaA
potassium dyhydrogen phosphate	KH_2PO_4	1.04873.1000	Merck KGaA
Pyrodoxine hydrochloride	$C_8H_{11}NO_3 \cdot HCl$	95180	Sigma-Aldrich, Fluka
Riboflavin	$C_{17}H_{20}N_4O_6$	R-7649	Sigma-Aldrich
SDS	$C_{12}H_{25}NaO_4S$	1.13760.1000	Merck KGaA
Sodium acetate	$C_2H_3O_2Na$	S8750	Sigma-Aldrich
sodium chloride	NaCl	27810.295	VWR Chemicals
Sodium chloride	NaCl	27810.295	VWR
Sodium pyruvate	$C_3H_3NaO_3$	P8574	Sigma-Aldrich
Sucrose	$C_{12}H_{22}O_{11}$	84100	Sigma-Aldrich
Thiamine hydroxychloride	$C_{12}H_{17}ClN_4OS \cdot HCl$	T4625	Sigma-Aldrich
Trifluoracetic acid (TFA)	CF_3COOH	302031	Sigma-Aldrich
Trisma® base	$NH_2C(CH_2OH)_3$	T1503	Sigma-Aldrich
Triton-X-100	$C_{14}H_{22}O(C_2H_4O)n$ (n = 9-10)	9002-93-1	Sigma-Aldrich
Trypsin from hog pancreas		93615	Sigma-Aldrich, Fluka
Uridine	$C_9H_{12}N_2O_6$	U6381	Sigma-Aldrich
Yeast extract			
Zinc sulphate heptahydrate	$ZnSO_4 \cdot 7H_2O$	96500	Sigma-Aldrich, Fluka

2.8 Equipment

Table 9 List of all special equipment used in this study. Regular laboratory equipment is not listed.

Equipment	Model	Supplier
FastPrep	FastPrep® - 24	MP^{TM} Biomedicals
Gel imager	GelDoc TM XR+	BioRad
Gel imager II	Azure Imager c400	Azure biosystems
HPLC machine	Dionex UltiMate 3000	Thermo-Fisher Scientific
HPLC column		Grace Davison Discovery Scientific
Microscope	LSM700	Zeiss
Spectrophotometer	NanoDrop 2000	Thermo-Fisher Scientific
PCR machine	ProFlex PCR systems	Applied Biosystems by Life Technologies
Vacuum pump connected to a condensation trap	Gel pump GP100	Savant

2.9 Recipes for growth mediums and general buffers

2.9.1 Solutions used when making C-medium

Yeast extract solution

40 g yeast extract

360 mL dH_2O

6 mL 37% HCl

16 g active coal

The mixture was stirred for 10 minutes and then incubated at 4°C for 2 hours. After the incubation, the solution was filtered through a column of celite overnight. The pH was adjusted to 7.8 with NaOH. The final volume was adjusted to 400 mL with dH_2O. The solution was sterile filtered and stored in 4 mL aliquots at -80°C.

ADAMS I

150 µL 0.5 mg/mL Biotine

75 mg Nicotinic acid

87.5 mg Pyridoxine hydrochloride (4°C)

300 mg Calcium pantothenate (4°C)

80 mg Thiamine hydrochloride

35 mg Riboflavin

The pH was adjusted to 7.0. The volume was adjusted to 0.5 L with dH_2O. The solution was sterile-filtered and stored at 4°C.

ADAMS II

500 mg Iron(II)sulphate heptahydrate

500 mg Copper sulfate pentahydrate

500 mg Zinc sulfate heptahydrate

200 mg Mangan(II)chloride tetrahydrate

10 mL 37% HCl

The volume was adjusted to 100 mL with dH_2O. The solution was sterile-filtered and stored at 4°C.

ADAMS III

128 mL ADAMS I

3.2 mL 10X ADAMS II

1.6 g Asparagine monohydrate

160 mg Choline

0.4 g Calcium chlorine anhydride

16 g Magnesium chloride hexahydrate

The pH was adjusted to 7.6. The volume was adjusted to 800 mL with dH_2O. The solution was sterile-filtered and stored at 4°C.

Pre-C-medium

The following components were added, and dH_2O was added to make up a final volume of 4 L:

45 mg L-Cysteine Hydrochloride Monohydrate

8 g Sodium acetate

20 g Bacto™ Casitone, Pancreatic Digest of Casein

24 mg L-Tryptophan

34 g Dipotassium phosphate

The solution was divided into 450 mL batches and autoclaved before storage at room temperature.

C-medium

To 150 mL pre-C-medium, the following components were added:

150 µL $MnCl_2$ 0,4 mM

1.5 mL glucose 20% (w/v)

3.75 mL ADAMS III

110 µL glutamine 3% (w/v)

2.25 mL Na pyruvate 2% (w/v)

95 µL sucrose 1,5 M

1.5 mL uridine adenosine 2 mg/mL

1.5 mL albumin/BSA 8%

3.75 mL yeast extract

The solution was sterile-filtered before use. C-medium was made new every day and stored at 4°C.

2.9.2 Petri dishes containing agar and antibiotics for growing transformants

TH agar for Petri dishes

To 0.5 L of dH_2O, the following components were added:

15 g Todd Hewitt broth powder (Becton, Dickinson, and Company)

7.5 g agar powder

The solution was autoclaved and cooled slightly before the respective antibiotic was added, and the mixture was poured into Petri dishes. Streptomycin was added for a final concentration of 200 µg/mL, and kanamycin was added for a final concentration of 400 µg/mL.

2.9.3 Buffers and other solutions used for gel electrophoresis

50x Tris-Acetate-EDTA (TAE)

424 g Tris base

57.1 mL Acetic acid

100 mL 0.5 M EDTA at pH 8.0

The volume was adjusted to 1 L with dH_2O.

6x Loading buffer for electrophoresis

- 240 µL 1 M Tris-HCl
- 1 mM EDTA
- 40% sucrose (w/v)
- 0.025% bromophenol blue

48 µL of EDTA, 240 µL of Tris-HCl, and 1.6 g of sucrose were added to an Eppendorf tube, and dH_2O was added to a combined volume of 4 mL. A pipette tip of bromophenol blue was added to the mixture until the color was strong.

1 kb DNA ladder (50 mg/mL)

50 µL 1 kb ladder

200 µL 10x loading buffer

750 µL dH_2O

The solution was mixed and kept at 4°C.

Agarose mixture for gel electrophoresis

For a solution of 1% agarose to water, 4 g of agarose powder was used in 400 mL of 1xTAE buffer. For each gel made, 50 mL of this solution was combined with 1 µL peqGREEN (Saveen Werner) and poured into a mold with added combs to create wells.

2.9.4 Buffers and solutions for SDS-PAGE and bocillin FL gels

100 mM Sodium phosphate buffer, pH = 7.2

6.8 mL Na2HPO4

3.16 mL NaH2PO4

20 mM Sodium phosphate buffer, pH = 7.2, 0.2% Triton-X-100

100 mM Sodium phosphate buffer, pH = 7.2

Triton-X-100

10 mL of the sodium phosphate buffer and 0.1 g of Triton-X-100 were combined with dH_2O, which made up the volume of 50 mL.

10x Tris-glycine running buffer

30 g Tris base (0.25M)

144 g Glycine (1.92 M)

40 mL 20% SDS

The final volume was adjusted with dH_2O to be 1 L.

2x SDS Sample buffer

0.125 M Tris-HCl, pH 6.8

4 % SDS

0.3 M 2% β-2-mercaptoethanol (or 0.2 M DTT)

20 % Glycerol

0.01 % Bromophenol blue

10% polyacrylamide, separation gel, two gels

6.42 mL 30% acrylamide

3.5 mL 2% bisacrylamide

5 mL buffer, pH = 8.8

4.25 mL dH_2O

200 µL 10% SDS

200 µL 10% APS (ammonium persulphate)

10 µL TEMED

After mixing acrylamide, bisacrylamide, buffer, and dH_2O, the solution was degassed for 5 minutes before adding the remaining components. The APS solution was made fresh each time it was used by weighing 0.05 g of APS and mixing it with 500 µL of water.

4% polyacrylamide, stacking gel, two gels

1 mL 30% acrylamide

550 µL 2% bisacrylamide

2.5 mL buffer, pH = 6.8

5.7 mL dH_2O

100 µL bromophenol blue

200 µL 10% SDS

150 µL 10% APS (ammonium persulphate)

10 µL TEMED

After mixing acrylamide, bisacrylamide, buffer, and dH_2O, the solution was degassed for 5 minutes before adding the remaining components. The APS solution was made fresh each time it was used.

2.9.5 Buffers and solutions used for microscopy

PBS solution:

8 g/L sodium chloride

0.2 g/L potassium chloride

1.44 g/L disodium phosphate

0.24 g/L potassium dihydrogen phosphate

pH was adjusted to 7.4. The final volume was adjusted to 1 L.

Agarose for microscopy

25 mL PBS solution

0.3 g agarose

This solution was heated up until the agarose was dissolved. This gives an agarose percentage of 1.2%.

2.9.6 Buffers and solutions used for cell wall isolation

100 mM Na-phosphate buffer pH 7.0 for LytA digestion

57.7 mL 1 M Na_2HPO_4

42.3 mL 1M NaH_2PO_4

The final volume was 100 mL.

100 mM Na-phosphate buffer pH 7.0 for LytA digestion

57.7 mL 1 M Na_2HPO_4

42.3 mL 1M NaH_2PO_4

The final volume was 100 mL.

1 M Tris-HCl buffer

15.15 g of Tris base was dissolved in 100 mL dH_2O. The pH was adjusted using eighter NaOH or HCl.

LytA digestion treatment of pneumococcal cell wall

The following reagent was added to an Eppendorf tube:

100 mM phosphate buffer, pH: 7.0[1]

1 mg cell wall[2]

1.7 mg/mL LytA

All reagents were mixed, and dH2O was added to a final volume of 100 µL.

Due to only a small amount of cell wall being purified for Pen6 Δ*pbp1b*, only 0.2 mg in 0.5 L of C-medium, the 0.2 mg was added, and the final volume for this sample was 50 µL.

[1]For JM2, JM3, JM4, and JM5, the concentration of this buffer was 50 mM. These samples, therefore, had twice the volume of the buffer added. The remaining samples had the concentration of buffer listed here.

[2]Based on how much water was added to make up a final concentration of 20 mg/mL, this volume varied from sample to sample.

2.9.7 HPLC solutions

Buffer A: 0.05% TFA (trifluoracetic acid)

500 µL TFA was added into dH_2O to a final volume of 1 L. This gave a final concentration of TFA of 0.05%.

Buffer B: 0.05% TFA in acetonitrile

125 µL TFA was added into 100% acetonitrile to a final concentration of 250 mL. This gave a final concentration of TFA of 0.05%.

2.10 Growth and storage of *S. pneumoniae*

The strains were grown at 37°C anaerobically. An OxoidTM AnaeroGenTM 3.5 L sachet (Thermo Scientific) was added to the container with the cells plated on agar plates to create the anaerobic conditions. The AnaeroGenTM sachets will react with the oxygen in their surroundings and reduce the level of O_2 available to <1% within 30 minutes. This process also produces CO_2 (Thermo Scientific, 2001).

2.11 Polymerase chain reaction

Polymerase chain reaction (PCR) is a technique used for amplifying a piece of DNA into large numbers of the same DNA (Saiki, Mullis 1987). The PCR instrument is sensitive enough to amplify a DNA sequence from a single cell into an amount that can be further analyzed. PCR can also add on, delete, and modify the template DNA. To amplify a DNA sequence, there must be some prior knowledge of the sequence information available. This is to design primers that will attach optimally to the target sequence. Many methods have also been developed for getting around this problem if knowledge about the sequence is impossible to obtain (Clark et al., 2019).

A DNA template, primers, all four nucleotides, and a DNA polymerase are needed to perform the PCR. The DNA template must contain the target sequence. The sequence of the primers defines the target sequence to be amplified on the template DNA, one upstream and one downstream. DNA polymerase is used to produce new DNA molecules. During the PCR, two primers anneal to their complementary sequences at either end of the target sequence on a denatured piece of the DNA sample. The DNA polymerase will synthesize a complementary strand from the primers. This results in two new strands of DNA. In the following cycles, the newly made DNA strands are denatured, primers are annealed, and the DNA polymerase will attach itself and copy the target regions. This results in multiple copies of the target sequence (Clark et al., 2019). Due to the exponential rate of copies being produced and the number of target sequences that should double each cycle, the number of DNA fragments can reach 100 billion in just a few hours. This enables scientists to start with minimal amounts of DNA molecules and amplify them into large, workable amounts (Mullis, 1990).

2.11.1 Making DNA fragments using Phusion PCR

The Phusion® DNA polymerase was used when the end-product from the PCR was used in transformations. This is because this DNA polymerase has high proofreading, which is essential in transformations. After all, the template being amplified for transformations should not contain any mutations as it can cause the gene to lose its function. All components listed in Table 10 were added to a PCR strip. The Phusion® polymerase was kept in an ice block while working. The Phusion® buffer contains Mg^{2+}, which facilitates optimal polymerase activity. In some PCR mixtures that did not work initially, additional Mg^{2+} was added to aid the reaction. If additional Mg^{2+} was added, this was done by adding 1 µL of Mg^{2+} and 1 µL less water. The amount of each component in the PCR mix is shown in the Table below.

Table 10 List of all reagents and the amount added in the PCR mix used for creating DNA fragments to be used in transformations.

Component	Final concentration/volume
0,5 µL 2U/µL Phusion® High-Fidelity DNA polymerase	0,02 U/ µL
10 µL 5x Phusion® High-Fidelity buffer	1x
2.5 µL 10 µM Primer forward	0.5 µM
2.5 µL 10 µM Primer reverse	0.5 µM
1 µL 10 mM dNTPs	0.2 mM
1 µL template DNA	20-100 ng
32.5 µL dH_2O	
Total volume	50

The settings for the PCR run with Phusion are shown in Table 11. The time of the extension depended on the length of the PCR product. Phusion uses about 30 seconds per 1000 bp. So, if the product were 3000 bp long, the extension time would be 1 minute and 30 seconds.

Table 11 The settings for the PCR run with Phusion® polymerase when making DNA fragments for transformations.

Temperature, ^{O}C	Time, minutes	Stage	Cycles
95	10	Initial denaturation	1
95	0.5	Denaturation	
60	0.5	Annealing	25
72	xx	Extension	
68	3	Final extension	1
4	-		

2.11.2 Screening transformants with RedTaq® using PCR

To screen the transformants, four colonies were picked from plates with kanamycin, and 7-8 colonies were picked from plates with streptomycin. The colonies were picked with a sterile toothpick each. First, the toothpick collected a colony; then, it was dabbed into 10 µL of sterile dH_2O in one well in a PCR strip to leave bacteria in the water and use it for the screening. The toothpick was then dropped into a falcon tube containing 3 mL of C-medium. The falcon tube was placed in a water bath at 37^{O}C to allow the bacteria to grow. When the accuracy of the end-product from the PCR is not very important, like in screening, RedTaq® is used. This is because this DNA polymerase is less accurate than the Phusion® High-Fidelity DNA polymerase.

For the screening with RedTaq®, all components for the PCR mix were combined in an Eppendorf tube, and 10 µL of the mixture was added into each of the four PCR tubes, which already contained the bacteria in 10 of dH_2O. The components and volumes of each component are shown in Table 12.

Table 12 List of all reagents and the amount used in the PCR mix for screening transformants.

Component	Volume, µL
2x RedTaq	40
Primer forward	2.5
Primer reverse	2.5
Total volume	45

The settings for the PCR run with RedTaq® are shown in Table 13. The time of the extension depended on the length of the PCR product. RedTaq® uses about 1 minute per 1000 bp. So, if the product were 2500 bp long, the extension time would be 2 minutes and 30 seconds.

Table 13 The settings used for the PCR run with RedTaq® during screenings of transformants.

Temperature, ^{O}C	Time, minutes	Stage	Cycles
95	10	Initial denaturation	1
95	0.5	Denaturation	
60	0.5	Annealing	25
72	xx	Extension	
68	3	Final extension	1
4	-		

2.12 Gel electrophoresis of the PCR product

Gel electrophoresis is a commonly used technique within molecular biology. This technique is used to separate fragments of DNA or RNA based on their size. This is done by sending a current through a gel in the electrophoresis chamber. Since DNA is a negatively charged molecule, it will move through the gel towards the positive charge. The distance the fragments move through the gel depends on their size (Clark et al., 2019).

The most used type of gel for gel electrophoresis is agarose gel. This gel is optimal for molecules with a similar molecular weight to DNA, which will be between 50-20 000 base pairs. A different gel should be used if the molecule is of a higher or lower molecular weight than this. The agarose gel uses agarose powder from seaweed mixed with a liquid buffer. Upon heating, this creates a clear liquid that will solidify when it is cooled down. The solidified gel contains many tiny pores and cavities filled with water. These pores will slow down the larger molecules since they get caught in the pores. The smaller ones will not get caught as much and will therefore move through the gel faster than the larger ones, and their band will therefore be lower in the gel. DNA fragments of similar size will migrate through the gel at the same speed and emerge in the gel at the same position. A standardized molecular weight size marker, also called a molecular ladder, is used to compare the distance the band has traveled in the gel compared to the size of the fragments in the band. The ladder comprises fragments with a known molecular weight (Clark et al., 2019).

A loading buffer is added to the samples before adding the samples to the gel. This allows better visualization of the sample when pipetting it into the wells, and the glycerol in the loading buffer increases the density of the sample, so it falls to the bottom of the well in the gel. The gel has peqGREEN added to it. This is added so that the bands can be visualized under UV light after the electrophoresis is done (Clark et al., 2019). The bands can be visualized because peqGREEN will fluoresce once bound to DNA and illuminated (Thermo Scientific, 2006).

Gel electrophoresis was used for two things in this experiment. The first thing was to separate the product after the PCR with Phusion so that it could be cut out of the gel as one band and be purified. The second use was to verify the size of the product after screening colonies from the transformations. This was done to ensure the transformants had taken in the DNA fragment.

After the PCR with RedTaq, the solution was pipetted into an agarose gel to undergo electrophoresis and run for about 30 minutes. The bands in the gel were visualized under UV light using a GelDoc TM XR+ (BoiRad). The size of the bands was compared to the calculated size of the genes. Strains were only carried on within the study if the screening matched the theoretical length of the genes.

2.13 Clean-up of the PCR product after the gel extraction

500 µL of NTI buffer was added to the Eppendorf tube containing the gel and DNA cut-out piece. The tube was placed in a water bath at 55 ^{O}C for 5 minutes. The solution was transferred from the tube to a spin column containing a silica membrane to collect the DNA. The centrifuge tube with the solution was centrifuged at 11 000 g for 30 seconds. 700 µL of NT3 was added to the filter as the first wash step. The tube was centrifuged at 11 000 g for 30 seconds. This wash step was repeated once more. The silica membrane was dried by centrifuging the tube at 11 000 g for 1 minute. The filter section of the tube was placed in an Eppendorf tube to collect the DNA. 15 µL of NE elution buffer was added to the tube. The tube was centrifuged at 11 000 g for 1 minute. This step was repeated once more. The concentration of the DNA was measured on a NanoDrop 2000 spectrophotometer.

2.14 Transformation of *S. pneumoniae*

S. Pneumoniae was transformed by natural transformation. Exponentially growing *S. pneumoniae* at OD_{550} = 0.05 – 0.1 was added with 100 – 200 ng of transforming DNA and induced to competence by adding a final concentration of 250 ng/mL CSP-1. The tubes were then incubated at 37 ^{O}C for 2 hours. Finally, 30 µL from the transformant and the negative control were plated onto a TH-agar, each containing the appropriate antibiotic for the transformation.

2.15 Microscopy

OD_{550} was measured until it reached between 0,3 and 0,4 for each strain before microscopic imaging.

The agarose gel used in microscopy was made by melting 1,2% agarose in 1x PBS buffer. The gel solution was heated in the microwave for 1 minute until the agar was dissolved completely. Once the agar was dissolved, the solution was kept in a water bath at 55 ^{O}C to prevent the agar from solidifying.

The agar mixture was added in drops onto a microscope slide with 12 wells. A thin glass slide was placed on the agarose and pushed down to create a thin layer of solidified agarose. Next, 0.5 µL of each sample was added to a well each, and a cover glass was placed on top and gently pushed down on the agarose to immobilize the cells. The bacteria were examined using a Zeiss LM700 microscope with a 100x phase contrast objective. Images were captured using an ORCA-Flash 4.0 V2 Digital CMOS camera (Hamamatsu Phonetics) with a 100x phase contrast objective and further processed using the ImageJ software.

2.16 Analysis of cell wall from *S. pneumoniae.*

2.16.1 Isolation of cell wall

The cell wall from each sample was isolated by following the protocol published by Vollmer et al. in 2007, with some modifications.

Cells were grown in 0,5 L of C-medium to an OD550 of 0,35-0,5. The cells were harvested by centrifugation at 10 000 g for 10 minutes. Next, the cells were resuspended in 40 mL ice-cold 50 mM Tris/HCl with pH 7,0. The resuspended cells were added dropwise into 120 mL of a 5% boiling SDS solution and stirred heavily for about 10 minutes. The solution was cooled to room temperature before the crude cell wall material was collected by centrifugation at 12 000 g for 10 minutes at room temperature. The solution was kept at room temperature since SDS precipitates at low temperatures.

The SDS was washed from the cells by repeated resuspension and centrifugation with the first two steps of 20 mL of 1 M NaCl and then with four steps of 20 mL of dH_2O. After the last

centrifugation, the pellet obtained was resuspended in 2 mL of dH_2O and added to a fast-prep tube with 0,5 g of acid-washed glass beads (<106 µm). The cell walls were broken mechanically in the Fast-prep machine in 6 pulses of 6.5 m/s for 20 seconds each, with 1-minute breaks between each pulse. When the cell walls had been fragmented, the supernatant was transferred to a new Eppendorf tube after the glass beads had had time to sediment. The beads were washed a few times with dH_2O to ensure the maximum amount of cell wall was extracted. The remaining whole cells and glass debris in the transferred supernatant were removed by slow centrifugation at 2 000 g for 5 minutes. The supernatant was transferred to a new tube and centrifuged at 25 000 g for 15 minutes at room temperature. This pelleted the cell wall material. The pellet was resuspended in 2 mL of 100 mM Tris/HCl with pH 7,5 with 20 mM MgSO4. Next, 10 µg/mL DNase and 50 µg/mL RNase were added to break down any residual DNA and RNA, and the samples were incubated at 37 ^{O}C with continuous stirring for 2 hours. After 2 hours, 10 mM CaCl2 and 100 µg/mL trypsin were added to the samples. The trypsin would hydrolyze any proteins left in the samples at this point. The samples were incubated overnight at 37 ^{O}C with continuous stirring.

8 % SDS solution was added to the sample solutions to give a final concentration of 1% SDS. The SDS is added to the solution to inactivate the enzymes (K. Weber & Kuter, 1971). The samples were then incubated at 80 ^{O}C for 15 minutes. The total volume of the sample solution was adjusted to 20 mL using dH_2O, and the cell walls were sedimented by centrifugation at 13 000 g for 30 minutes at room temperature. The cell wall pellet was resuspended in 10 mL of 8M LiCl, incubated at 37 ^{O}C for 15 minutes, and centrifuged like before. Next, the pellet was resuspended in 10 mL 100 mM EDTA with pH 7,0, incubated at 37 ^{O}C for 15 minutes, and centrifuged like before. The pellet was washed with 20 mL of dH_2O, 20 mL of acetone, and 20 mL of dH_2O with the same centrifugation as before between each wash. The pellet obtained after the last centrifugation was resuspended in 1 mL of water, transferred to a pre-weighed Eppendorf tube to be able to determine the final weight of the purified cell walls and centrifuged to remove as much water as possible while keeping the cell wall wet. Finally, the cell walls were dried in a vacuum centrifuge (Savant).

2.16.2 LytA treatment of cell wall

This protocol uses LytA to digest the cell walls. The gene *lytA* encodes an N-acetylmuramic acid L-alanine amidase that cleaves the pneumococcal cell wall. Then, it hydrolyses the bond between

MurNac and the first L-Ala of the stem peptides in peptidoglycan. This way, LytA can release all stem peptides from the cell wall material (Balachandran et al., 2001; Mosser & Tomasz, 1969).

The dried cell walls were resuspended in dH_2O to a final concentration of 25 mg/mL. Next, 1 mg of the purified cell wall was digested with a LytA treatment using the reactants listed in section 2.9.6. The reaction mixture was mixed in the tube and incubated at 37 ^{O}C overnight. After incubation, the samples were heated to 95 ^{O}C in a heating block for 20 minutes to precipitate LytA. Next, the samples were centrifuged in a bench centrifuge at 20 000 g for 10 minutes. The supernatant was transferred to new Eppendorf tubes to leave the precipitated LytA and glycan behind. The samples were centrifuged at 20 000 g for 5 minutes, and the supernatant was collected one final time to ensure no insoluble material was applied to the HPLC column. The pH of the samples was adjusted to 3 by adding small amounts of 20% orthophosphoric acid, starting with 1,5 µL. The pH was verified using pH paper.

2.16.3 HPLC analysis

LytA-released stem peptides were analyzed using C-18 reverse-phase HPLC. The mobile phase was 0,05% TFA in dH2O, and the eluent solution was 0,05% TFA in 100% acetonitrile. All samples were loaded using 40 µL volume, except for the sample JM5, which was loaded with 25 µL of its solution. The column used was C-18. The program for separating peptides was set up using a flow of 0.5 mL/minute and an absorbance of 206 nm. Before starting the program and between each sample, there was a 15-minute wash of the system. Each sample had an elution time of 120 minutes in a range of acetonitrile from 0% to 15%.

2.17 Bocillin assay

Nucleic acids are negatively charged and will move toward the positive charge during av electrophoresis. On the other hand, proteins have a more complex overall charge caused by different charges coming from different amino acids in the protein. The proteins can have a positive or negative charge or be neutral. The number of positive vs. negative amino acids gives the protein's total charge. If there are more positives than negatives, the overall charge of the protein is positive, and vice versa. If a mixture of proteins with their original charge were to be electrophoresed, the positive would migrate toward the cathode and the negative towards the

anode. The neutral proteins would hardly move at all. To avoid this, the proteins are boiled in sodium dodecyl sulfate (SDS) to separate proteins based on their molecular weight. This detergent will ruin the folded structure of the proteins, leaving them as long strands of denatured proteins. In addition to being a detergent, the SDS also has a hydrophobic tail. This tail has a negative charge. The SDS will coil around the denatured proteins, giving an overall negative charge for all proteins. The amount of SDS binding is proportional to the length of the protein. Now, the proteins can be separated by size (Clark et al., 2019).

Cells were grown to an OD_{550} = 0,2 in 5 mL of C-medium. The cells were pelleted and lysed by resuspending them in 100 µL 20 mM sodium phosphate buffer with pH 7,2 containing 0,2% Triton X-100. The tube was incubated in a 37 ^{O}C water bath for 5 minutes to lyse the cells fully (Triton X-100 activates the LytA autolysin). The lysate was stored at -80 ^{O}C. When the PBPs were going to be labeled with bocillin, 15 µL of each sample was mixed with 2 µL of bocillin from a stock with a concentration of 25 µM, giving a final concentration of bocillin at 3,3 µM. Next, the samples were heated in a water bath at 37 ^{O}C for 30 minutes. The labeled proteins were mixed with a 2x SDS sample buffer in a 1:1 ratio to prepare the samples for separation and boiled for 5 minutes to denature the proteins. The sample buffer contains SDS and β-mercaptoethanol. The SDS and the β-mercaptoethanol will denature all proteins present in the sample once heated up. The sample buffer also dyes the sample mixture blue, later used to indicate how long the sample should migrate in the gel.

SDS-PA-gels for bocillin analyses were cast using the Mini protein gel cast system from Biorad. The separation gel was made by mixing the components listed in section 2.9.4. The 30% acrylamide, 2% bisacrylamide buffer at pH 8,8, and dH_2O were mixed and degassed for 5 minutes. Then, the SDS, APS, and TEMED were added to initialize the polymerization of the polyacrylamide gel. 3,2 mL of the separation solution was quickly added into each mold. The gel was immediately leveled by carefully flooding the top half of the mold with dH_2O. After the gel had polymerized, the stacking gel was made by mixing the components listed in section 2.9.4. The stacking gel was made in the same way as the separation gel. The dH_2O was removed completely from the mold, and 1 mL of the stacking gel was added into the mold onto the separation gel. A comb for making 10 wells was inserted into the top of the stacking gel, and the gel was allowed to polymerize fully.

10 µL of the sample was added to each well, and the electrophoresis was performed at 100V until the samples migrated to the separation gel. The samples were then separated at 200V until the dye had left the gel. The samples were further separated at this voltage for an additional 90 minutes for the PBPs to separate throughout the gel fully. The bocillin-labeled PBPs were visualized by fluorescence from the fluorescent bocillin in an Azure Imager c400.

3 Results

This project aimed to investigate the contribution of low-affinity PBP2b to a branched structured cell wall in *S. pneumoniae*. The presence of low-affinity PBP2b increase the relative amount of branched muropeptides in the cell wall, which was found by a previous master's student in the Molecular Microbiology group at NMBU (Heggenhougen, 2019). The hypothesis was, therefore, that a low-affinity version of PBP2b either prefers branched structured muropeptides or is less active, leading to compensating cell wall synthesis by one or more of the other PBPs. To study this further, knockout strains of *pbp2b* and single knockouts of the class A PBPs (*pbp1a*, *pbp1b,* and *pbp2a*) were created and phenotypically tested for changes in cell wall composition.

3.1 Knockout strains – screening and phenotypic verification

Two penicillin-resistant lab-generated mutants of *S. pneumoniae,* strain RSG77, and Pen6, were chosen as the foundational genetic backgrounds for this project. RSG77 is a strain created at the MolMik group. The strain is a penicillin-sensitive R6 derivative that has been repeatedly transformed with genomic DNA from a highly resistant *Streptococcus oralis* Uo5 and selected based on increasing Penicillin G concentration. The Pen6 strain is a well-known strain created by Zighelboim in 1980 that has been obtained by a similar method using a resistant clinical isolate from South Africa as a DNA donor. Typical for both these strains is that they display a highly branched cell wall structure and have a high minimum inhibitory concentration (MIC) for penicillin (Zighelboim & Tomasz, 1980). This resistance level depends on branched structured muropeptides since the MIC drops when the *murM* gene is deleted (Crisóstomo et al., 2006; S. R. Filipe et al., 2002; A. M. Smith & Klugman, 2001). Due to the observed phenotype in an RSG77 Δ*murM* mutant, this strain was particularly interesting in this project. The strain Pen6 was included to control that potential results from this study could be repeated in other well-known strains.

One of the main aims of this study was to determine whether low-affinity PBP2b is responsible for the increased incorporation of branched muropeptides in the cell wall of resistant strains. An approach to test this would be to analyze the cell wall of a Δ*pbp2b* mutant. However, the *pbp2b* gene is essential in *S. pneumoniae*. A way to circumvent the essentiality of *pbp2b* is to exploit the

fact that certain suppressor mutation alleviates the essentiality of this gene. Namely, if the gene *eloR* is deleted, *pbp2b* can also be deleted, or if a truncated version of the cell division protein MreC (MreC*) is expressed, *pbp2b* can also be deleted (Stamsås et al., 2017). Going through *eloR* and *mreC** was done because RSG77 has shown a correlation between PBP2b, *eloR,* and MurM (see 1.7). It was unsure if *eloR* would give any results, so going through both from the start would save some time if the Δ*pbp2b* strain did not yield any results. Because of this, the mutant strains lacking eighter *eloR* or *murM* were made simultaneously.

For this study, 14 new mutants were made: seven from RSG77 and seven from Pen6 (Table 2). In addition, four strains, JM7, JM10, JM13, and JM14, were made using other strains from this study. The rest were made directly from eighter RSG77 or Pen6 (Figure 9).

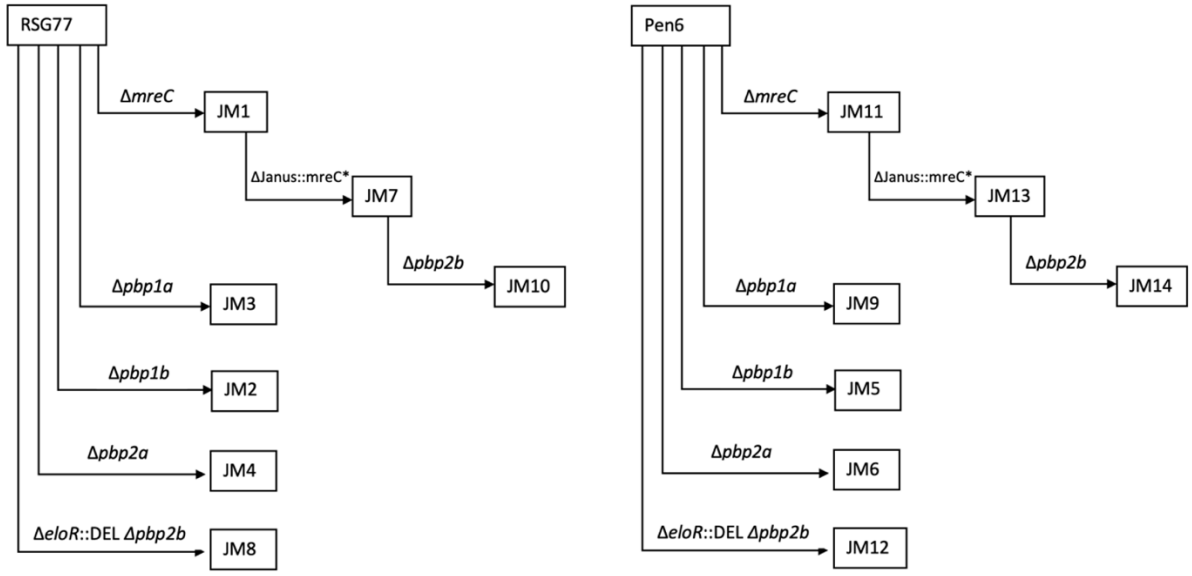

Figure 9 Overview of all mutant strains created in this study and how they relate to each other and RSG77 or Pen6.

During the transformations, almost all the strains were transformed without a problem and had too many colonies to count. The strain JM9 (Pen6, Δ*pbp1a*) took several attempts to make because no transformant grew on the agar plate. Since this transformant would not grow on the kanamycin plates, the theory was either that the transformation had failed or that the PCR product was wrong. New primers were ordered to uncover if the PCR product was the problem. After a few tries with these new primers and different combinations of primers, colonies grew abundantly. This indicated

that the initial primers used were not a good match for the Pen6 genome and that the new primers ordered after genome sequencing worked the way they should.

Due to the limited access to the genome of Pen6, it took a while to figure out which primers would anneal well to the targeted genes. The strain JM11 took several tries to get right because of this. New primers were ordered and used to make the PCR product, which resulted in some colonies growing. The number of colonies was about 30 for this strain at this point. When JM11 was used to make JM13, it was initially difficult to successfully transform the PCR product into JM11 to create JM13. After many tries with different primers for the PCR product, it was decided that a new JM11 should be attempted made. This decision was made because the likelihood of this strain being the problem was significant due to the difficulty of making the mutant strain in the first place and the suspiciously low number of colonies presented. The new JM11 was made and presented too many colonies to count. The new JM11 was used to make JM13, and the transformation worked on the first try, with an abundance of colonies present for this strain as well. The strains with *eloR* knocked out, JM8 and JM12, were left in the incubator for two days instead of one like the rest. This was due to the *eloR* knockout being known from the literature to grow slowly because of the mutation's effect on the cells.

The strains selected for with Streptomycin, JM7 and JM13 both presented fewer colonies than the rest, which were selected for using kanamycin. They grew roughly between 50 and 100 colonies each. They also had a couple of colonies on negative control. This is normal when selecting using streptomycin because of the balance between resistant and sensitive *rpsL* in the cells.

All strains made in this study were screened with PCR (See 2.11.2). This was done to verify that the size corresponded to what was expected based on the size of the PCR product and if Janus was present.

3.1.1 Verification of morphological changes in knockout strains

In addition to the PCR screening, the knockout mutants were verified in the form of phenotypical characteristics using phase contrast microscopy. The same changes in morphology were expected for the strains derived from RSG77 and Pen6.

All mutants were observed under a microscope to see if the morphology of the cells had changed the way it was expected for the respective knockouts, based on what has been reported in the literature. The strain RSG77 was expected not to deviate far from the morphology of the wild-type R6 it was made from. This morphology is typically elongated diplococci that do not form long chains or clusters, but can form short chains. RSG77 and Pen6 show this expected morphology (Figure 10 A and I). Previous research has shown that the deletion of *eloR* gives a characteristic morphology of short and chained cells (Stamsås et al, 2017). The Δ*eloR* strain from RSG77 and Pen6 shows shorter cells, which grow in chains (Figure 10 D and L). Because the changes in morphology are consistent with what has previously been found, the correct gene had likely been knocked out in both strains.

Expression of a truncated MreC (MreC*) and depletion of *pbp2b* results in shorter cells growing in chains compared to the wild-type (Berg et al., 2013; Stamsås et al., 2017). When introducing MreC* to delete *pbp2b* in the RGS77 and Pen6 strains, the resulting *mreC**, Δ*pbp2b* mutant displayed the expected morphology of shorter cells organized in chains. However, the chaining was not as extreme in Pen6 as in RSG77 (Figure 10 B, C, J, and K). Like the expression of MreC*, deletion of *eloR* also allows deletion of *pbp2b*. An Δ*eloR* mutant is reported to be shorter and rounder than wild-type cells. As expected, the Δ*eloR* Δ*pbp2b* mutants of RSG77 and Pen6 were shorter and rounder than wild-type cells in addition to those grown in chains (like *pbp2b* depleted cells) (Figure 10 E and M). These changes in morphology, which match with the predictions based on findings from the literature, indicate that the correct genes have been knocked out in all these cells.

Studies by Paik et al. in 1999 and by Hoskins et al. in 1999 showed that single knockouts of the class A PBP genes had no notable changes to the morphology of the cells. The morphology of the knockouts Δ*pbp1a*, Δ*pbp1b,* and Δ*pbp2a* in RSG77 and Δ*pbp1b* and Δ*pbp2a* in Pen6 showed no changes in morphology (Figure 10 F, G, H, O, and P). However, in Pen6, the mutant Δ*pbp1a* showed an unexpected change in morphology (Figure 10 N). The shape of the cells is the same, but they vary in size and grow in clusters. This indicated that knocking out *pbp1a* in Pen6 might be more noticeable or less compensable for the cells, which leads to an abnormal morphology compared to the genetic background. This should have the same morphology as Pen6 (Figure 10 I and N).

The strains JM1 and JM11 was not used in the results, only to make the strains JM7 and JM13. They are therefore not present in any figures in the results.

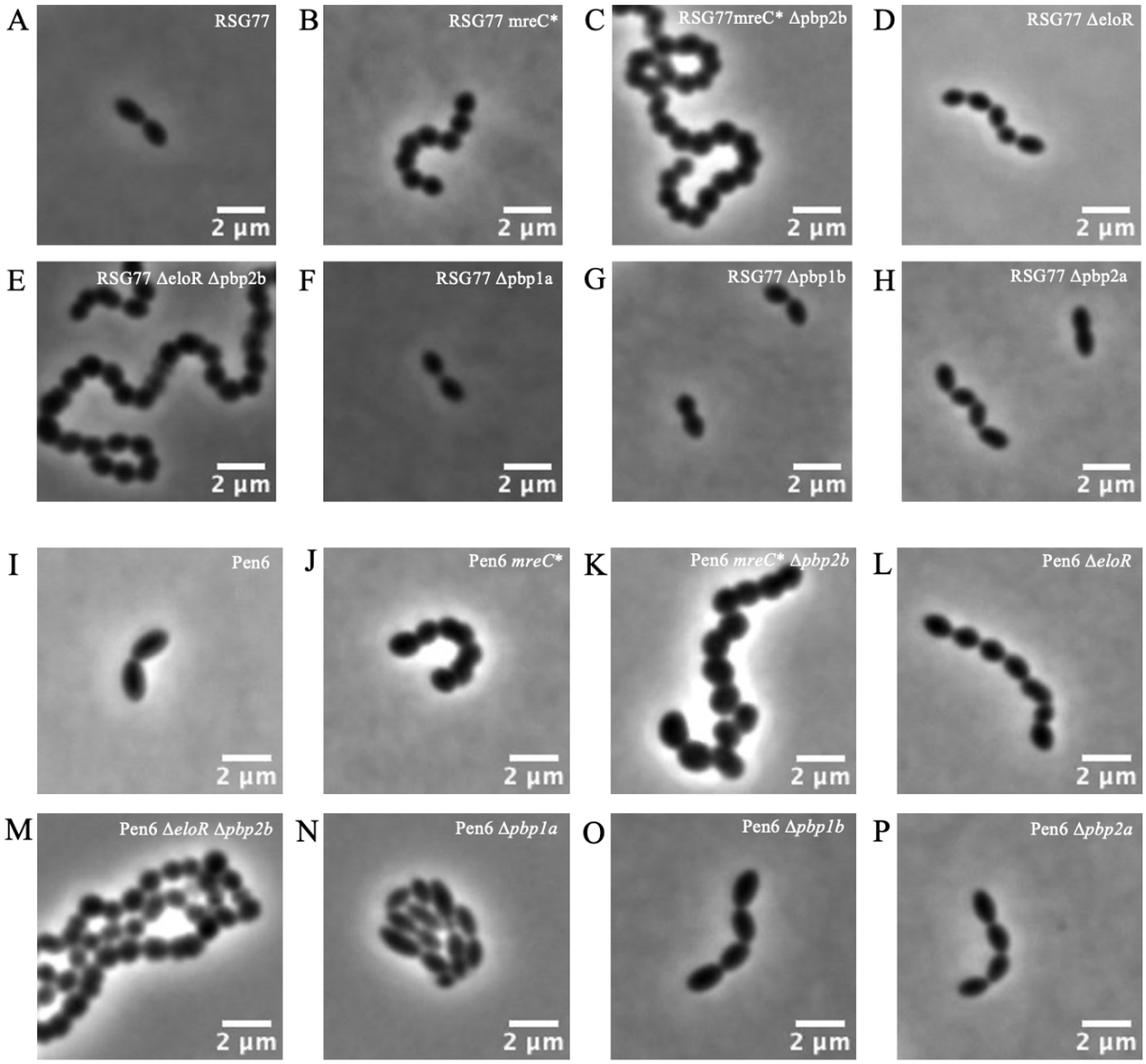

Figure 10 Microscopy images of 12 out of 14 strains made in this study, as well as RSG77 with and without *eloR* and Pen6 with and without *eloR*. A) RSG77, B) RSG77 *mreC**, C) RSG77 *mreC** Δ*pbp2b*, D) RSG77 Δ*eloR*, E) RSG77 Δ*eloR* Δ*pbp2b*, F) RSG77 Δ*pbp1a*, G) RSG77 Δ*pbp1b*, H) RSG77 Δ*pbp2a*, I) Pen6, J) Pen6 *mreC**, K) Pen6 *mreC** Δ*pbp2b*, L) Pen6 Δ*eloR*, M) Pen6 Δ*eloR* Δ*pbp2b*, N) Pen6 Δ*pbp1a*, O) Pen6 Δ*pbp1b* and P) Pen6 Δ*pbp2a*.

3.1.2 Using fluorescently labeled penicillin to confirm knockout strains

The PBPs were fluorescently labeled and separated on an SDS-PAGE to further confirm the deletion of the different pbp genes in the mutants described above (Figure 11). It was important to determine if a change occurred before and after *pbp2b* had been knocked out in the strains lacking *eloR* or *mreC**. It was also pivotal to confirm that the correct genes had been knocked out in the respective strains to validate that the morphological effect was caused by the knockout of *pbp2b*, *eloR,* or *mreC*,* as well as the class A PBPs. This method would indicate the presence of PBPs to verify if the correct PBPs had been knocked out. There were some slight differences between the strains in the amount of protein loaded on the gel, which can explain some of the differences in brightness visible in the images (Figure 11).

The proteins are well separated in all three gels, but only a few bands are showing due to the presence of many low-affinity PBPs. Using the bands for RH425 as a reference, the bands have separated well. However, some bands are not showing, either because the PBP is knocked out and is not present or because the PBPs are low-affinity. These will, therefore, not bind penicillin as much as the PBPs in RH425 and will be either weak or not visible at all.

Generally, it is not easy to separate the band 1a/1b because they are almost the same molecular weight. It was therefore, as expected, not possible to separate these bands in Figure 11. The bands for 2x, 2a, and 2b separated well for RH425 (Figure 11 A and C).

In Figure 11 A, all RSG77 mutant strains and RSG77 itself show no bands for PBP2x and PBP2b. In the two strains here where *pbp2b* is knocked out, the band for PBP2b is absent because the protein is absent. The rest of the strains present with a low-affinity PBP2b. All strains here also present with a low-affinity PBP2x. Pen6 Δ*eloR* in the same Figure, shows a weak band for PBP2b. This indicates that PBP2b might gain some affinity and bind slightly more penicillin once EloR is no longer present in the cell. This band disappears when *pbp2b* is knocked out in the same strain (Figure 11 A, Pen6 Δ*eloR* and Pen6 Δ*eloR* Δ*pbp2b*).

In Figure 11 B, two out of three bands are present from PBP2x, PBP2a, and PBP2b. The upper band is most likely the band for PBP2x, based on the slight distance expected between PBP2x and PBP2a from the separation of RH425 in Figure 11 A and C. The upper band, which is thinner and weaker than the PBP2a band, indicates that PBP2x is also a low-affinity PBP in these strains (Figure 11 B). The brightness from the bands from strain Pen6 *mreC** Δ*pbp2b* is greater than for

the rest of the strain in Figure 11 B. The difference in signal here is also seen in the 1a/1b band and is, therefore, most likely just from a difference in the amount of protein added.

For RSG77Δ*pbp1a* and Pen6Δ*pbp1a* in Figure 11 C, there is hardly any difference between the combination of signals from the mutants from the two different genetic backgrounds. The combination of bands is interesting to use to confirm if the same mutation in different genetic backgrounds have the same composition of low-affinity- and high-affinity PBPs in the cell. The bands for PBP2x, PBP2b, and PBP1a were expected to be stronger in both RSG77 and Pen6. Since the bands do not show, it indicates that not enough PBPs for each band bind penicillin with a high affinity.

Since the combination of bands has not changed between RSG77 and Pen6 and their Δ*pbp1a* mutant (Figure 11 C), the effect of *pbp1a* being knocked out is seemingly hardly noticeable to the cell. In the strains RSG77 Δ*pbp1b* and Pen6 Δ*pbp1b* (Figure 11 C), the band for 1a/1b is gone, but the band for 2a is stronger for RSG77 Δ*pbp1b* than RSG77 is, and slightly weaker for Pen6 Δ*pbp1b* compared to Pen6. For RSG77 Δ*pbp2a* and Pen6 Δ*pbpa2* (Figure 11 C), the band for 2a is gone compared to RSG77 and Pen6, as expected. The band for 1a/1b also appears slightly weaker in RSG77 Δ*pbp2a*, while it seems to be gone entirely in Pen6 Δ*pbp2a*.

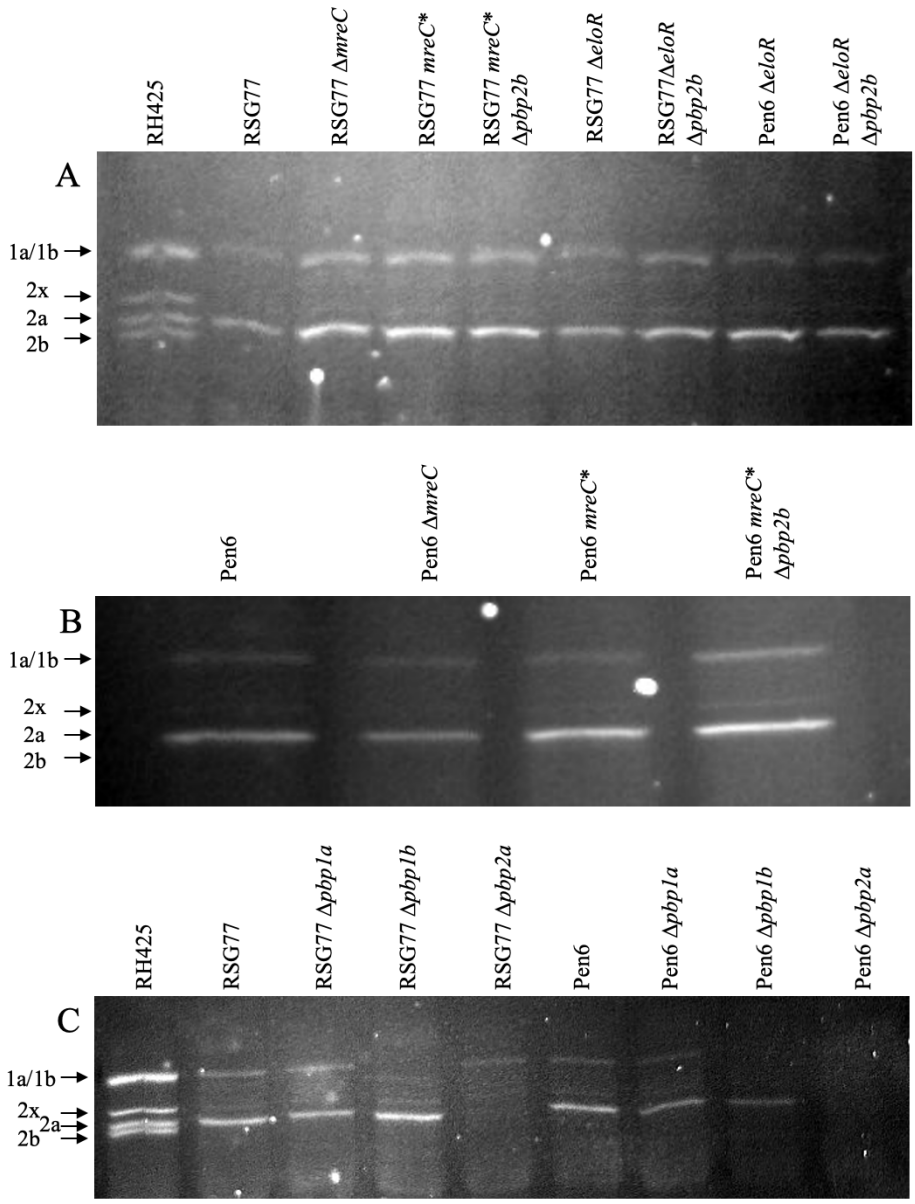

Figure 11 Gel images from bocillin FL labeled PBPs in the following strains: *A)* RH425, RSG77, RSG77 Δ*mreC,* RSG77 *mreC*,* RSG77 *mreC** Δ*pbp2b,* RSG77 Δ*eloR,* RSG77 Δ*eloR* Δ*pbp2b,* Pen6 Δ*eloR* and Pen6 Δ*eloR* Δ*pbp2b. B)* Pen6, Pen6 Δ*mreC,* Pen6 *mreC** and Pen6 *mreC** Δ*pbp2b. C)* RH425, RSG77, RSG77 Δ*pbp1a,* RSG77 Δ*pbp1b,* RSG77 Δ*pbp2a,* Pen6, Pen6 Δ*pbp1a,* Pen6 Δ*pbp1b* and Pen6 Δ*pbp2a.*

3.2 Deletion of *pbp2b* gave no change in stem peptide composition in the cell wall

After using the SDS-PAGE to support the theory that the correct PBPs had been knocked out, meaning that the changes in morphology were most likely due to the deletions and knockouts, the composition of the cell wall was analyzed using HPLC. The muropeptides present in the samples were eluted over 120 minutes and measured the UV absorbance at 206 nm. The chromatograms from the HPLC analysis were compared to the known chromatograms of Pen6 (Figure 12).

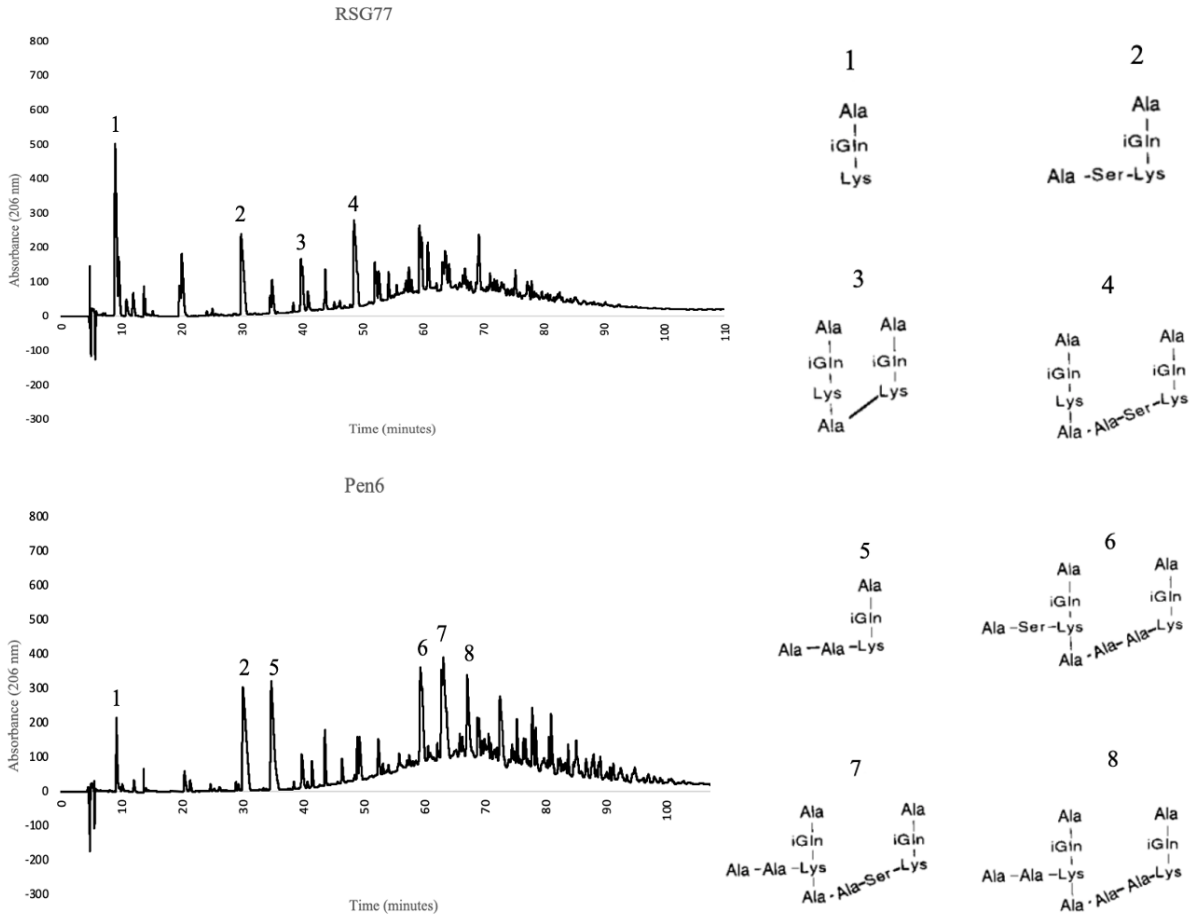

Figure 12 Illustration of where the different muropeptides appear in the HPLC chromatograms of RSG77 and Pen6. Figure part 1-8 shows the different muropeptides analyzed in this study. Parts 1, 2, 3, and 5 are linear muropeptides, and 4, 6, 7, and 8 are branched muropeptides. The time was measured in minutes and is indicated on the x-axis. The absorbance was measured in UV absorption at 206 nm and is indicated on the y-axis. Figure modified from *S. Filipe & Tomasz, 2000.*

To investigate the contribution of low-affinity PBP2b to a branched structured cell wall, *pbp2b* was knocked out in an Δ*eloR* or *mreC** genetic background. The cell wall composition in these mutants was compared to that of the genetic backgrounds (Figure 12). The results showed no major differences in the stem peptide composition when both *pbp2b* and eighter *eloR* or *mreC** were knocked out (Figure 13). There are minor changes to the cell wall composition in general, but there are no large changes indicating any drastic changes in any of the HPLC graphs.

The chromatograms for the RSG77 strain and the *eloR* knockout and *mreC** strands, both with and without PBP2b, show some minor variations in the area under the peaks but not as significant as it was expected to be. All chromatograms follow the same general curvature within the same genetic background, as seen in Figure 12.

The ratio of linear to branched muropeptides, the peak at 40 minutes divided by the peak at 50 minutes, in RSG77 *mreC** Δ*pbp2b* and RSG77 Δ*eloR* Δ*pbp2b* is 0,81 and 0,85, respectively. The ratio for the same peaks for RSG77 is 0,38. Based on the area of the peaks, this indicates that the amount of linear muropeptides increases when *pbp2b* is knocked out in RSG77 and that the amount of branched muropeptides is unchanged. The area of the peaks in each chromatogram should be interpreted as a whole, but there was not enough time for that in this study.

Pen6 does not show the same peaks at RSG77 because the two strains have different types of branched muropeptides. While RSG77 has the type indicated as number 4 in Figure 12, Pen 6 has the three variants shown as 6, 7, and 8 in the same Figure. Based on the structure of the muropeptides in Pen6, this strain has more branching than in RSG77 due to the extra branch, which is not cross-linked.

The HPLC chromatograms for RSG77 *mreC**, RSG77 Δ*eloR*, Pen6 *mreC**, and Pen6 Δ*eloR* did not deviate much from the mutant they were used to make. They were, therefore, not included in the results. All four graphs are listed in Appendix A1-A4.

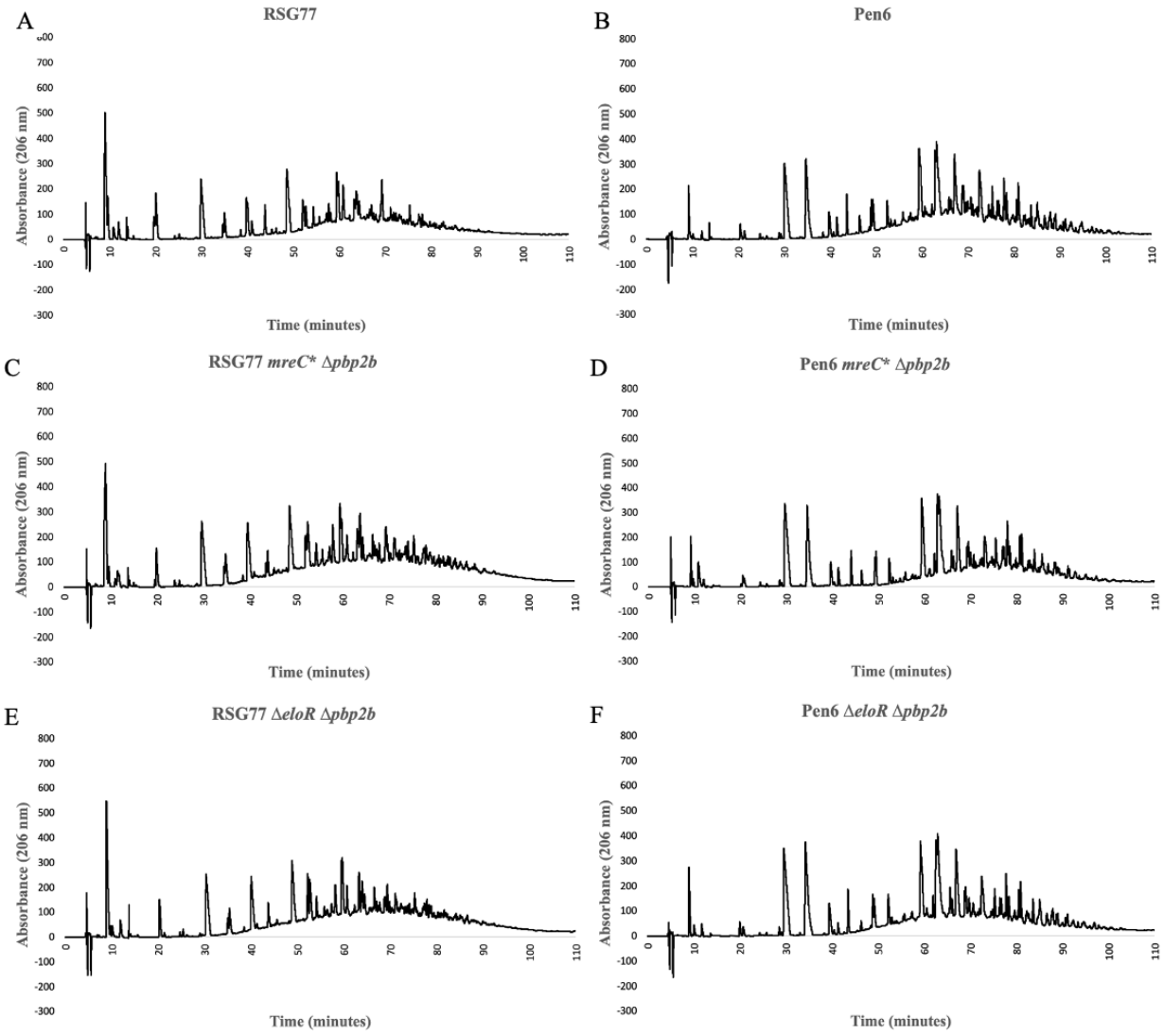

Figure 13 HPLC chromatograms of A) RSG77, B) Pen6, C) RSG77 *mreC** Δ*pbp2b*, D) Pen6 *mreC** Δ*pbp2b*, E) RSG77 Δ*eloR* Δ*pbp2b* and F) Pen6 Δ*eloR* Δ*pbp2b*. The time was measured in minutes and is indicated on the x-axis. The absorbance was measured in UV absorption at 206 nm and is indicated on the y-axis.

3.3 Could class A PBPs rescue the lack of PBP2b and cause a more branched cell wall?

Based on previous observations by Heggenhougen and employees in the Molecular Microbiology group at NMBU (see 1.7), we hypothesized that *pbp2b* might be responsible for the increased incorporation of branched muropeptides found in the cell wall of penicillin-resistant isolates. However, the results obtained in this study indicated that this might not be the case. The changes

in peaks for the strains from this experiment compared to RSG77 and Pen6 were expected to be greater based on the abovementioned hypothesis, although this did not seem to be the case (Figure 12). Hence, the contribution of class A PBPs to cell wall branching was examined. The theory was that perhaps one or more of the class A PBPs compensate for the expression of a less efficient low-affinity PBP2b in penicillin-resistant strains. Therefore, the class A PBP encoding genes (*pbp1a*, *pbp1b,* and *pbp2a*) were knocked out individually in the RSG77 and Pen6 strains by placing a Janus cassette inside the respective gene. The same procedures for the previously mentioned strains were repeated for the three PBPs in class A, and the mutants' cell wall stem peptide composition was analyzed using HPLC.

The results showed no major differences between the mutants lacking *pbp1a*, *pbp1b,* or *pbp2a* in both RSG77 and Pen6. For RSG77, a knockout of the class A PBPs seemed to slightly impact the size of the peaks for linear and branched muropeptides. However, there were also some minor changes to other peaks, so the small changes in peaks should be investigated within each chromatogram.

For Pen6, a knockout of *pbp1a* resulted in more of the peptide Ala-iGln-Lys-Ala-Ala eluting at 20 minutes (Figure 2, red square), whereas a knockout of *pbp1b* and *pbp2a* did not result in any changes to the stem peptide composition of the cell wall (Figure 14 D, F, and H). In Figure 14 F, the amount of added cell wall was less than the rest. Therefore, the changes seen in composition between this chromatogram and the other mutants of Pen6 are not comparable. The general curvature is like the other mutants, but the ratios cannot be compared.

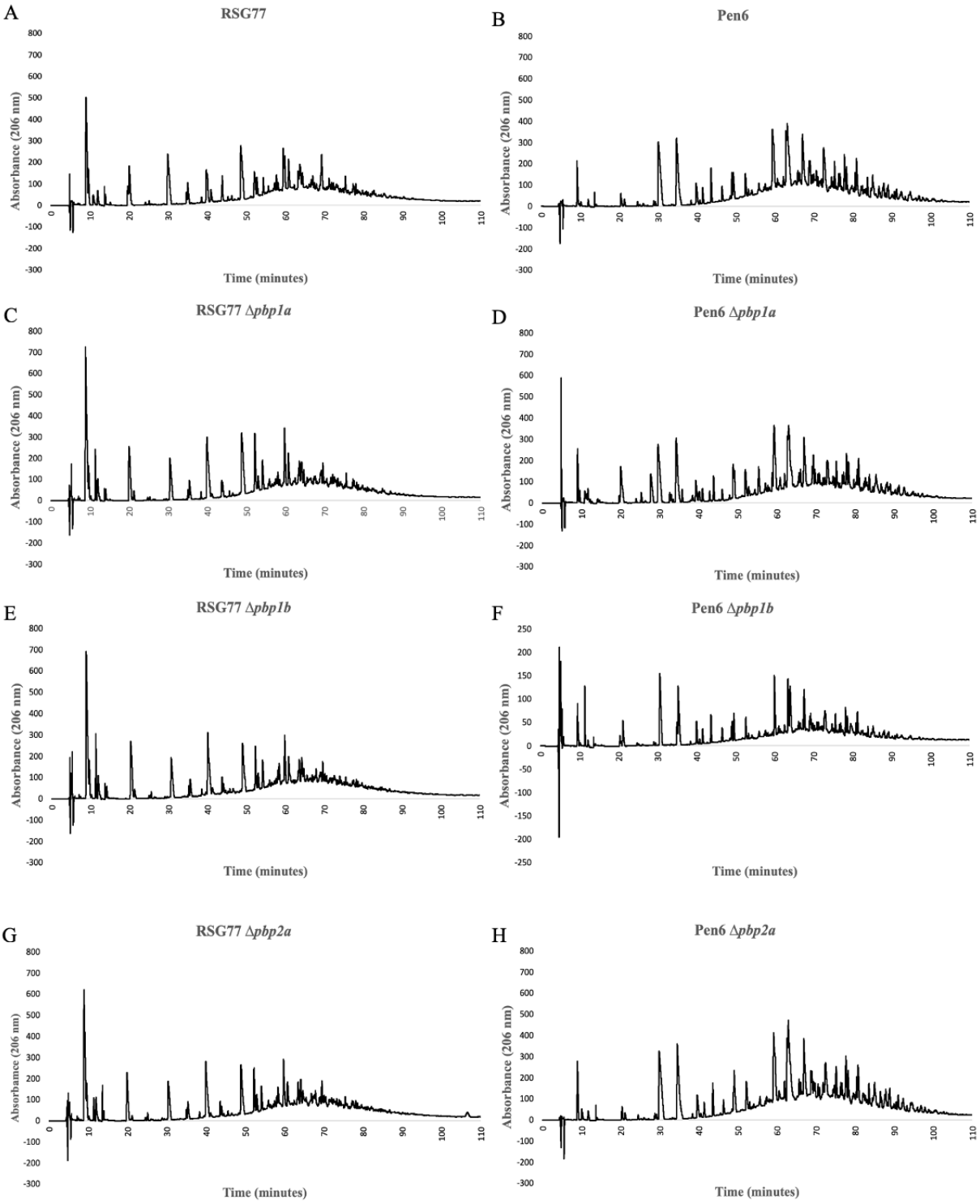

Figure 14 HPLC chromatograms of A) RSG77, B) Pen6, C) RSG77 Δ*pbp1a*, D) Pen6 Δ*pbp1a*, E) RSG77 Δ*pbp1b*, F) Pen6 Δ*pbp1b*, G) RSG77 Δ*pbp2a* and H) Pen6 Δ*pbp2a*. In figure F, the amount of cell wall added to the HPLC column was less than for the rest and the scale is therefore different from the rest of the chromatograms. See 2.9.6 LytA treatment for more information about the volume added of Pen6 Δ*pbp1b*. The time was measured in minutes and is indicated on the x-axis. The absorbance was measured in UV absorption at 206 nm and is indicated on the y-axis.

4 Discussion

The pneumococcal cell wall consists of both branched and non-branched linear muropeptides. As previously mentioned, analyses of penicillin-resistant clinical isolates have shown that these more often increase branched muropeptides and that branched lipid II precursors used for peptidoglycan synthesis are critical for resistance (S. Filipe & Tomasz, 2000). Resistant pneumococci express low-affinity PBPs that are not inhibited by penicillin. It has been hypothesized that one or more low-affinity PBPs prefer branched lipid II over non-branched and that branched lipid II outcompetes penicillin for the active site in these PBP versions. When branched lipid II is unavailable, e.g., when *murM* is knocked out, resistance is lost. Until now, it has not been investigated which PBPs contribute to the increased incorporation of branched stem peptides in the cell wall of resistant isolates. Previous results found by a master´s student in the Molecular Microbiology group at NMBU (Heggenhougen, 2019) showed that introducing low-affinity PBP2b into a sensitive lab strain led to a shift towards branched muropeptides in the ratio between branched and linear muropeptides. We wanted, based on this, to explore the possibilities of low-affinity PBP2b being responsible for the increase in branching in highly resistant strains. This led to us making a deletion mutant of *pbp2b* in resistant strains to see if the number of branched muropeptides decreased. The strains chosen as the base for the study were RSG77 and Pen6. These were selected because they are both strains with a highly branched cell wall, they both have a high MIC for penicillin, and the resistance level will drop when ΔmurM because the resistance level depends on branched muropeptides. The Pen6 strain was included as a control to ensure that the results obtained in this study could also be replicated in a published strain.

Figure 10 F and N showed some unexpected results. In RSG77, the knockout of *pbp1a* has not shown any changes in morphology, but in Pen6, this same mutation gave the same shape to the cells, but they varied in size and grew in clusters. The mutation was expected to have the same impact on both RSG77 and Pen6, so this morphological discrepancy was unexpected. This indicated that knocking out *pbp1a* in Pen6 might be less compensable for the cells. It might lead to an abnormal morphology compared to Pen6, meaning that the absence of PBP1a affects the morphology in Pen6. Figure 11C indicated no changes in the composition of the different high-affinity PBPs in the two mutant strains. This might suggest that PBP1a is as important for the morphology in the *S. penumoniae* strain Pen6 as it is in *Streptococcus mutans* (Wen et al., 2015).

When *pbp2a* is knocked out, only a weak band from PBP1a/PBP1b is showing in RSG77 Δ*pbp2a*, but no other bands are showing in RSG77 or Pen6 (Figure 11 C). This indicates that no high-affinity PBP will increase to compensate for the loss of PBP2a. There might be low-affinity PBP doing this, but that is not possible to decipher from these images.

The bocillin labeling can also indicate how the affinity to β-lactam antibiotic changed from the wild-type RH425 to the strains made in this experiment. This could tell us something about which PBPs are low-affinity and which ones are not, which can be interesting information about the mutant strains made in this study (Figure 11).

4.1 Effect of PBP2b depletion on a branched structured phenotype

One of this thesis' primary goals was to determine if low-affinity PBP2b is responsible for incorporating branched stem peptides in the peptidoglycan of penicillin-resistant pneumococci. This was done by making knockout mutants of *pbp2b* in both RSG77 and Pen6. Low-affinity PBP2b was the PBP hypothesized to be the one dependent on branching based on what previous studies have found. If this was the case, one would expect a difference in the number of branched peptidoglycan strands in the cell wall when *pbp2b* is knocked out. However, the cell wall analysis results showed no noticeable changes to the amount of branching present between the wild types and the knockout strains of *pbp2b* (Figure 13).

Based on the hypothesis, the difference in ratio between branched and linear muropeptides from the HPLC analyses for *pbp2b* knockouts was expected to deviate more than what it proved to do if the hypothesis were correct. This was the same in both genetic backgrounds tested. Based on this, it seems that low-affinity PBP2b might not be the only main contributor to branching after all. When the low-affinity PBP2b is introduced to the cell, the amount of branching increases, but when the low-affinity PBP2b is knocked out, the amount of branching does not change. This might be because low-affinity PBP2b functions so poorly that the phenotype does not change even when the protein is knocked out. This does, despite this, not mean that PBP2b does not contribute to branching. It could mean that some of the other PBPs compensate for the absence of PBP2b to create a cell wall structure like PBP2b would.

In this study, there was not enough time to measure the MIC for any of the strains. The MIC of a strain has been shown to be dependent on branched structured muropeptides since the MIC drops when the *murM* gene is deleted (Weber et al., 2000). In the master´s thesis of Heggengougen in 2019, it was made a strain containing a low-affinity PBP2x and PBP1a. This strain had a MIC of roughly 1 μg/mL. The MIC increased when a low-affinity PBP2b was put into this strain. A theory about low-affinity PBP2b is that it functions so poorly that its job of incorporating branched muropeptides is handed over to another PBP. If this is the case, knocking out the low-affinity PBP2b should not change the MIC significantly due to it not doing anything that will cause a change in MIC. In the Δ*pbp2b* strains made in this study, the MIC should therefore decrease from that of the genetic backgrounds unless the PBP2b is low-affinity.

As previously mentioned, PBP2b interacts with RodA, a transglycosylase that connects glycan strands for PBP2b by transpeptidation. These proteins are involved in the elongasome, the peripheral part of cell wall synthesis (Angeles et al., 2020). The *pbp2b* knockout mutants display a rounded and shortened morphology growing in long chains (Figure 10). This change in morphology has been shown in other studies and is precisely what makes it plausible that different processes are involved in elongation and cell division. Since the cells are no longer elongated, it is reasonable to believe, based on the microscopy images, that the entire elongasome is inactivated due to *pbp2b*, *eloR,* and *mreC* being knocked out.

As mentioned, Heggenhougen´s results in 2019 indicated a link between the low-affinity PBP2b and increased levels of branched muropeptides in the cell wall (Heggenhougen, 2019). Further, recent unpublished data in the Molecular Microbiology group showed that a particular version of the low-affinity PBP2b is required for the cell to become highly penicillin-resistant and dependent on MurM and EloR for resistance. When knocking out *murM* in this specific strain (RSG77), the morphology had the same characteristic changes as one would expect if *pbp2b* is knocked out (shortened cells growing in long chains), which is not seen in a regular knockout of *murM*. Since the knockout of *murM has* been shown to eliminate the presence of branched muropeptide, it seems that in this mutant, the elongasome (with PBP2b) stops working in the absence of branched lipid II. However, when the elongation of the cells is inactivated, either by deletion of *eloR* or double knockout of *eloR* and *pbp2b* as well as *mreC***Δpbp2b*, the structure of the cell wall is not changed.

This means that the results obtained in this project indicate that neither PBP2b nor the elongasome is as important as first believed for increased branching.

4.2 Class A PBPs involvement in cell wall composition

Our hypothesis was that low-affinity PBP2b either has a higher affinity for branched muropeptides or works less efficiently. This could force the other PBPs to compensate for the dysfunctional PBP2b. Perhaps these other PBPs have a higher preference for branched lipid II. It has been shown *in vitro* that a low-affinity version of PBP2x has reduced transpeptidase activity compared to wild-type PBP2x (Zhao et al., 1997). If low-affinity PBP2b has a higher affinity for branched muropeptides, we expected to see some kind of change in the HPLC graphs before and after it was knocked out (Figure 13). Since we do not see this, other proteins might be sensing the structure of peptidoglycan, like StkP (see 1.4.1), which regulates other proteins involved in cell wall synthesis to modulate their activity. This is an explanation for how the introduction of low-affinity PBP2b can increase branching, which is what Heggenhougen found in 2019.

The new hypothesis was that if the low-affinity PBP2b is knocked out, maybe one of the PBPs in class A would be able to compensate for the loss of PBP2b and its reason for increasing branching, and there will, therefore, not be any noticeable differences in the amount of branching present in the cell wall. For this reason, the same experiment was also performed on all class A PBPs. By knocking out one of the class A PBPs in each strain, it would be possible to detect any changes in the amount of branching present and conclude if one of the class A PBP could be dependent on branched lipid II substrate. However, based on the cell wall analyses of the strains with the different PBPs knocked out, there was no reason to believe this was the case. There were no significant differences in cell wall composition before or after the knockout of the class A PBPs. The new direction of the hypothesis was, therefore, also ruled out. It means that one class A PBP is likely not alone responsible for increased branched stem peptides in the cell wall. However, class A PBPs might have overlapping roles and can partially substitute each other's function (Straume et al., 2020). Therefore, it would have been interesting to analyze the cell walls of class A PBP double knockouts or perhaps the cell walls of pneumococci in which all three class A PBPs were inhibited.

The knockout combination of PBP1a and PBP2a is lethal for the cell and, therefore, impossible to do (Berg et al., 2014; Paik et al., 1999). This is indicative that these two proteins have overlapping essential functions. A change in branching caused by the knockout of one of these two PBPs would, therefore, not be visible because the other PBP takes over the job of branching immediately. Because of this, it would be interesting to see if a knockout-depletion of these two PBP1a and PBP2a would give any changes in the amount of branching in the cell wall. By doing a knockout of one PBP and a depletion of the other, the composition of the cell wall of this knockout-depletion can be measured. This has been done before, but not in a strain without high branching and without analyzing the cell wall composition. Another approach could be using a moenomycin antibiotic, which inhibits the transglycosylase activity of class A PBPs (Van Heijenoort et al., 1987; Wallhausser et al., 1965). The enzymes would still be able to perform transpeptidation, but their processivity in peptidoglycan synthesis would stop. Hence, it would most probably prevent them from incorporating new peptidoglycan material. If moenomycin treatment of RSG77 and Pen6 resulted in reduced branching in the cell wall, it would suggest that class A PBPs are important for branched cell walls in resistant strains.

4.3 What is happening in the cell wall – a new alternative hypothesis

Since neither deletion of *pbp2b* nor any of the class A PBPs resulted in a dramatic decrease of incorporation of branched stem-peptides in the cell wall, only two PBPs are left untested. PBP3 has not been found to have eighter transglycosylation or transpeptidation abilities. This PBP is, therefore, not likely to be the PBP dependent on branching since it has no way to influence the amount of branching appearing in the cell wall. This leaves low-affinity PBP2x as the possible candidate responsible for the branched cell wall phenotype. PBP2x is active in septal peptidoglycan synthesis (see 1.4.1) and an essential gene in *S. pneumoniae* (no suppressor mutations are known to allow deletion of *pbp2x* in *S. penumoniae*). Because of its essentiality, it was not included in this study. However, making PBP2x deficient cells, e.g., by using a gene depletion system, it would be possible to gradually switch off the pbp2x transcription and analyze the cell wall. PBP2x is the first PBP to be inhibited by penicillin due to it being the PBP with the highest affinity towards penicillin (Berg et al., 2013; Lalble & Hakenbeck, 1987). If PBP2x uses branched lipid II to keep the penicillin away from its active site, it would then make sense that the

cells lose their resistance when the branching is gone in a *murM* mutant. Then PBP2x might be inhibited by penicillin even if it is a low-affinity PBP. Since PBP2x is an essential protein, the cells would then stop dividing. Working with depletion mutants instead of knockout mutants can take more time, and the amount of time available for this study was limited to looking into the knockout of *pbp2b* through *eloR* and *mreC,* as well as the class A PBPs.

When PBP2x is attacked by β-lactams and a low-affinity PBP2b is introduced to the genome, the attack changes focus to this PBP. If PBP2x turns out to be the one that prefers when branched lipid II is incorporated in the cell wall when a low-affinity PBP2b is introduced, the PBP2x must work harder to incorporate the branching to be able to bind to it. If the branching were removed, the PBP2x would then be inhibited by penicillin again.

4.4 Who decides when branching is incorporated?

An aspect of the background for this study is the reason for the incorporation of branched muropeptides into the cell wall. The low-affinity PBP2b has a higher affinity for branched muropeptides than penicillin. Why does a low-affinity PBP2b aid in increasing the branching when RodA is responsible for the polymerization of the glycan strands? PBP2b must cross-link the glycan stands it is given, it cannot choose which strands it gets, but it is still, in some way, part of incorporating the branching. RodA has nothing to do with the incorporation of the branched muropeptides. Can this mean that the low-affinity PBP2b refuses to cross-link glycan strands that are not branched and that the linear glycan strands are recycled and returned as, hopefully, branched peptides? If this is the case, can the reason for the continued incorporation of other muropeptides (Figure 12) be that the low-affinity PBP2b does such a poor job at incorporating the branched that another PBP aids in the transpeptidation and that this is not as strictly selective as PBP2b is? These are some possible theories into why low-affinity PBP2b incorporates branched muropeptides into the cell wall.

5 Conclusion and future work

This project aimed to investigate the contribution of low-affinity PBP2b to a branched structured cell wall in *S. pneumoniae*. The results indicated that *pbp2b* is not the one solely responsible for this, and neither are the class A PBPs. Based on the cell wall composition analysis, the only likely PBP left to depend on branching is low-affinity PBP2x. As previously explained, this was not included in this study due to time restrictions. Further work should be done on low-affinity PBP2x to determine whether this is involved in the increase of branched muropeptides. The same way of analyzing this study's cell wall composition can be used on *pbp2x*. This protein can, however, not be knocked out as it is an essential gene in the cell. This gene will therefore need to be depleted using a gene depletion system.

It would be interesting to measure the MIC of all knockout strains made in this study. This could give further insight into the effect PBP2b and the class A PBPs have on the cell and its resistance towards penicillin.

This study made single knockout mutants of the class A PBPs. Mutant strains containing double knockouts of eighter Δ*pbp1a*Δ*pbp1b* or Δ*pbp1b*Δ*pbp2a* can be made. This might indicate if any of the PBPs from class A are responsible for the increased branching and if some PBPs work together to keep the branching at a stable level. If there are changes between the single and double knockouts, this will indicate teamwork between two PBPs in keeping the branched muropeptides in the cell wall. The knockout combination of *pbp1a* and *pbp2a* is known to be lethal for the cell, and a mutant strain of Δ*pbp1a*Δ*pbp2a* can, therefore, not be made (Berg et al., 2014; Paik et al., 1999). To do a knockout and a depletion instead of a double knockout of these two PBPs to see the changes in cell wall composition, might give further knowledge about these PBPs involvement in a branched structured cell wall.

Antibiotic-resistant pneumococci are an increasing concern to the general health of the public. The recent findings from the MolMik group at NMBU (See 1.7), make it highly interesting to investigate further each PBPs contributions to the branching of the cell wall. Since a branched structured cell wall is one of the main characteristics of penicillin-resistant pneumococcal isolates, the significance of finding its main contributor is highly important. The cells lose their resistance when branched lipid II is not present. By potentially hindering the cells from using branched lipid II, we can continue to treat infections caused by penicillin-resistant strains with the penicillin

available today. This means a prolonged lifespan of already existing antibiotics. Penicillin is the most important group of antibiotics we have. By finding out how to inhibit either MurM or branched lipid II, it could be possible to use that mechanism of inhibition to create new antibiotics. Investigating antibiotic resistance mechanisms is still crucial in stopping the spread and stagnation of new multiresistant strains.

6 References

Angeles, D., Maciá Valero, A., Bohorquez, L., & Scheffers, D.-J. (2020). The pasta domains of bacillus subtilis PBP2B strengthen the interaction of PBP2B with DIVIB. *Microbiology*, *166*. https://doi.org/10.1099/mic.0.000957

Balachandran, P., Hollingshead, S. K., Paton, J. C., & Briles, D. E. (2001). The Autolytic Enzyme LytA of Streptococcus pneumoniae Is Not Responsible for Releasing Pneumolysin. *Journal of Bacteriology*, *183*(10), 3108–3116. https://doi.org/10.1128/JB.183.10.3108-3116.2001

Barreteau, H., Kovač, A., Boniface, A., Sova, M., Gobec, S., & Blanot, D. (2008). Cytoplasmic steps of peptidoglycan biosynthesis. *FEMS Microbiology Reviews*, *32*(2), 168–207. https://doi.org/10.1111/j.1574-6976.2008.00104.x

Bartual, S. G., Straume, D., Stamsås, G. A., Muñoz, I. G., Alfonso, C., Martínez-Ripoll, M., Håvarstein, L. S., & Hermoso, J. A. (2014). Structural basis of PcsB-mediated cell separation in Streptococcus pneumoniae. *Nature Communications*, *5*, 3842. https://doi.org/10.1038/ncomms4842

Beilharz, K., Nováková, L., Fadda, D., Branny, P., Massidda, O., & Veening, J.-W. (2012). Control of cell division in Streptococcus pneumoniae by the conserved Ser/Thr protein kinase StkP. *Proceedings of the National Academy of Sciences of the United States of America*, *109*(15), E905–E913. https://doi.org/10.1073/pnas.1119172109

Berg, K. H., Biørnstad, T. J., Johnsborg, O., & Håvarstein, L. S. (2012). Properties and Biological Role of Streptococcal Fratricins. *Applied and Environmental Microbiology*, *78*(10), 3515–3522. https://doi.org/10.1128/AEM.00098-12

Berg, K. H., Stamsås, G. A., Straume, D., & Håvarstein, L. S. (2013). Effects of Low PBP2b Levels on Cell Morphology and Peptidoglycan Composition in Streptococcus pneumoniae R6. *Journal of Bacteriology*, *195*(19), 4342–4354. https://doi.org/10.1128/JB.00184-13

Berg, K. H., Straume, D., & Håvarstein, L. S. (2014). The function of the transmembrane and cytoplasmic domains of pneumococcal penicillin-binding proteins 2x and 2b extends beyond that of simple anchoring devices. *Microbiology*, *160*(8), 1585–1598. https://doi.org/10.1099/mic.0.078535-0

Bisson Filho, A. W., Hsu, Y.-P., Squyres, G. R., Kuru, E., Wu, F., Jukes, C., Sun, Y., Dekker, C., Holden, S., VanNieuwenhze, M. S., Brun, Y. V., & Garner, E. C. (2017). Treadmilling by FtsZ Filaments Drives Peptidoglycan Synthesis and Bacterial Cell Division. *Science (New York, N.Y.)*, *355*(6326), 739–743. https://doi.org/10.1126/science.aak9973

Boudes, M., Sanchez, D., Graille, M., van Tilbeurgh, H., Durand, D., & Quevillon-Cheruel, S. (2014). Structural insights into the dimerization of the response regulator ComE from Streptococcus pneumoniae. *Nucleic Acids Research*, *42*(8), 5302–5313. https://doi.org/10.1093/nar/gku110

Briggs, N. S., Bruce, K. E., Naskar, S., Winkler, M. E., & Roper, D. I. (2021). The

Pneumococcal Divisome: Dynamic Control of Streptococcus pneumoniae Cell Division. *Frontiers in Microbiology*, *12*. https://www.frontiersin.org/articles/10.3389/fmicb.2021.737396

Bui, N. K., Eberhardt, A., Vollmer, D., Kern, T., Bougault, C., Tomasz, A., Simorre, J.-P., & Vollmer, W. (2012). Isolation and analysis of cell wall components from Streptococcus pneumoniae. *Analytical Biochemistry*, *421*(2), 657–666. https://doi.org/10.1016/j.ab.2011.11.026

Bupp, K., & van Heijenoort, J. (1993). The final step of peptidoglycan subunit assembly in Escherichia coli occurs in the cytoplasm. *Journal of Bacteriology*, *175*(6), 1841–1843.

Bycroft, B. W., & Shute, R. E. (1985). The molecular basis for the mode of action of Beta-lactam antibiotics and mechanisms of resistance. *Pharmaceutical Research*, *2*(1), 3–14. https://doi.org/10.1023/A:1016305704057

Campbell, E. A., Choi, S. Y., & Masure, H. R. (1998). A competence regulon in Streptococcus pneumoniae revealed by genomic analysis. *Molecular Microbiology*, *27*(5), 929–939. https://doi.org/10.1046/j.1365-2958.1998.00737.x

Chambers, H. F. (1999). Penicillin-Binding Protein-Mediated Resistance in Pneumococci and Staphylococci. *The Journal of Infectious Diseases*, *179*(Supplement_2), S353–S359. https://doi.org/10.1086/513854

Chewapreecha, C., Harris, S. R., Croucher, N. J., Turner, C., Marttinen, P., Cheng, L., Pessia, A., Aanensen, D. M., Mather, A. E., Page, A. J., Salter, S. J., Harris, D., Nosten, F., Goldblatt, D., Corander, J., Parkhill, J., Turner, P., & Bentley, S. D. (2014). Dense genomic sampling identifies highways of pneumococcal recombination. *Nature Genetics*, *46*(3), Artikkel 3. https://doi.org/10.1038/ng.2895

Clark, D. P., McGehee, M. R., & Pazdernik, N. J. (2019). *Molecular Biology* (third edition). AP Cell press, Elsevier Inc.

Cornick, J. E., & Bentley, S. D. (2012). *Streptococcus pneumoniae: The evolution of antimicrobial resistance to beta-lactams, fluoroquinolones and macrolides | Elsevier Enhanced Reader*. https://doi.org/10.1016/j.micinf.2012.01.012

Crisóstomo, M. I., Vollmer, W., Kharat, A. S., Inhülsen, S., Gehre, F., Buckenmaier, S., & Tomasz, A. (2006). Attenuation of penicillin resistance in a peptidoglycan O-acetyl transferase mutant of Streptococcus pneumoniae. *Molecular Microbiology*, *61*(6), 1497–1509. https://doi.org/10.1111/j.1365-2958.2006.05340.x

Dalhoff, A., Janjic, N., & Echols, R. (2006). Redefining penems. *Biochemical Pharmacology*, *71*(7), 1085–1095. https://doi.org/10.1016/j.bcp.2005.12.003

de Boer, P. A. J. (2010). Advances in understanding E.coli cell fission. *Current opinion in microbiology*, *13*(6), 730–737. https://doi.org/10.1016/j.mib.2010.09.015

De Las Rivas, B., García, J. L., López, R., & García, P. (2002). Purification and Polar Localization of Pneumococcal LytB, a Putative Endo-β-N-Acetylglucosaminidase: The Chain-Dispersing Murein Hydrolase. *Journal of Bacteriology*, *184*(18), 4988–5000. https://doi.org/10.1128/JB.184.18.4988-5000.2002

Den Blaauwen, T., de Pedro, M. A., Nguyen-Distèche, M., & Ayala, J. A. (2008). Morphogenesis of rod-shaped sacculi. *FEMS Microbiology Reviews*, *32*(2), 321–344. https://doi.org/10.1111/j.1574-6976.2007.00090.x

Di Guilmi, A. M., Mouz, N., Andrieu, J.-P., Hoskins, J., Jaskunas, S. R., Gagnon, J., Dideberg, O., & Vernet, T. (1998). Identification, Purification, and Characterization of Transpeptidase and Glycosyltransferase Domains of Streptococcus pneumoniae Penicillin-Binding Protein 1a. *Journal of Bacteriology*, *180*(21), 5652–5659.

Du, S., & Lutkenhaus, J. (2017). Assembly and activation of the Escherichia coli divisome. *Molecular Microbiology*, *105*(2), 177–187. https://doi.org/10.1111/mmi.13696

Duncan, K., Van Heijenoort, J., & Walsh, C. T. (1990). Purification and characterization of the D-alanyl-D-alanine-adding enzyme from Escherichia coli. *Biochemistry*, *29*(9), 2379–2386. https://doi.org/10.1021/bi00461a023

Egan, A. J. F., & Vollmer, W. (2013). The physiology of bacterial cell division. *Annals of the New York Academy of Sciences*, *1277*(1), 8–28. https://doi.org/10.1111/j.1749-6632.2012.06818.x

Ehmann, D. E., Jahić, H., Ross, P. L., Gu, R.-F., Hu, J., Kern, G., Walkup, G. K., & Fisher, S. L. (2012). Avibactam is a covalent, reversible, non–β-lactam β-lactamase inhibitor. *Proceedings of the National Academy of Sciences of the United States of America*, *109*(29), 11663–11668. https://doi.org/10.1073/pnas.1205073109

Feil, E. J., & Spratt, B. G. (2001). Recombination and the population structures of bacterial pathogens. *Annual Review of Microbiology*, *55*, 561–590. https://doi.org/10.1146/annurev.micro.55.1.561

Fenton, A. K., Manuse, S., Flores-Kim, J., Garcia, P. S., Mercy, C., Grangeasse, C., Bernhardt, T. G., & Rudner, D. Z. (2018). Phosphorylation-dependent activation of the cell wall synthase PBP2a in Streptococcus pneumoniae by MacP. *Proceedings of the National Academy of Sciences of the United States of America*, *115*(11), 2812–2817. https://doi.org/10.1073/pnas.1715218115

Filipe, S. R., Pinho, M. G., & Tomasz, A. (2000). Characterization of the murMN operon involved in the synthesis of branched peptidoglycan peptides in Streptococcus pneumoniae. *The Journal of Biological Chemistry*, *275*(36), 27768–27774. https://doi.org/10.1074/jbc.M004675200

Filipe, S. R., Severina, E., & Tomasz, A. (2001). Functional Analysis of Streptococcus pneumoniae MurM Reveals the Region Responsible for Its Specificity in the Synthesis of Branched Cell Wall Peptides*. *Journal of Biological Chemistry*, *276*(43), 39618–39628. https://doi.org/10.1074/jbc.M106425200

Filipe, S. R., Severina, E., & Tomasz, A. (2002). The murMN operon: A functional link between antibiotic resistance and antibiotic tolerance in Streptococcus pneumoniae. *Proceedings of the National Academy of Sciences of the United States of America*, *99*(3), 1550–1555. https://doi.org/10.1073/pnas.032671699

Filipe, S., & Tomasz, A. (2000). Inhibition of the expression of penicillin resistance in Streptococcus pneumoniae by inactivation of cell wall muropeptide branching genes.

Proceedings of the National Academy of Sciences, *97*, 4891–4896. https://doi.org/10.1073/pnas.080067697

Fiser, A., Filipe, S. R., & Tomasz, A. (2003). Cell wall branches, penicillin resistance and the secrets of the MurM protein. *Trends in Microbiology*, *11*(12), 547–553. https://doi.org/10.1016/j.tim.2003.10.003

Fleurie, A., Cluzel, C., Guiral, S., Freton, C., Galisson, F., Zanella-Cleon, I., Di Guilmi, A.-M., & Grangeasse, C. (2012). Mutational dissection of the S/T-kinase StkP reveals crucial roles in cell division of Streptococcus pneumoniae. *Molecular Microbiology*, *83*(4), 746–758. https://doi.org/10.1111/j.1365-2958.2011.07962.x

Fleurie, A., Lesterlin, C., Manuse, S., Zhao, C., Cluzel, C., Lavergne, J.-P., Franz-Wachtel, M., Macek, B., Combet, C., Kuru, E., VanNieuwenhze, M. S., Brun, Y. V., Sherratt, D., & Grangeasse, C. (2014). MapZ beacons the division sites and positions FtsZ-rings in Streptococcus pneumoniae. *Nature*, *516*(7530), 259–262. https://doi.org/10.1038/nature13966

Ganaie, F., Saad, J. S., McGee, L., van Tonder, A. J., Bentley, S. D., Lo, S. W., Gladstone, R. A., Turner, P., Keenan, J. D., Breiman, R. F., & Nahm, M. H. (2020). A New Pneumococcal Capsule Type, 10D, is the 100th Serotype and Has a Large cps Fragment from an Oral Streptococcus. *mBio*, *11*(3), e00937-20. https://doi.org/10.1128/mBio.00937-20

García, P., González, M. P., García, E., López, R., & García, J. L. (1999). LytB, a novel pneumococcal murein hydrolase essential for cell separation. *Molecular Microbiology*, *31*(4), 1275–1277. https://doi.org/10.1046/j.1365-2958.1999.01238.x

Garcia-Bustos, J. F., Chait, B. T., & Tomasz, A. (1987). Structure of the peptide network of pneumococcal peptidoglycan. *Journal of Biological Chemistry*, *262*(32), 15400–15405. https://doi.org/10.1016/S0021-9258(18)47739-3

Georgopapadakou, N. H., & Liu, F. Y. (1980). Penicillin-binding proteins in bacteria. *Antimicrobial Agents and Chemotherapy*, *18*(1), 148–157.

Georgopapadakou, N., Hammarström, S., & Strominger, J. L. (1977). Isolation of the penicillin-binding peptide from D-alanine carboxypeptidase of Bacillus subtilis. *Proceedings of the National Academy of Sciences of the United States of America*, *74*(3), 1009–1012.

Gérard, P., Vernet, T., & Zapun, A. (2002). Membrane Topology of the Streptococcus pneumoniae FtsW Division Protein. *Journal of Bacteriology*, *184*(7), 1925–1931. https://doi.org/10.1128/JB.184.7.1925-1931.2002

Ghachi, M. E., Derbise, A., Bouhss, A., & Mengin-Lecreulx, D. (2005). Identification of Multiple Genes Encoding Membrane Proteins with Undecaprenyl Pyrophosphate Phosphatase (UppP) Activity in Escherichia coli*. *Journal of Biological Chemistry*, *280*(19), 18689–18695. https://doi.org/10.1074/jbc.M412277200

Ghuysen, J.-M. (1994). Molecular Structures of Penicillin-Binding Proteins and Beta-Lactamases. *Trends in Microbiology*, *2*(10). https://doi.org/10.1016/0966-842X(94)90614-9

Goehring, N. W., & Beckwith, J. (2005). Diverse Paths to Midcell: Assembly of the Bacterial Cell Division Machinery. *Current Biology*, *15*(13), R514–R526. https://doi.org/10.1016/j.cub.2005.06.038

Goffin, C., & Ghuysen, J.-M. (1998). Multimodular Penicillin-Binding Proteins: An Enigmatic Family of Orthologs and Paralogs. *Microbiology and Molecular Biology Reviews*, *62*(4), 1079–1093.

Grebe, T., & Hakenbeck, R. (1996). Penicillin-binding proteins 2b and 2x of Streptococcus pneumoniae are primary resistance determinants for difierent classes of β-lactam antibiotics. *Antimicrobial Agents and Chemotherapy*, *40*(4), 829–834. Scopus. https://doi.org/10.1128/aac.40.4.829

Griffith, Fred. (1928). The Significance of Pneumococcal Types. *The Journal of Hygiene*, *27*(2), 113–159.

Grishin, N. V. (1998). The R3H motif: A domain that binds single-stranded nucleic acids. *Trends in Biochemical Sciences*, *23*(9), 329–330. https://doi.org/10.1016/S0968-0004(98)01258-4

Hakenbeck, R., & Kohiyama, M. (1982). Purification of Penicillin-Binding Protein 3 from Streptococcus pneumoniae. *European Journal of Biochemistry*, *127*(2), 231–236. https://doi.org/10.1111/j.1432-1033.1982.tb06860.x

Hakenbeck, R., Tarpay, M., & Tomasz, A. (1980). Multiple changes of penicillin-binding proteins in penicillin-resistant clinical isolates of Streptococcus pneumoniae. *Antimicrobial Agents and Chemotherapy*, *17*(3), 364–371. https://doi.org/10.1128/AAC.17.3.364

Hansman, D., & Bullen, M. M. (1967). A RESISTANT PNEUMOCOCCUS. *The Lancet*, *290*(7509), 264–265. https://doi.org/10.1016/S0140-6736(67)92346-X

Hardie, J. m., & Whiley, R. a. (1997). Classification and overview of the genera Streptococcus and Enterococcus. *Journal of Applied Microbiology*, *83*(S1), 1S-11S. https://doi.org/10.1046/j.1365-2672.83.s1.1.x

Hare, K. M., Morris, P., Smith-Vaughan, H., & Jane Leach, A. (2008). RANDOM COLONY SELECTION VERSUS COLONY MORPHOLOGY FOR DETECTION OF MULTIPLE PNEUMOCOCCAL SEROTYPES IN NASOPHARYNGEAL SWABS. *The Pediatric Infectious Disease Journal*, *27*(2), 178. https://doi.org/10.1097/INF.0b013e31815bb6c5

Heggenhougen, M. V. (2019). *A penicillin resistant Streptococcus pneumoniae in the making: Characterizing resistance development and cell fitness after acquiring low-affinity penicillin-binding protein and a mosaic MurM* [Master´s thesis, Norwegian Unicersity of Life Sciences]. https://nmbu.brage.unit.no/nmbu-xmlui/handle/11250/2620475

Helassa, N., Vollmer, W., Breukink, E., Vernet, T., & Zapun, A. (2012). The membrane anchor of penicillin-binding protein PBP2a from Streptococcus pneumoniae influences peptidoglycan chain length. *The FEBS Journal*, *279*(11), 2071–2081. https://doi.org/10.1111/j.1742-4658.2012.08592.x

Henriques, A. O., Glaser, P., Piggot, P. J., & Moran Jr, C. P. (1998). Control of cell shape and elongation by the rodA gene in Bacillus subtilis. *Molecular Microbiology*, *28*(2), 235–247. https://doi.org/10.1046/j.1365-2958.1998.00766.x

Higgins, M. L., & Shockman, G. D. (1976). Study of cycle of cell wall assembly in Streptococcus faecalis by three-dimensional reconstructions of thin sections of cells. *Journal of Bacteriology*, *127*(3), 1346–1358.

Hsieh, W. C., & Ho, S. W. (1975). Evaluation of antibacterial activities of cephalosporin antibiotics: Cefazolin, cephaloridine, cephalothin, and cephalexin. *Zhonghua Minguo Wei Sheng Wu Xue Za Zhi = Chinese Journal of Microbiology*, *8*(1), 1–11.

Håvarstein, L. S., Coomaraswamy, G., & Morrison, D. A. (1995). An unmodified heptadecapeptide pheromone induces competence for genetic transformation in Streptococcus pneumoniae. *Proceedings of the National Academy of Sciences*, *92*(24), 11140–11144. https://doi.org/10.1073/pnas.92.24.11140

Håvarstein, L. S., Gaustad, P., Nes, I. F., & Morrison, D. A. (1996). Identification of the streptococcal competence-pheromone receptor. *Molecular Microbiology*, *21*(4), 863–869. https://doi.org/10.1046/j.1365-2958.1996.521416.x

Ikeda, M., Wachi, M., Jung, H. K., Ishino, F., & Matsuhashi, M. (1991). The Escherichia coli mraY gene encoding UDP-N-acetylmuramoyl-pentapeptide: Undecaprenyl-phosphate phospho-N-acetylmuramoyl-pentapeptide transferase. *Journal of Bacteriology*, *173*(3), 1021–1026.

Johnsborg, O., Eldholm, V., & Håvarstein, L. S. (2007). Natural genetic transformation: Prevalence, mechanisms and function. *Research in Microbiology*, *158*(10), 767–778. https://doi.org/10.1016/j.resmic.2007.09.004

Johnsborg, O., & Håvarstein, L. S. (2009). Pneumococcal LytR, a Protein from the LytR-CpsA-Psr Family, Is Essential for Normal Septum Formation in Streptococcus pneumoniae. *Journal of Bacteriology*, *191*(18), 5859–5864. https://doi.org/10.1128/JB.00724-09

Kawamura, Y., Hou, X. G., Sultana, F., Miura, H., & Ezaki, T. (1995). Determination of 16S rRNA sequences of Streptococcus mitis and Streptococcus gordonii and phylogenetic relationships among members of the genus Streptococcus. *International Journal of Systematic Bacteriology*, *45*(2), 406–408. https://doi.org/10.1099/00207713-45-2-406

Kell, C. M., Sharma, U. K., Dowson, C. G., Town, C., Balganesh, T. S., & Spratt, B. G. (1993). Deletion analysis of the essentiality of penicillin-binding proteins 1A, 2B and 2X of Streptococcus pneumoniae. *FEMS Microbiology Letters*, *106*(2), 171–175. https://doi.org/10.1111/j.1574-6968.1993.tb05954.x

Lalble, G., & Hakenbeck, R. (1987). Penicillin-binding proteins in ?-lactam-resistant laboratory mutants of Streptococcus pneumoniae. *Molecular Microbiology*, *1*(1), 355–363. https://doi.org/10.1111/j.1365-2958.1987.tb01942.x

Lamanna, M. M., Manzoor, I., Joseph, M., Ye, Z. A., Benedet, M., Zanardi, A., Ren, Z., Wang, X., Massidda, O., Tsui, H.-C. T., & Winkler, M. E. (2022). Roles of RodZ and class A PBP1b in the assembly and regulation of the peripheral peptidoglycan

elongasome in ovoid-shaped cells of Streptococcus pneumoniae D39. *Molecular Microbiology*, *118*(4), 336–368. https://doi.org/10.1111/mmi.14969

Land, A. D., & Winkler, M. E. (2011). The Requirement for Pneumococcal MreC and MreD Is Relieved by Inactivation of the Gene Encoding PBP1a. *Journal of Bacteriology*, *193*(16), 4166. https://doi.org/10.1128/JB.05245-11

Lattar, S. M., Wu, X., Brophy, J., Sakai, F., Klugman, K. P., & Vidal, J. E. (2018). A Mechanism of Unidirectional Transformation, Leading to Antibiotic Resistance, Occurs within Nasopharyngeal Pneumococcal Biofilm Consortia. *mBio*, *9*(3), e00561-18. https://doi.org/10.1128/mBio.00561-18

Leaver, M., & Errington, J. (2005). Roles for MreC and MreD proteins in helical growth of the cylindrical cell wall in Bacillus subtilis. *Molecular Microbiology*, *57*(5), 1196–1209. https://doi.org/10.1111/j.1365-2958.2005.04736.x

Lee, M. S., & Morrison, D. A. (1999). Identification of a new regulator in Streptococcus pneumoniae linking quorum sensing to competence for genetic transformation. *Journal of Bacteriology*, *181*(16), 5004–5016. Scopus. https://doi.org/10.1128/jb.181.16.5004-5016.1999

Liger, D., Masson, A., Blanot, D., Van Heijenoort, J., & Parquet, C. (1995). Over-production, Purification and Properties of the Uridine-diphosphate-N -Acetylmuramate: L-alanine Ligase from Escherichia coli. *European Journal of Biochemistry*, *230*(1), 80–87. https://doi.org/10.1111/j.1432-1033.1995.0080i.x

Löwe, J. (1998). Crystal Structure Determination of FtsZ fromMethanococcus jannaschii. *Journal of Structural Biology*, *124*(2), 235–243. https://doi.org/10.1006/jsbi.1998.4041

Massidda, O., Nováková, L., & Vollmer, W. (2013). From models to pathogens: How much have we learned about Streptococcus pneumoniae cell division? *Environmental Microbiology*, *15*(12), 3133–3157. https://doi.org/10.1111/1462-2920.12189

Maurer, P., Todorova, K., Sauerbier, J., & Hakenbeck, R. (2012). Mutations in Streptococcus pneumoniae Penicillin-Binding Protein 2x: Importance of the C-Terminal Penicillin-Binding Protein and Serine/Threonine Kinase-Associated Domains for Beta-Lactam Binding. *Microbial Drug Resistance*, *18*(3), 314–321. https://doi.org/10.1089/mdr.2012.0022

McCausland, J. W., Yang, X., Squyres, G. R., Lyu, Z., Bruce, K. E., Lamanna, M. M., Söderström, B., Garner, E. C., Winkler, M. E., Xiao, J., & Liu, J. (2021). Treadmilling FtsZ polymers drive the directional movement of sPG-synthesis enzymes via a Brownian ratchet mechanism. *Nature Communications*, *12*(1), Artikkel 1. https://doi.org/10.1038/s41467-020-20873-y

McGee, L., McDougal, L., Zhou, J., Spratt, B. G., Tenover, F. C., George, R., Hakenbeck, R., Hryniewicz, W., Lefévre, J. C., Tomasz, A., & Klugman, K. P. (2001). Nomenclature of Major Antimicrobial-Resistant Clones of Streptococcus pneumoniae Defined by the Pneumococcal Molecular Epidemiology Network. *Journal of Clinical Microbiology*, *39*(7), 2565–2571. https://doi.org/10.1128/JCM.39.7.2565-2571.2001

Meeske, A. J., Riley, E. P., Robins, W. P., Uehara, T., Mekelanos, J. J., Kahne, D., Walker, S., Kruse, A. C., Bernhardt, T. G., & Rudner, D. Z. (2016). SEDS proteins are a widespread family of bacterial cell wall polymerases. *Nature*, *537*(7622), 634–638. https://doi.org/10.1038/nature19331

Michaud, C., Mengin-Lecreulx, D., van HEIJENOORT, J., & Blanot, D. (1990). Over-production, purification and properties of the uridine-diphosphate-N-acetylmuramoyl-l-alanyl-d-glutamate: Meso-2,6-diaminopimelate ligase from Escherichia coli. *European Journal of Biochemistry*, *194*(3), 853–861. https://doi.org/10.1111/j.1432-1033.1990.tb19479.x

Mitchell, T. (2004). The pathogenesis of streptococcal infections: From Tooth decay to meningitis. *Nature reviews. Microbiology*, *1*, 219–230. https://doi.org/10.1038/nrmicro771

Morlot, C., Noirclerc-Savoye, M., Zapun, A., Dideberg, O., & Vernet, T. (2004). The d,d-carboxypeptidase PBP3 organizes the division process of Streptococcus pneumoniae. *Molecular Microbiology*, *51*(6), 1641–1648. https://doi.org/10.1046/j.1365-2958.2003.03953.x

Morlot, C., Pernot, L., Le Gouellec, A., Di Guilmi, A. M., Vernet, T., Dideberg, O., & Dessen, A. (2005). Crystal Structure of a Peptidoglycan Synthesis Regulatory Factor (PBP3) from Streptococcus pneumoniae*. *Journal of Biological Chemistry*, *280*(16), 15984–15991. https://doi.org/10.1074/jbc.M408446200

Mortier-Barrière, I., Velten, M., Dupaigne, P., Mirouze, N., Piétrement, O., McGovern, S., Fichant, G., Martin, B., Noirot, P., Le Cam, E., Polard, P., & Claverys, J.-P. (2007). A Key Presynaptic Role in Transformation for a Widespread Bacterial Protein: DprA Conveys Incoming ssDNA to RecA. *Cell*, *130*(5), 824–836. Scopus. https://doi.org/10.1016/j.cell.2007.07.038

Mosser, J. L., & Tomasz, A. (1969). *Choline-containing Teichoic Acid As a Structural Component of Pneumococcal Cell Wall and Its Role in Sensitivity to Lysis by an Autolytic Enzyme*. https://doi.org/10.1016/S0021-9258(18)63393-9

Mullis, K. B. (1990). The Unusual Origin of the Polymerase Chain Reaction. *Scientific American*, *262*(4), 56–65. https://doi.org/10.1038/scientificamerican0490-56

Nagai, K., Davies, T. A., Jacobs, M. R., & Appelbaum, P. C. (2002). Effects of amino acid alterations in penicillin-binding proteins (PBPs) 1a, 2b, and 2x on PBP affinities of penicillin, ampicillin, amoxicillin, cefditoren, cefuroxime, cefprozil, and cefaclor in 18 clinical isolates of penicillin-susceptible, -intermediate, and -resistant pneumococci. *Antimicrobial Agents and Chemotherapy*, *46*(5), 1273–1280. Scopus. https://doi.org/10.1128/AAC.46.5.1273-1280.2002

NCIRD, Division of bacterial diseases. (2022, februar 28). *Streptococcus pneumoniae: Information for Clinicians | CDC*. https://www.cdc.gov/pneumococcal/clinicians/streptococcus-pneumoniae.html

Nelson, A. L., Roche, A. M., Gould, J. M., Chim, K., Ratner, A. J., & Weiser, J. N. (2007). Capsule Enhances Pneumococcal Colonization by Limiting Mucus-Mediated

Clearance. *Infection and Immunity*, *75*(1), 83–90. https://doi.org/10.1128/IAI.01475-06

Noirclerc-Savoye, M., Lantez, V., Signor, L., Philippe, J., Vernet, T., & Zapun, A. (2013). Reconstitution of Membrane Protein Complexes Involved in Pneumococcal Septal Cell Wall Assembly. *PLoS ONE*, *8*(9), e75522. https://doi.org/10.1371/journal.pone.0075522

Nováková, L., Sasková, L., Pallová, P., Janeček, J., Novotná, J., Ulrych, A., Echenique, J., Trombe, M.-C., & Branny, P. (2005). Characterization of a eukaryotic type serine/threonine protein kinase and protein phosphatase of Streptococcus pneumoniae and identification of kinase substrates. *The FEBS Journal*, *272*(5), 1243–1254. https://doi.org/10.1111/j.1742-4658.2005.04560.x

O'Brien, K. L., Wolfson, L. J., Watt, J. P., Henkle, E., Deloria-Knoll, M., McCall, N., Lee, E., Mulholland, K., Levine, O. S., & Cherian, T. (2009). Burden of disease caused by Streptococcus pneumoniae in children younger than 5 years: Global estimates. *The Lancet*, *374*(9693), 893–902. https://doi.org/10.1016/S0140-6736(09)61204-6

Paik, J., Kern, I., Lurz, R., & Hakenbeck, R. (1999). Mutational Analysis of the Streptococcus pneumoniae Bimodular Class A Penicillin-Binding Proteins. *Journal of Bacteriology*, *181*(12), 3852–3856.

Perez, A. J., Cesbron, Y., Shaw, S. L., Bazan Villicana, J., Tsui, H.-C. T., Boersma, M. J., Ye, Z. A., Tovpeko, Y., Dekker, C., Holden, S., & Winkler, M. E. (2019). Movement dynamics of divisome proteins and PBP2x:FtsW in cells of Streptococcus pneumoniae. *Proceedings of the National Academy of Sciences of the United States of America*, *116*(8), 3211–3220. https://doi.org/10.1073/pnas.1816018116

Peterson, S., Cline, R. T., Tettelin, H., Sharov, V., & Morrison, D. A. (2000). Gene expression analysis of the Streptococcus pneumoniae competence regulons by use of DNA microarrays. *Journal of Bacteriology*, *182*(21), 6192–6202. Scopus. https://doi.org/10.1128/JB.182.21.6192-6202.2000

Peterson, S. N., Sung, C. K., Cline, R., Desai, B. V., Snesrud, E. C., Luo, P., Walling, J., Li, H., Mintz, M., Tsegaye, G., Burr, P. C., Do, Y., Ahn, S., Gilbert, J., Fleischmann, R. D., & Morrison, D. A. (2004). Identification of competence pheromone responsive genes in Streptococcus pneumoniae by use of DNA microarrays. *Molecular Microbiology*, *51*(4), 1051–1070. https://doi.org/10.1046/j.1365-2958.2003.03907.x

Pinho, M. G., Kjos, M., & Veening, J.-W. (2013). How to get (a)round: Mechanisms controlling growth and division of coccoid bacteria. *Nature Reviews Microbiology*, *11*(9), Artikkel 9. https://doi.org/10.1038/nrmicro3088

Pratviel-Sosa, F., Mengin-Lecreulx, D., & van HEIJENOORT, J. (1991). Over-production, purification and properties of the uridine diphosphate N-acetylmuramoyl-l-alanine: D-glutamate ligase from Escherichia coli. *European Journal of Biochemistry*, *202*(3), 1169–1176. https://doi.org/10.1111/j.1432-1033.1991.tb16486.x

Quevillon-Cheruel, S., Campo, N., Mirouze, N., Mortier-Barrière, I., Brooks, M. A., Boudes, M., Durand, D., Soulet, A.-L., Lisboa, J., Noirot, P., Martin, B., Van Tilbeurgh, H.,

Noirot-Gros, M.-F., Claverys, J.-P., & Polard, P. (2012). Structure-function analysis of pneumococcal DprA protein reveals that dimerization is crucial for loading RecA recombinase onto DNA during transformation. *Proceedings of the National Academy of Sciences of the United States of America*, *109*(37), E2466–E2475. Scopus. https://doi.org/10.1073/pnas.1205638109

Rice, L. B. (2002). Association of different mobile elements to generate novel integrative elements. *Cellular and Molecular Life Sciences CMLS*, *59*(12), 2023–2032. https://doi.org/10.1007/s000180200002

Rogers, H. J., Perkins, H. R., & Ward, J. B. (1980). *Microbial Cell Walls and Membranes.* Chapman and Hall. https://doi.org/10.1007/978-94-011-6014-8

Sasková, L., Nováková, L., Basler, M., & Branny, P. (2007). Eukaryotic-Type Serine/Threonine Protein Kinase StkP Is a Global Regulator of Gene Expression in Streptococcus pneumoniae. *Journal of Bacteriology*, *189*(11), 4168–4179. https://doi.org/10.1128/JB.01616-06

Sauvage, E., Kerff, F., Terrak, M., Ayala, J. A., & Charlier, P. (2008). The penicillin-binding proteins: Structure and role in peptidoglycan biosynthesis. *FEMS Microbiology Reviews*, *32*(2), 234–258. https://doi.org/10.1111/j.1574-6976.2008.00105.x

Scheffers, D.-J., & Pinho, M. G. (2005). Bacterial Cell Wall Synthesis: New Insights from Localization Studies. *Microbiology and Molecular Biology Reviews*, *69*(4), 585–607. https://doi.org/10.1128/MMBR.69.4.585-607.2005

Severin, A., & Tomasz, A. (1996). Naturally occurring peptidoglycan variants of Streptococcus pneumoniae. *Journal of Bacteriology*, *178*(1), 168–174. https://doi.org/10.1128/jb.178.1.168-174.1996

Sham, L.-T., Butler, E. K., Lebar, M. D., Kahne, D., Bernhardt, T. G., & Ruiz, N. (2014). MurJ is the flippase of lipid-linked precursors for peptidoglycan biogenesis. *Science (New York, N.Y.)*, *345*(6193), 220–222. https://doi.org/10.1126/science.1254522

Sjodt, M., Rohs, P. D. A., Gilman, M. S. A., Erlandson, S. C., Zheng, S., Green, A. G., Brock, K., Taguchi, A., Kahne, D., Walker, S., Marks, D. S., Rudner, D. Z., Bernhardt, T. G., & Kruse, A. C. (2020). Structural coordination of polymerization and crosslinking by a SEDS-bPBP peptidoglycan synthase complex. *Nature microbiology*, *5*(6), 813–820. https://doi.org/10.1038/s41564-020-0687-z

Smith, A. M., & Klugman, K. P. (2001). Alterations in MurM, a Cell Wall Muropeptide Branching Enzyme, Increase High-Level Penicillin and Cephalosporin Resistance in Streptococcus pneumoniae. *Antimicrobial Agents and Chemotherapy*, *45*(8), 2393–2396. https://doi.org/10.1128/AAC.45.8.2393-2396.2001

Smith, T., Lehmann, D., Montgomery, J., Gratten, M., Riley, I. D., & Alpers, M. P. (1993). Acquisition and invasiveness of different serotypes of *Streptococcus pneumoniae* in young children. *Epidemiology and Infection*, *111*(1), 27–39. https://doi.org/10.1017/S0950268800056648

Soucy, S. M., Huang, J., & Gogarten, J. P. (2015). Horizontal gene transfer: Building the web of life. *Nature Reviews Genetics*, *16*(8), Artikkel 8. https://doi.org/10.1038/nrg3962

Spratt, B. G. (1977). Properties of the Penicillin-Binding Proteins of Escherichia coli K12. *European Journal of Biochemistry*, *72*(2), 341–352. https://doi.org/10.1111/j.1432-1033.1977.tb11258.x

Stamsås, G. A., Straume, D., Ruud Winther, A., Kjos, M., Frantzen, C. A., & Håvarstein, L. S. (2017). Identification of EloR (Spr1851) as a regulator of cell elongation in Streptococcus pneumoniae. *Molecular Microbiology*, *105*(6), 954–967. https://doi.org/10.1111/mmi.13748

Straume, D., Piechowiak, K. W., Olsen, S., Stamsås, G. A., Berg, K. H., Kjos, M., Heggenhougen, M. V., Alcorlo, M., Hermoso, J. A., & Håvarstein, L. S. (2020). Class A PBPs have a distinct and unique role in the construction of the pneumococcal cell wall. *Proceedings of the National Academy of Sciences*, *117*(11), 6129–6138. https://doi.org/10.1073/pnas.1917820117

Straume, D., Stamsås, G. A., Berg, K. H., Salehian, Z., & Håvarstein, L. S. (2017). Identification of pneumococcal proteins that are functionally linked to penicillin-binding protein 2b (PBP2b). *Molecular Microbiology*, *103*(1), 99–116. https://doi.org/10.1111/mmi.13543

Straume, D., Stamsås, G. A., & Håvarstein, L. S. (2014, november 4). *Natural transformation and genome evolution in Streptococcus pneumoniae | Elsevier Enhanced Reader*. https://doi.org/10.1016/j.meegid.2014.10.020

Suvorov, M., Vakulenko, S. B., & Mobashery, S. (2007). Cytoplasmic-Membrane Anchoring of a Class A β-Lactamase and Its Capacity in Manifesting Antibiotic Resistance. *Antimicrobial Agents and Chemotherapy*, *51*(8), 2937–2942. https://doi.org/10.1128/AAC.00011-07

Taguchi, A., Welsh, M. A., Marmont, L. S., Lee, W., Sjodt, M., Kruse, A. C., Kahne, D., Bernhardt, T. G., & Walker, S. (2019). FtsW is a peptidoglycan polymerase that is functional only in complex with its cognate penicillin-binding protein. *Nature microbiology*, *4*(4), 587–594. https://doi.org/10.1038/s41564-018-0345-x

Thermo Fisher, S. (2001). *Oxoid—Product Detail*. http://www.oxoid.com/UK/blue/prod_detail/prod_detail.asp?pr=AN0025&c=UK&lang=EN

Thermo Fisher, S. (2006). *DNA Stains—NO*. https://www.thermofisher.com/uk/en/home/life-science/dna-rna-purification-analysis/nucleic-acid-gel-electrophoresis/dna-stains.html

Tipper, D. J., & Strominger, J. L. (1965). Mechanism of action of penicillins: A proposal based on their structural similarity to acyl-D-alanyl-D-alanine. *Proceedings of the National Academy of Sciences of the United States of America*, *54*(4), 1133–1141.

Tomasz, A. (1966). Model for the Mechanism Controlling the Expression of Competent State in Pneumococcus Cultures. *Journal of Bacteriology*, *91*(3), 1050–1061.

Troeger, C., Blacker, B., Khalil, I. A., Rao, P. C., Cao, J., Zimsen, S. R. M., Albertson, S. B., Deshpande, A., Farag, T., Abebe, Z., Adetifa, I. M. O., Adhikari, T. B., Akibu, M., Al Lami, F. H., Al-Eyadhy, A., Alvis-Guzman, N., Amare, A. T., Amoako, Y. A., Antonio, C. A. T., … Reiner, R. C. (2018). Estimates of the global, regional, and

national morbidity, mortality, and aetiologies of lower respiratory infections in 195 countries, 1990–2016: A systematic analysis for the Global Burden of Disease Study 2016. *The Lancet Infectious Diseases*, *18*(11), 1191–1210. https://doi.org/10.1016/S1473-3099(18)30310-4

Trouve, J., Zapun, A., Arthaud, C., Durmort, C., Di Guilmi, A. M., Söderström, B., Pelletier, A., Grangeasse, C., Bourgeois, D., Wong, Y.-S., & Morlot, C. (2021). Nanoscale dynamics of peptidoglycan assembly during the cell cycle of Streptococcus pneumoniae. *Current Biology*, *31*(13), 2844-2856.e6. https://doi.org/10.1016/j.cub.2021.04.041

Tsui, H.-C. T., Boersma, M. J., Vella, S. A., Kocaoglu, O., Kuru, E., Peceny, J. K., Carlson, E. E., VanNieuwenhze, M. S., Brun, Y. V., Shaw, S. L., & Winkler, M. E. (2014). Pbp2x localizes separately from Pbp2b and other peptidoglycan synthesis proteins during later stages of cell division of Streptococcus pneumoniae D39. *Molecular Microbiology*, *94*(1), 21–40. https://doi.org/10.1111/mmi.12745

Tsui, H.-C. T., Zheng, J. J., Magallon, A. N., Ryan, J. D., Yunck, R., Rued, B. E., Bernhardt, T. G., & Winkler, M. E. (2016). Suppression of a deletion mutation in the gene encoding essential PBP2b reveals a new lytic transglycosylase involved in peripheral peptidoglycan synthesis in Streptococcus pneumoniae D39. *Molecular Microbiology*, *100*(6), 1039–1065. https://doi.org/10.1111/mmi.13366

Typas, A., Banzhaf, M., Gross, C. A., & Vollmer, W. (2011). From the regulation of peptidoglycan synthesis to bacterial growth and morphology. *Nature reviews. Microbiology*, *10*(2), 123–136. https://doi.org/10.1038/nrmicro2677

Valverde, R., Edwards, L., & Regan, L. (2008). Structure and function of KH domains. *The FEBS Journal*, *275*(11), 2712–2726. https://doi.org/10.1111/j.1742-4658.2008.06411.x

Van Den Ent, F., Leaver, M., Bendezu, F., Errington, J., De Boer, P., & Löwe, J. (2006). Dimeric structure of the cell shape protein MreC and its functional implications. *Molecular Microbiology*, *62*(6), 1631–1642. https://doi.org/10.1111/j.1365-2958.2006.05485.x

van der Poll, T., & Opal, S. M. (2009). Pathogenesis, treatment, and prevention of pneumococcal pneumonia. *The Lancet*, *374*(9700), 1543–1556. https://doi.org/10.1016/S0140-6736(09)61114-4

Van Heijenoort, Y., Leduc, M., Singer, H., & Van Heijenoort, J. (1987). Effects of Moenomycin on Escherichia coli. *Microbiology*, *133*(3), 667–674. https://doi.org/10.1099/00221287-133-3-667

Vollmer, W., Blanot, D., & De Pedro, M. A. (2008). Peptidoglycan structure and architecture. *FEMS Microbiology Reviews*, *32*(2), 149–167. https://doi.org/10.1111/j.1574-6976.2007.00094.x

Vollmer, W., Hakenbeck, R., & Chhatwal, S. (2007). Preparation and analysis of pneumococcal murein (peptidoglycan). I *Molecular biology of streptococci* (s. 531–536). Horizon Bioscience.

Vollmer, W., Massidda, O., & Tomasz, A. (2019). The Cell Wall of Streptococcus pneumoniae. *Microbiology Spectrum*, *7*(3), 7.3.19. https://doi.org/10.1128/microbiolspec.GPP3-0018-2018

Wachi, M., Doi, M., Okada, Y., & Matsuhashi, M. (1989). New mre genes mreC and mreD, responsible for formation of the rod shape of Escherichia coli cells. *Journal of Bacteriology*, *171*(12), 6511–6516.

Wahl, B., O'Brien, K. L., Greenbaum, A., Majumder, A., Liu, L., Chu, Y., Lukšić, I., Nair, H., McAllister, D. A., Campbell, H., Rudan, I., Black, R., & Knoll, M. D. (2018). Burden of Streptococcus pneumoniae and Haemophilus influenzae type b disease in children in the era of conjugate vaccines: Global, regional, and national estimates for 2000–15. *The Lancet. Global Health*, *6*(7), e744–e757. https://doi.org/10.1016/S2214-109X(18)30247-X

Wallhausser, K. H., Nesemann, G., Prave, P., & Steigler, A. (1965). Moenomycin, a new antibiotic. I. Fermentation and isolation. *Antimicrobial Agents and Chemotherapy*, *5*, 734–736.

Weber, B., Ehlert, K., Diehl, A., Reichmann, P., Labischinski, H., & Hakenbeck, R. (2000). The fib locus in Streptococcus pneumoniae is required for peptidoglycan crosslinking and PBP-mediated β-lactam resistance. *FEMS Microbiology Letters*, *188*(1), 81–85. https://doi.org/10.1111/j.1574-6968.2000.tb09172.x

Weber, K., & Kuter, D. J. (1971). Reversible Denaturation of Enzymes by Sodium Dodecyl Sulfate. *Journal of Biological Chemistry*, *246*(14), 4504–4509. https://doi.org/10.1016/S0021-9258(18)62040-X

Ween, O., Gaustad, P., & Håvarstein, L. S. (1999). Identification of DNA binding sites for ComE, a key regulator of natural competence in Streptococcus pneumoniae. *Molecular Microbiology*, *33*(4), 817–827. https://doi.org/10.1046/j.1365-2958.1999.01528.x

Weil-Olivier, C., van der Linden, M., de Schutter, I., Dagan, R., & Mantovani, L. (2012). Prevention of pneumococcal diseases in the post-seven valent vaccine era: A European perspective. *BMC Infectious Diseases*, *12*, 207. https://doi.org/10.1186/1471-2334-12-207

Wen, Z. T., Bitoun, J. P., & Liao, S. (2015). PBP1a-Deficiency Causes Major Defects in Cell Division, Growth and Biofilm Formation by Streptococcus mutans. *PLOS ONE*, *10*(4), e0124319. https://doi.org/10.1371/journal.pone.0124319

WHO publishes list of bacteria for which new antibiotics are urgently needed. (2017). https://www.who.int/news/item/27-02-2017-who-publishes-list-of-bacteria-for-which-new-antibiotics-are-urgently-needed

Winther, A., Kjos, M., Stamsås, G., Håvarstein, L., & Straume, D. (2019). Prevention of EloR/KhpA heterodimerization by introduction of site-specific amino acid substitutions renders the essential elongasome protein PBP2b redundant in Streptococcus pneumoniae. *Scientific Reports*, *9*, 3681. https://doi.org/10.1038/s41598-018-38386-6

Winther, A. R. (2020). *Cell-shape regulation in Streptococcus pneumoniae: EloR/KhpA, a new regulatory pathway administering cellelongation* [Philosophiae Doctor (PhD) Thesis, Norwegian Unicersity of Life Sciences]. https://nmbu.brage.unit.no/nmbu-xmlui/handle/11250/2681247

Winther, A. R., Kjos, M., Herigstad, M. L., Håvarstein, L. S., & Straume, D. (2021). EloR Interacts with the Lytic Transglycosylase MltG at Midcell in Streptococcus pneumoniae R6. *Journal of Bacteriology*, *203*(9), e00691-20. https://doi.org/10.1128/JB.00691-20

Yeats, C., Finn, R. D., & Bateman, A. (2002). The PASTA domain: A β-lactam-binding domain. *Trends in Biochemical Sciences*, *27*(9), 438–440. https://doi.org/10.1016/S0968-0004(02)02164-3

York, A., Lloyd, Adrian. J., del Genio, C. I., Shearer, J., Hinxman, Karen. J., Fritz, K., Fulop, V., Dowson, Christopher. G., Khalid, S., & Roper, David. I. (2021). Structure-based modeling and dynamics of MurM, a Streptococcus pneumoniae penicillin resistance determinant present at the cytoplasmic membrane. *Structure*, *29*(7), 731-742.e6. https://doi.org/10.1016/j.str.2021.03.001

Zapun, A., Contreras-Martel, C., & Vernet, T. (2008). Penicillin-binding proteins and β-lactam resistance. *FEMS Microbiology Reviews*, *32*(2), 361–385. https://doi.org/10.1111/j.1574-6976.2007.00095.x

Zapun, A., Vernet, T., & Pinho, M. G. (2008). The different shapes of cocci. *FEMS Microbiology Reviews*, *32*(2), 345–360. https://doi.org/10.1111/j.1574-6976.2007.00098.x

Zhao, G., Yeh, W. K., Carnahan, R. H., Flokowitsch, J., Meier, T. I., Alborn, W. E., Becker, G. W., & Jaskunas, S. R. (1997). Biochemical characterization of penicillin-resistant and -sensitive penicillin-binding protein 2x transpeptidase activities of Streptococcus pneumoniae and mechanistic implications in bacterial resistance to beta-lactam antibiotics. *Journal of Bacteriology*, *179*(15), 4901–4908.

Zighelboim, S., & Tomasz, A. (1980). Penicillin-binding proteins of multiply antibiotic-resistant South African strains of Streptococcus pneumoniae. *Antimicrobial Agents and Chemotherapy*, *17*(3), 434–442.

Appendix

A1 HPLC chromatogram of RSG77 *mreC**

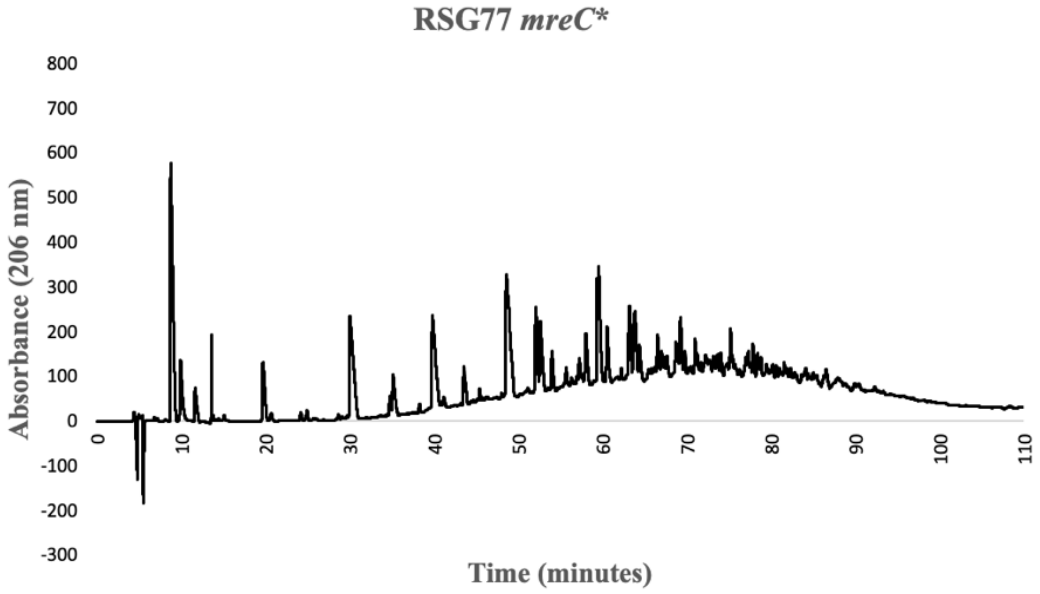

Figure 15 HPLC chromatogram of RSG77 *mreC**. This strain was used to make the strain RSG77 *mreC** Δ*pbp2b.*

A2 HPLC chromatogram of RSG77 Δ*eloR*

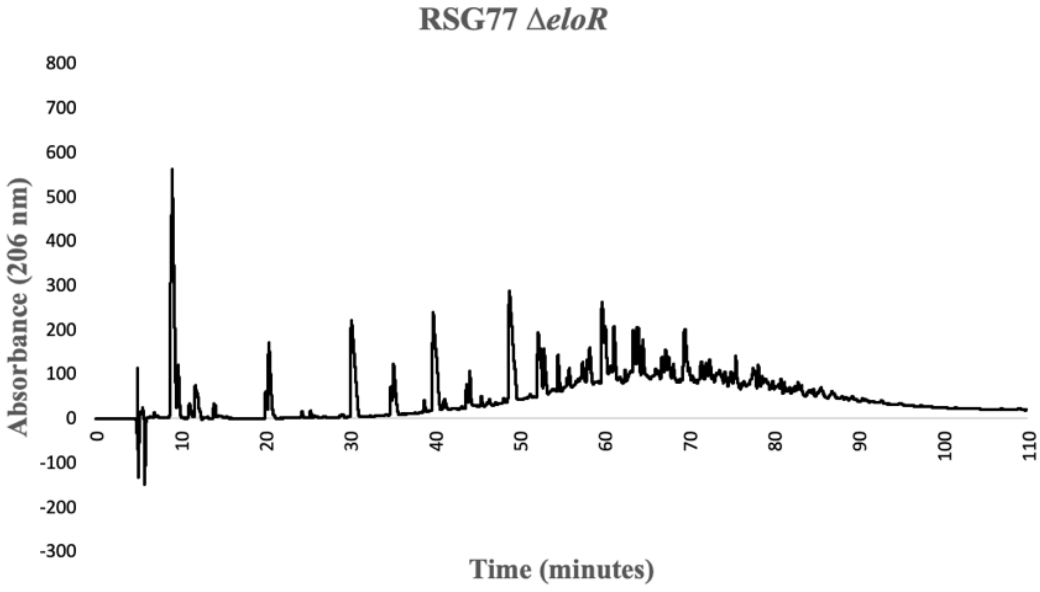

Figure 16 HPLC chromatogram of RSG77 Δ*eloR*. This strain was used to make the strain RSG77 Δ*eloR* Δ*pbp2b*.

A3 HPLC chromatogram of Pen6 *mreC**

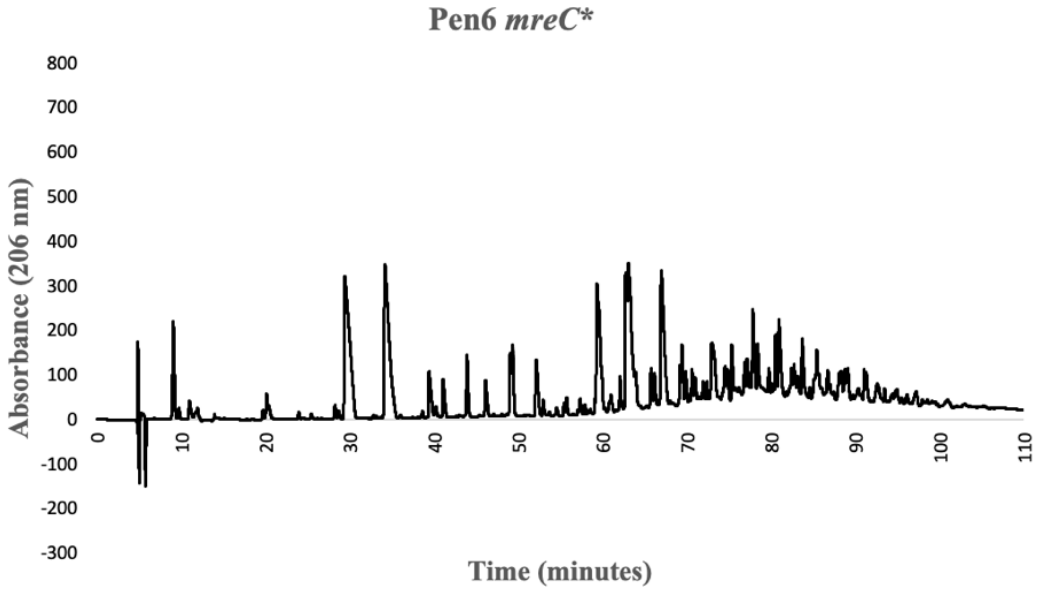

Figure 17 HPLC chromatogram of Pen6 *mreC**. This strain was used to make the strain Pen6 *mreC** Δ*pbp2b*.

A4 HPLC chromatogram of Pen6 Δ*eloR*

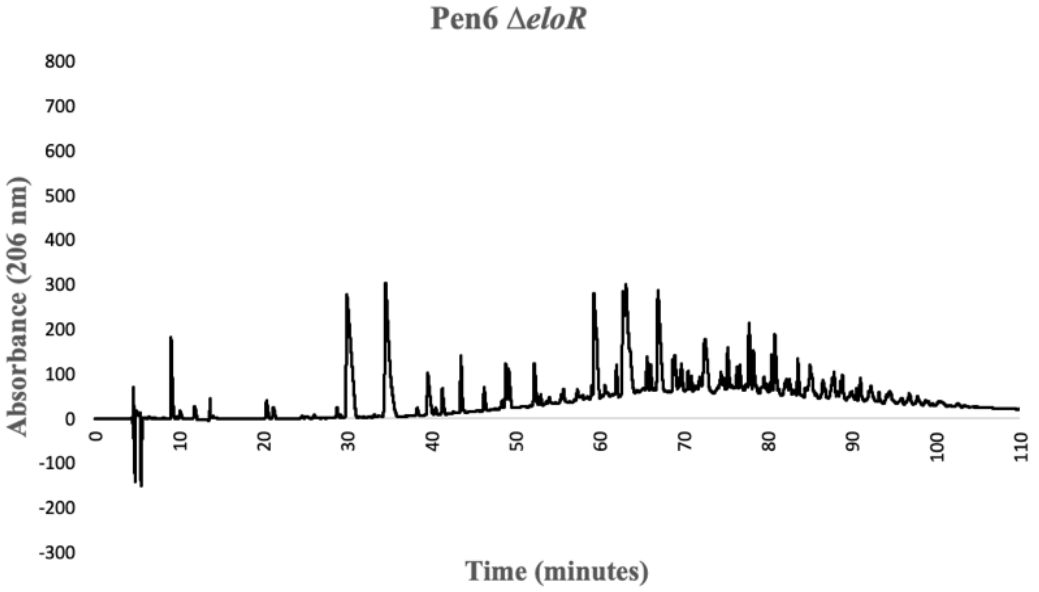

Figure 18 HPLC chromatogram of Pen6 Δ*eloR*. This strain was used to make the strain Pen6 Δ*eloR* Δ*pbp2b*.

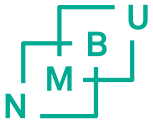

Norges miljø- og biovitenskapelige universitet
Noregs miljø- og biovitskapelege universitet
Norwegian University of Life Sciences

Postboks 5003
NO-1432 Ås
Norway